POLITECNICO DI TORINO

Master of Science in Civil Engineering

MASTER'S DEGREE THESIS

SEISMIC VULNERABILITY ASSESSMENT OF FOGGIA AIRPORT AND RETROFITTING SOLUTION WITH EXOSKELETONS

Supervisor:

Prof. Marco Domaneschi

Co-supervisors:

Prof. Raffaele Cucuzza

Candidate:

Carlos Jesus Orozco Bustamante

OCTOBER 2023 - A.Y. 2022/2023

Abstract

Seismic regulations began to be implemented worldwide in the late 1980s. Prior to that, the construction philosophy primarily focused on gravitational loads. The case study of Foggia Airport highlights several deficiencies [1] that rendered the building vulnerable to seismic activity. The need to keep the facilities operational during the intervention led to the adoption of exoskeletons, a technique that acts as an appendage to the main structure by absorbing a significant portion of the horizontal forces and relieving the existing building [14] . Conversely, some structures with inherent structural deficiencies fail to achieve a 75% mass participation factor during modal analysis, a critical limitation for generating a modal profile that simulates seismic forces using a unidirectional, monotonically increasing force in evaluating structural behavior in the nonlinear range through pushover analysis. Multi-modal distribution used in pushover analysis [19] enables the derivation of a force profile by combining the most influential modes into a unidirectional vector of forces.

This work is divided into three main chapters. The first chapter encompasses a literature review and a summary of the current state of structural deficiency classification, external retrofitting intervention techniques, and theoretical support for the static nonlinear analysis procedure. Through this chapter, we observe the evolution of external structures coupled to existing buildings with the aim of improving horizontal response. Moreover, we discuss suitable alternatives for analyzing existing structures with multiple deficiencies. The multimodal distribution in pushover analysis [19] provides a reliable option to assess a building with multiple frequencies that reaches 85% of the mass participation factor, a problem presented in the case study.

The second chapter provides a comprehensive description of the building's characteristics, a seismic assessment, modeling assumptions, and model calibration. The software used for modeling the structure was SAP2000 integrated with MATLAB through OAPI. Additionally, it presents the preliminary analysis, shedding light on the issues open for discussion. This chapter describes the characteristics of the structure, materials, in situ survey outcomes, and inspections.

In addition, it presents the FEM model and the hypotheses assumed to build it up; different reduced models were used to verify the reliability of the nonlinear forces and calibrate the input parameters of the nonlinear forces. It includes the correct selection of the constitutive law for the creation of plastic hinges and the pushover curve outcome. The end of this chapter provides conclusive evidence of potential structural damage under seismic actions.

The third main chapter offers the ultimate solution, employing orthogonal exoskeletons with semi-spherical morphology and horizontal deck bracings. Subsequently, the structure undergoes a nonlinear evaluation to determine the vulnerability index. The conclusions obtained reveal outstanding results concerning the overall performance under seismic conditions.

Contents

List of Figures

List of Tables

INTRODUCTION

In the continuously evolving realm of structural engineering, ensuring the safety of structures intended for human use stands as a paramount concern. Codes and regulations governing construction practices are primarily tasked with standardizing structures to uphold human safety. Historically, construction philosophy predominantly centered on addressing gravitational loads. However, as seismic resistance principles have gained prominence, the focus has shifted towards safeguarding structures against dynamic forces.

This document presents a case study involving a structure of significant regional importance, the Foggia Airport. With its recent transformation from a military complex to a public civil facility catering to commercial flights, local authorities raised concerns regarding the structure's ability to accommodate the increased non-permanent gravitational loads and maintain safety standards. Subsequently, an engineering firm was commissioned to conduct a comprehensive structural assessment. The survey yielded crucial information pertaining to the structural system, material properties, and key elements and arrangements within the facility. Unfortunately, the findings indicated the structure's inadequacy to withstand seismic demands.

However, the report's conclusion lacked sufficient empirical substantiation, prompting the need for a rigorous safety assessment of the Foggia Airport. This assessment, outlined in this document, employs two methodologies: linear dynamic analysis and non-linear static analysis in its initial phase. Furthermore, this document addresses the requirement established by the client, which involves the implementation of exoskeletons as an intervention strategy. Exoskeletons function as integrated systems that significantly enhance structural stiffness. While a common misconception may suggest that increased stiffness leads to higher excitation frequencies and shorter periods, ultimately elevating the magnitude of acceleration, the reality is more nuanced. Exoskeletons effectively redirect seismic forces, absorbing them into their framework and relieving the original structure of seismic demands.

The proposed solution within this document serves to demonstrate the efficacy of exoskeletons in rectifying structural deficiencies, harmonizing global responses across various frequency spectra, and enhancing overall structural performance.

To offer a comprehensive perspective on the retrofitting process, this document presents a finite element model (FEM) meticulously calibrated to depict building responses under both linear and nonlinear conditions, both before and after the introduction of exoskeletons. A robust theoretical framework is articulated to discuss model calibration, the constitutive laws governing plastic hinges, pushover analysis methodology, the derivation of participation factors under varying load profiles, and the ensuing safety assessments. Through this scientific exploration, we endeavor to contribute to the advancement of knowledge in the domain of structural engineering, with a specific focus on retrofitting strategies, and their implications for enhancing the safety and resilience of structures designed for human use.

Chapter 1

LITERATURE REVIEW AND STATE OF THE ART

1.1 Structural Deficiencies

Prior to delving into discussions of structural vulnerability, it is essential to introduce the concept of seismic deficiency. Seismic deficiency is defined as a critical state wherein buildings fail to meet specified seismic performance objectives. These performance objectives are established in accordance with prescriptive evaluation standards. A building that does not conform to seismic-resistant codes and regulations seeks to preserve its functionality following a significant seismic event by implementing intervention measures aimed at rectifying potential deficiencies[1]. The primary consideration when initiating the assessment of a building's seismic capacity lies in the availability and reliability of structural drawings, their correlation with as-built information, material properties, and the construction process. These factors collectively form the foundational basis for evaluating a structure's seismic resilience. Numerous procedures and standards for seismic evaluation are available within the field of engineering. These methodologies range from prescriptive approaches rooted in predefined regulations tailored to specific building typologies, to more intricate methods that prioritize the computation of a vulnerability index. This computation relies on the application of non-linear cyclic response analyses, carried out through either a static approach or a time history approach.

1.2 Seismic Evaluation

Seismic evaluation of existing buildings can be initiated by competent authorities at the national or regional level as part of their risk reduction programs. The primary objective is to ensure the preservation of a building in an optimal state following a seismic event or to guarantee its stability as per design criteria. Typically, buildings are selected for seismic evaluation based on key parameters such as structural system, age, geographical location, and combinations of various risk factors[1].

Seismic evaluations are also mandated under the following circumstances:

• When regional governmental authorities observe alterations in the type of occupancy, changes in the structural system, or significant structural modifications to a building.

• When property owners voluntarily seek seismic risk analysis to safeguard their economic investments or to maintain the intrinsic value of the building itself. The following addresses different approaches to evaluate the condition of an existing structure.

1.2.1 Comparison with requirements for new buildings

Prior to the 1980s, there existed limited standardized guidelines for the assessment of existing buildings in California. Consequently, the prevailing practice involved benchmarking these structures against the standards applicable during their original construction era. This approach frequently proved impractical, primarily due to constraints in classifying the building's construction system, restrictions stemming from the utilization of prohibited materials, or outright violations of established structural norms. The outcome of this practice often necessitated the introduction of an entirely new seismic retrofitting system, resulting in significant disruptions and financial burdens.[1]

1.2.2 Prescriptive standards

This methodology was established in response to growing concerns regarding the seismic assessment of aging structures situated along the western coast of the United States. Numerous organizations involved in seismic damage prevention collectively issued guidelines for the evaluation of buildings susceptible to potential seismic harm. Among the most prominent documents for seismic assessment of existing structures is ASCE 31-03: "Seismic Evaluation of Existing Buildings". Originally developed by FEMA as FEMA 310: "Handbook for the Seismic Evaluation of Existing Buildings – A Prestandard", FEMA 310 was subsequently incorporated into ASCE 31 as part of the standardization process conducted by the American Society of Civil Engineers.

1.2.3 Performance-based evaluation using expected non-linear response

The most intricate and advanced seismic evaluations are conducted through analytical methodologies that explicitly account for the anticipated non-linear behavior of structures during intense seismic events. One such analytical technique is the pushover analysis, as outlined in ATC 40 guidelines. [1]The outcomes of these analyses necessitate a comparison against predefined performance levels, including immediate occupancy, life safety, or collapse prevention criteria. As a result, American standards have advanced since 2006, mirroring similar progress in European standards, particularly exemplified by the Italian normative standards outlined in NTC-2018. This notable advancement in conjunction with the ongoing development of Finite Element Method (FEM) software has established this methodology as the most precise approach, yielding highly dependable results.

The analysis of nonlinearity within this methodology serves to gauge a building's capacity to endure dynamic forces prior to the onset of structural collapse. This contemporary approach aids users in comprehending various phases of a building's behavior and the potential mechanisms that come into play when specific structural elements transition into plastic deformation zones.

1.3 Categories of Seismic deficiencies

Irrespective of the chosen evaluation methodology, the identification of seismic deficiencies becomes imperative when predefined criteria hint at potential structural failures. These deficiencies are systematically categorized as follows[1]:

1. Global Strength Deficiency: This deficiency is often observed in older struc-

tures that lack proper design or adhere to primitive building codes with insufficient strength requirements. It primarily pertains to the lateral strength of the structural system at its effective global yield point, considering the resistance of structural elements;

2. Global Stiffness Deficiency: While strength and stiffness are frequently governed by the same existing elements or retrofitting techniques, these two deficiencies are typically assessed separately. Failing to meet standards in this context results from excessive drift demands placed on existing, inadequately designed components;

3. Configuration Deficiency: This category encompasses irregularities in the structural configuration that negatively impact performance. Current coding distinguishes between plan irregularities and vertical irregularities. The former is associated with issues in structural elements due to torsional responses or diaphragm shapes, while the latter relates to differences in floor heights with irregular mass distribution, leading to unusual force distributions and displacements. Retrofitting is often necessary to mitigate such issues, which are commonly found in older buildings;

4. Load Path Deficiency: This deficiency arises from the breakage of load paths, essentially disruptions between elements responsible for contributing to the global structural behavior and the diaphragms or load sources. It can be seen as the failure to activate the correct structural mechanisms;

5. Component Detailing Deficiency: This deficiency pertains to decisions that influence system behavior, often manifesting in the nonlinear range. Examples include the use of stirrups to enhance resistance through confinement or the incorporation of plates and flanges to provide stiffness in local steel elements. Conversely, it can involve the use of braced frame systems with brittle and weak connections incapable of effectively transmitting diagonal forces;

6. Diaphragm Deficiency: Diaphragms serve a pivotal role in the overall seismic system by acting as horizontal beams that span between lateral force-resisting elements. Deficiencies are observed when there is inadequate shear or bend-

ing strength, typically stemming from a lack of connectivity between members tasked with managing lateral forces;

7. Foundation Deficiency: This intuitive deficiency category encompasses a wide array of issues associated with the structural foundation. These issues are rooted in various base-related problems.

1.4 Seismic rehabilitation

Nonlinear techniques are primarily designed to provide a more robust prediction of structural performance, rather than merely adhering to arbitrary standards. Consequently, the comprehensive implementation of these techniques demands an extensive dataset to gain a thorough understanding of the structural behavior.

The process of rehabilitation encompasses a variety of strategies aimed at effecting changes in the existing structure. These strategies may directly address deficiencies identified during the evaluation phase, thereby altering the overall structural response. Alternatively, they can focus on enhancing specific local elements to prevent early failures under lateral forces.

1.4.1 Categories of Rehabilitation Measures

1. Add Elements: Introducing additional structural components.

2. Enhance Performance of Existing Elements: Improving the performance of pre-existing structural elements.

3. Improve Connections Between Components: Enhancing the connections between structural components.

4. Reduce Demand: Implementing measures to reduce the demands placed on the structure.

5. Remove Selected Components: Strategically removing certain structural elements.

1.4.2 Strategies for Developing Rehabilitation Schemes

After performing the vulnerability evaluation and detecting deficiencies in the structures that lead to an unsafe condition under seismic demand, we should consider different strategies that comply two different considerations:

Technical considerations

1. Ensuring a complete load path within the structure.

2. Providing adequate strength and stiffness to meet design standards.

3. Ensuring compatibility with and effective protection of the existing lateral and gravity support systems.

4. Establishing a suitable foundation for the rehabilitation efforts.

Non-Technical considerations

1. Evaluating construction costs associated with the proposed rehabilitation.

2. Assessing the seismic performance enhancement potential.

3. Considering short-term disruptions to occupants and the long-term functionality of the building.

4. Evaluating aesthetic aspects of the proposed changes.

1.5 Topology of Steel Moment resistant Structures

This type of buildings is completely assembled by steel beams and columns. Lateral forces are resisted by moment frames that develop stiffness through rigid connections of the beams and column created by angles, plates, and bolts or welding. Moment frames might be developed on all framing lines or only in selected bays. This topology has no structural walls or bracings connected to the structure[1].

Floors and roofs can function as flexible diaphragms, using materials like wood or untopped metal decks. Within the category of flexible diaphragms, we encounter scenarios involving either bare metal decks or metal decks with non-structural infill. This design approach is commonly employed in roofing systems that bear low gravity loads. The attachment of these decks to the steel structural members can be achieved through elements such as shear studs, screws, or shot pins. In certain cases, these deck elements may also serve as both chords and collectors within the diaphragm system.

These types of building were widely used prior 80's decade. Yet, there are deficiencies that are detected, mainly regarded to Global Strength and Global Stiffness. Concerning global strength, the weaknesses appear due to the insufficient frame strength, resulting high demands on the existing frames. The yielding or fractures in beam or columns elements could lead to excessive drifts and therefore severely damaged after seismic demand. On the other hand, global stiffness is an important aspect to take care about, this typology of buildings is much more flexible than other type of lateral force-resisting system, resulting highs inter-story drift and building dirtfts. Consequently, a great amount of damage appears in connections and non-structural elements. Another aspect is related to P delta effects. This typology is prone to be intervened by lateral elements like bracings or exostructures that gives additional strength and stiffness.

Another aspect to remark is the presence of soft story, a condition that happens when stiffness from one floor to the other changes abruptly. Low height buildings with light roofs and different mass per floor might carry on with this type of problems.

1.6 External structures for structural interventions

After performing a structural evaluation and safety assessment, the subsequent action to do if the safety condition is not present is to proceed with a retrofitting. Depending on the safety level, the intervention could be at local or global scale. The present sub-chapter introduces the evolution of the external structures as an alternative solution to retrofit structures with seismic deficiencies.

1.6.1 External Shear walls

This technique consists in a reinforced concrete shear wall coupled with the existing structures between one to a maximum of two storeys. They are placed orthogonal to the façade providing additional stiffness to control lateral displacement due to horizontal actions [11]. The structures that cannot be internally intervened due to their continuous use may be subject to retrofitting through external strategies. The case of many primary and secondary schools in rural areas in Turkey underwent this methodology. External shear walls proved to be efficient in enhancing the seismic behavior of a structure, the aim of this retrofitting practice was to overcome the potential damage of this typology of structures after Duzce earthquake [20].

Different experimental testing was performed to recreate the response of the existing buildings simulating the conditions in which the existing structures were

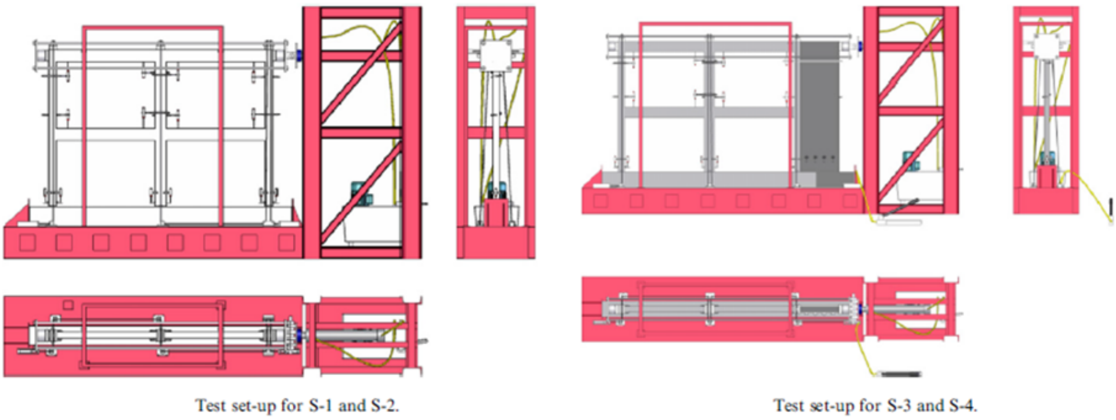

Figure 1.1: Testing set up for frames [11]

built up. The results of this procedure demonstrated the efficiency of the shear walls when they are coupled to frame with poor confinement and not very ductile.

It was proved that the coupled system can overcome 4 times the demand of the existing system. Therefore, they become a feasible solution for the limitations imposed by operational issues and easy to perform when there is enough space.

Moreover, further modifications were made during the evolution of the concept of shear walls. The first condition that was altered corresponds to the support restrains, depending on the modal shape and response of the building, it could be coherent to use a hinged connection to the ground for the coupled system. This methodology is called rocking wall[21].

The other concept that was introduced is the different typologies of connections between the coupled system and the original one. Generally, this is addressed to assess the behaviour of the building if the connection possesses dissipation of energy or transfer the energy directly through rigid links. A very interesting case of study that provides significant relevance regarding these two topics is Tokyo institute of technology built up in 1979 just before the Japanese seismic codding of 1981. This structure provided deficiencies under a hypothetic seismic scenario.

The assessment of this building provides a comparative between a non-retrofitted scenario and the other one coupling the system to a rocking wall with dissipative links. In the safety assessment performed the results concluded a vulnerable condition in the first, fourth, fifth, sixth and seventh floor in terms of interstorey drifts.

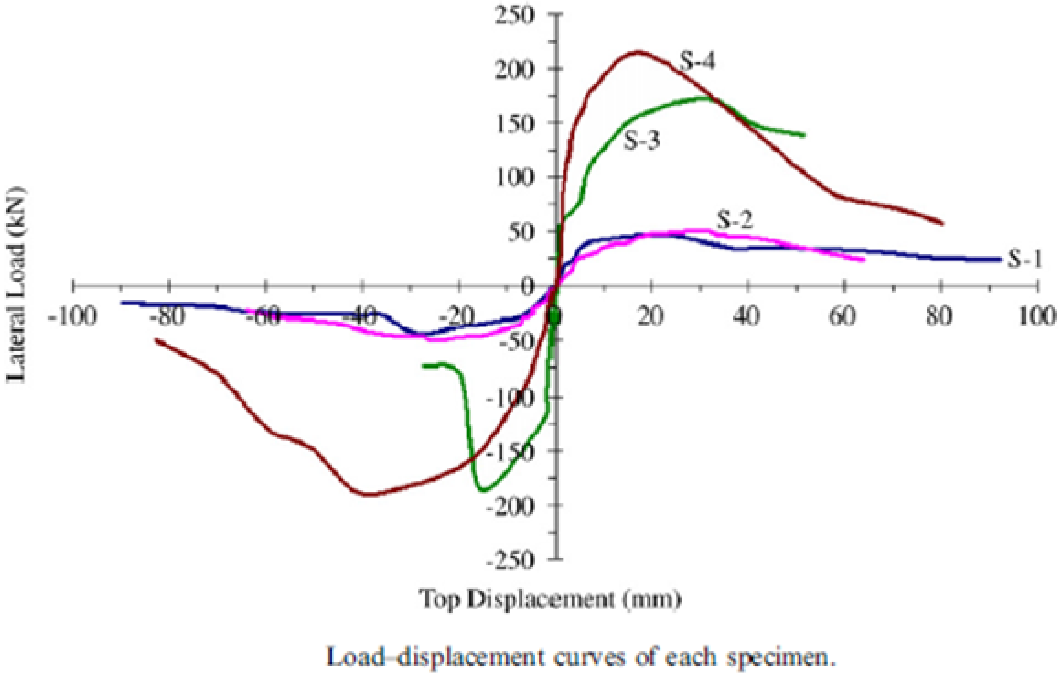

Figure 1.2: Load-Displacement curves for previous scheme [11]

The distribution of the deformation was very unpredictable and large displacements were meant to happen. The rocking wall allows the movement of a solid mass and normalize the shape of the building. This characteristic helps the global behavior to dissipate local failures and helping the building to achieve the maximum possible plastic hinges in a same time. This approach allows to have a control in the failure mode of the structure. On the other hand, dissipation allows to reduce the demand in the building.

Another approach arouses in the field of the external shear walls and maybe one the first kind of exoskeletons are the orthogonal steel shear walls. [10]. This solution comes to present a good alternative to improve the global strength and stiffness allowing the structure to achieve a greater shear base capacity. [16]. Moreover, such line of interventions compensates the local deficiencies by limiting the displacement demand [6].

In terms of local behaviour this kind of approach were tested and realized that they behave as monolithic walls [12]. Therefore, several authors refer this typology of intervention as steel shear walls and not exoskeletons. [13]. The use of steel bracings interventions present advantages with respect to construction costs. In

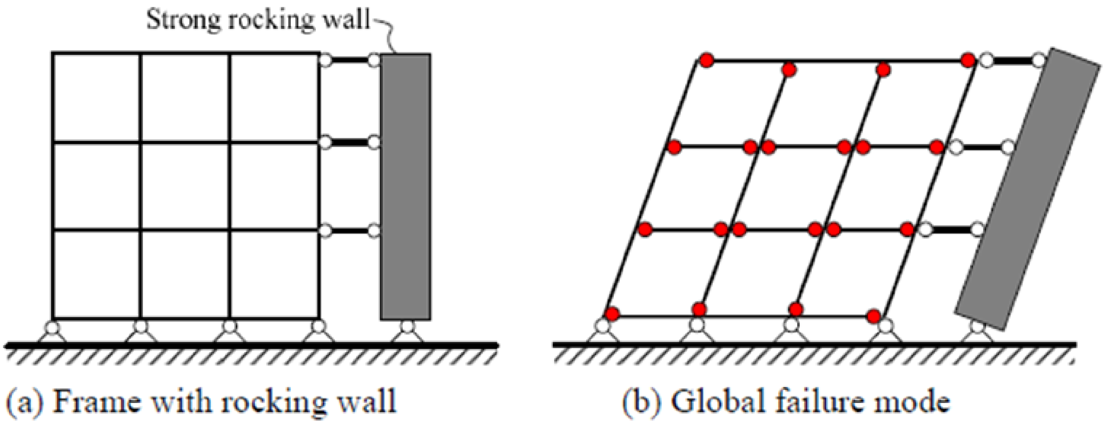

Figure 1.3: Moment resisting frame coupled to strong rocking walls [21]

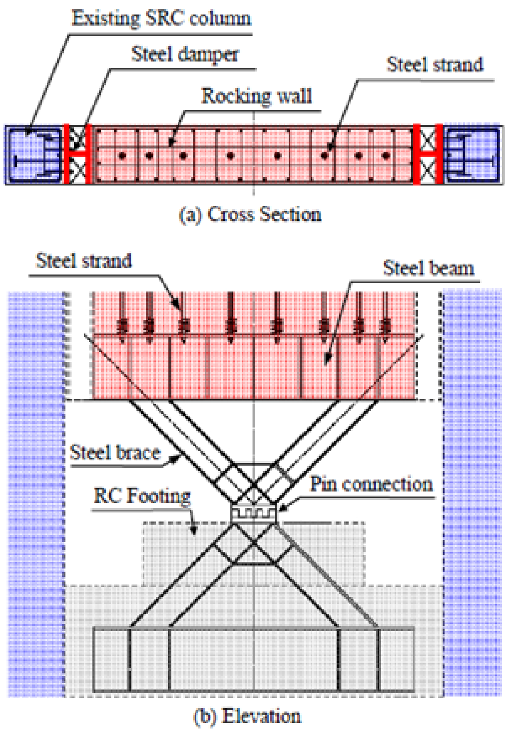

Figure 1.4: Detailing of rocking wall and steel damper [21]

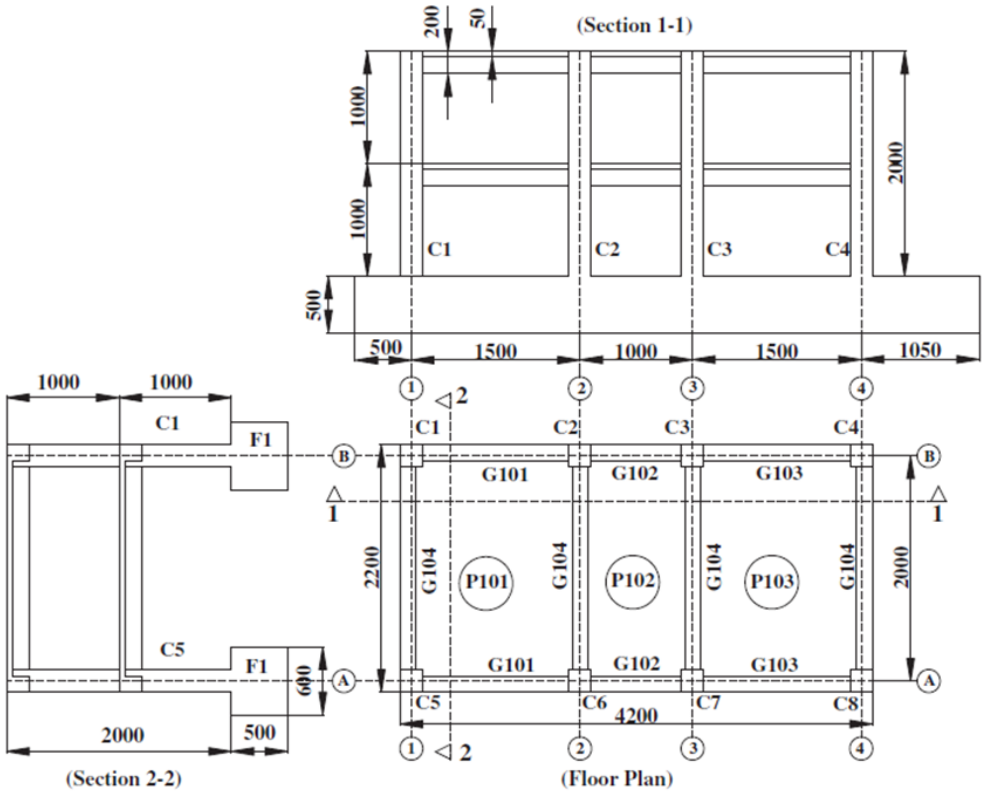

Figure 1.5: Layout of the retrofitted scaled model [10]

real life there is an important case of study that implemented such approaches, the Durango Building in Mexico City [9] the outcome suggested that no significant damage occurred in the earthquake of 1985.

To prove the advantage of this methodology an experimental test was contrasted to a FEM modeling [10]. A scaled 1/3, 3d model was tested under two conditions with and without external steel shear walls. Typical deficiencies presented in buildings designed for gravitational actions were taken into consideration. The type of bracings used was (V), the building is a single bay building in Y direction and three bay framed in X direction. Column dimensions are 200mmx200mm with bars of d=6mm (S220) in longitudinal direction. The ending regions were poorly confined with 90° stirrups, the concrete used correspond to a 30 MPa one. On the other hand, an external (SSW) steel shear wall was made with a rectangular cross section of (50x50x5). The SSW were placed only in the spam between edges (2) and (3) and they were anchored using epoxy anchors and stiffened plates.

Chapter 2

EVALUATION OF THE CASE STUDY “FOGGIA AIRPORT GINO LISA

The Foggia airport is a structure destinated to operate commercial flights in the northern part of the region of Puglia. The aim of this study is to provide technical proofs of the current structural vulnerability of the building under horizontal actions. Local authorities demanded such evaluation to prevent structural damages and therefore guaranteeing the operability of the building with the safest conditions for the users. For these purposes it was realized a survey that collect the technical as built information to determine the structural and seismic parameters that lead to a safety assessment of the existing structure.

In the present chapter we are specifically describing the actual structure, including on site parameters that affect the evaluation, processing the information collected in the survey, modeling a tridimensional FEM model of the actual building, performing the realization theory to interpret the outcome, and finally obtaining the final response of the building.

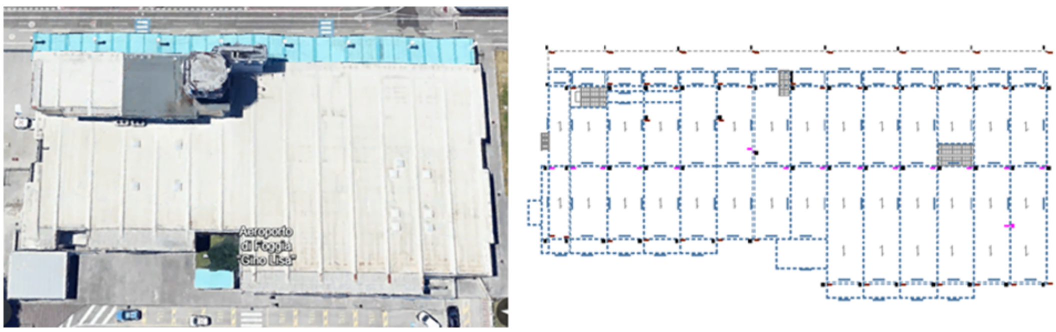

Figure 2.1: Current arrangement (left) and top view of the raised floor (right). Left picture taken from google images

2.1 Description of the structure

The structure evaluated in this chapter correspond to a commercial flight civil airport “Foggia Airport Gino Lisa” located at Viale degli aviator, 1 at the southern side of Foggia. The use of the airport for civil purposes started in 1968 and since then the airport has been operated intermittently maintaining the purpose to operate commercial flights. Due to the increase of activities in this airport the attention of local authorities demanded an evaluation to assess the current structural performance of the building.

Now days the structure also helds a tower of operations that is meant to be demolished due to a construction of a new one independent of the existing building. Therefore, to give an accurate response of the structure, it will be excluded from the analysis of this document.

The airport presents a structural system of moment resistant steel frames without lateral bracing. The slab of the raising floor is composed by a thin steel deck supported by IPE cross section beams mainly by IPE 330 and IPE 300. The other storeys present Gerber truss beams of different arrangement, they were elaborated by double angles and IPE sections. Either both areas of the storey, the roof and executives’ offices held a slab composed by a thin steel deck.

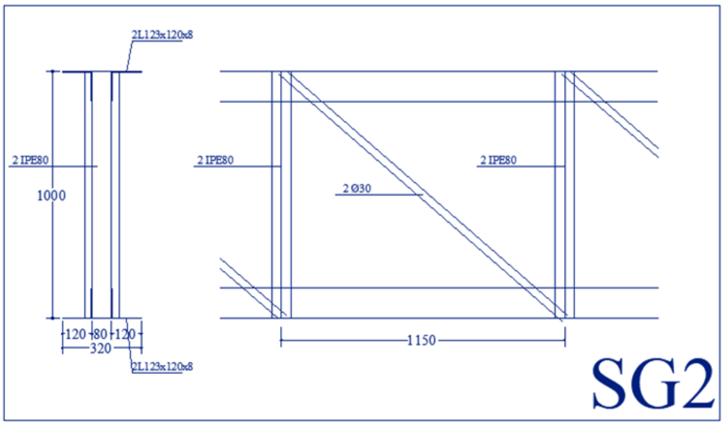

Figure 2.2: Representative section of main truss beam

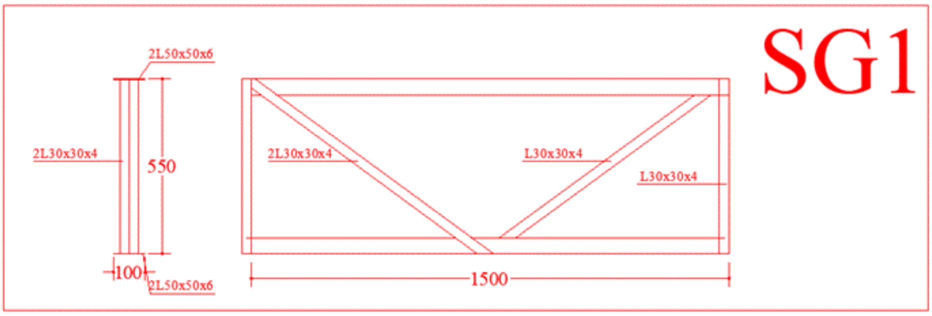

Figure 2.3: Representative section of secondary main beam

The topology of the building consists in a 3-storey building. From which starts:

- Zero Level: ground level (0m),
- First Storey: raised floor at +(1.4 m)
- Second Storey: at +(6.15) m from which the biggest area corresponds to the roof and the other part for internal operation offices.
- Third storey: It is the roof of the existing offices. + (14.25m)

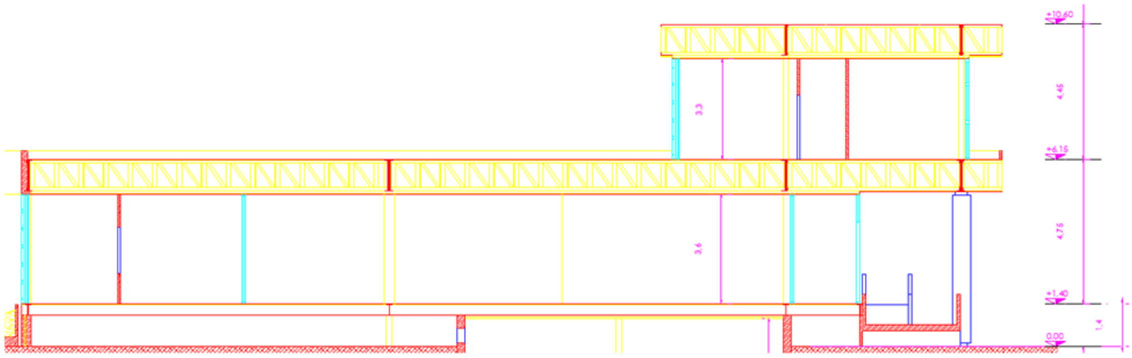

Figure 2.4: Elevation view of the building

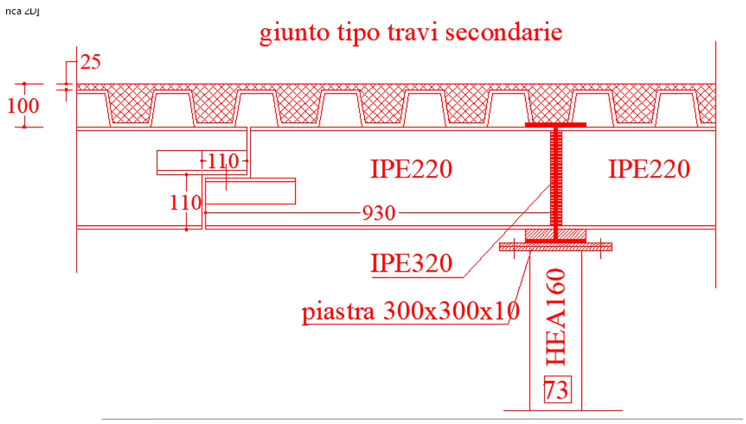

Figure 2.5: Detail of the steel deck at raising floor

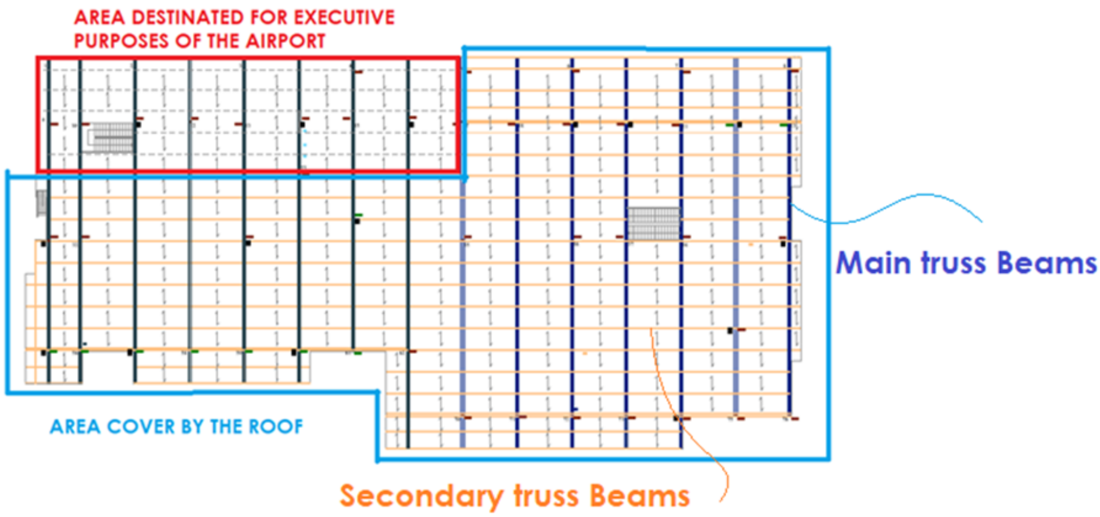

Figure 2.6: Layout of the second floor +6.15m

A good estimate of the area that covers the airport is 2960 m^2 from which 320 m^2 is for executives' purposes at the level +6.15m.

Concerning to the columns that are part of the seismic resistant system they are composed by cross sections of HEA 160 and HEA 180. Connections between main trusses beams and columns are considered rigid while connections between secondary beams and main beams are fully hinged connections. Photographic evidence shows reinforced plates at the ends of the main trusses to guarantee the bearing capacity of the elements.

2.1.1 Site characteristic of the project

After a detailed understanding of the case study's typology, we need to establish the site parameters related to seismic evaluation, wind actions, and external loads like snow. It's imperative to carry out this assessment to determine the overarching design conditions. In the context of seismic evaluation, everything is regulated by means of a probabilistic analysis due to the uncertainties associated with earthquake magnitude and frequency types. Pseudo acceleration spectra normalize a response based on ground acceleration records from a specific region. Each hazard level is assessed considering the probability of exceeding a seismic event within a defined time frame. Consequently, structures must be designed to withstand damage levels equivalent to the anticipated occurrence of strong earthquakes. On a different note, the determination of gravitational loads involves an estimative evaluation of the loads influencing or currently affecting a structure, with uncertainties or assumptions tied to their precise locations.

Parameters for Elastic spectrum	
Region	Puglia
Province	Foggia
Town	Foggia
Function critic damping Ratio	5%
Site longitude	15.55
Site Latitude	41.462
Limit state	SLU
Usage Class	III
Nominal Life (years)	50
Reference construction lifespan Vr (years)	75
Return period for SLV	712
Peak ground acceleration ag/g	0.1572
Magnification factor, F0	2.6
Reference period Tc*	0.4396
Spectrum type	SLV
Soil type	D
Topography	T1
Cc	1.88
Ss	1.794
St	1
Damping Ratio	2%
h/H ratio	1
Spectrum period Tb	0.2763
Spectrum period Tc	0.8288
Spectrum period Td	2.2288

Table 2.1: Parameters of Elastic spectrum

For this analysis to derive the spectrum the NTC says that the minimum value for considering the behavior factor is 1.5. This state could be very optimistic due to the absence of elements that provide ductility, the mechanism of failure of the structure and the flexibility that could experience. At this point there are several conditions that suggest brittle failure in the structure such as short columns effects on the raising floor level and the absence of bracings. Anyways this aspect is considered just for the linear dynamic analysis. The spectrum of reference will be the elastic spectrum.

The assessment of the structure is ranked in the life safety condition limit state SLV. The strategic purposes and the historical context of the airport demonstrate that is not totally fundamental. Therefore, the nominal life period was stablishing as 50 years but the usage class is ranked as level III. According to NTC 2018 the reference construction lifespan is:

$Vr = V_N C_U$

As it is exposed in the summary above

$Vr = 50 * 1.5 = 75$ years

And the probability of exceedance for the SLV is 10%. Calculating the return period, we obtain a result of 712 years.

$T_c = 0.4396s$

$S = S_s \cdot S_T \qquad (NTC - 08Eq \cdot 3.2.5)$

$\eta = \sqrt{10/(5+\xi)} \geq 0.55; \eta = \frac{1}{q} \qquad (NTCE \cdot q \cdot 3.26; 3.2.3.5)$

$T_b = \frac{T_c}{3} \qquad (NTC - 07Eq \cdot 3.2.8)$

$T_b = C_c \cdot T^*{}_c \qquad (NTC - 07Eq \cdot 3.2.7)$

$T_b = 4.0\frac{a_g}{g} + 1.6 \qquad (NTC - 07Eq \cdot 3.2.9)$

First stretch: $\quad 0 \leq T \leq T_B$

$$S_e\left(T\right) = a_g \bullet \; S \bullet \eta \bullet \; F_0 \left[\frac{T}{T_B} + \frac{1}{\eta \bullet F} + \left(1 - \frac{T}{T_B}\right)\right]$$

Second stretch: $\quad T_B \leq T \leq T_c$

$$S_e\left(T\right) = a_g \bullet \; S \bullet \eta \bullet \; F_0$$

Third stretch: $\quad T_C \leq T \leq T_D$

$$S_e\left(T\right) = a_g \bullet \; S \bullet \eta \bullet \; F_0 \bullet \left(\frac{T_C}{T}\right)$$

Fourth stretch: $\quad T_D \leq TS_e$

$$T_D \leq \; TS_e\,(T) = a_g \bullet \;\; S \bullet \eta \bullet \;\; F_0 \bullet \left(\frac{T_C T D}{T^2}\right)$$

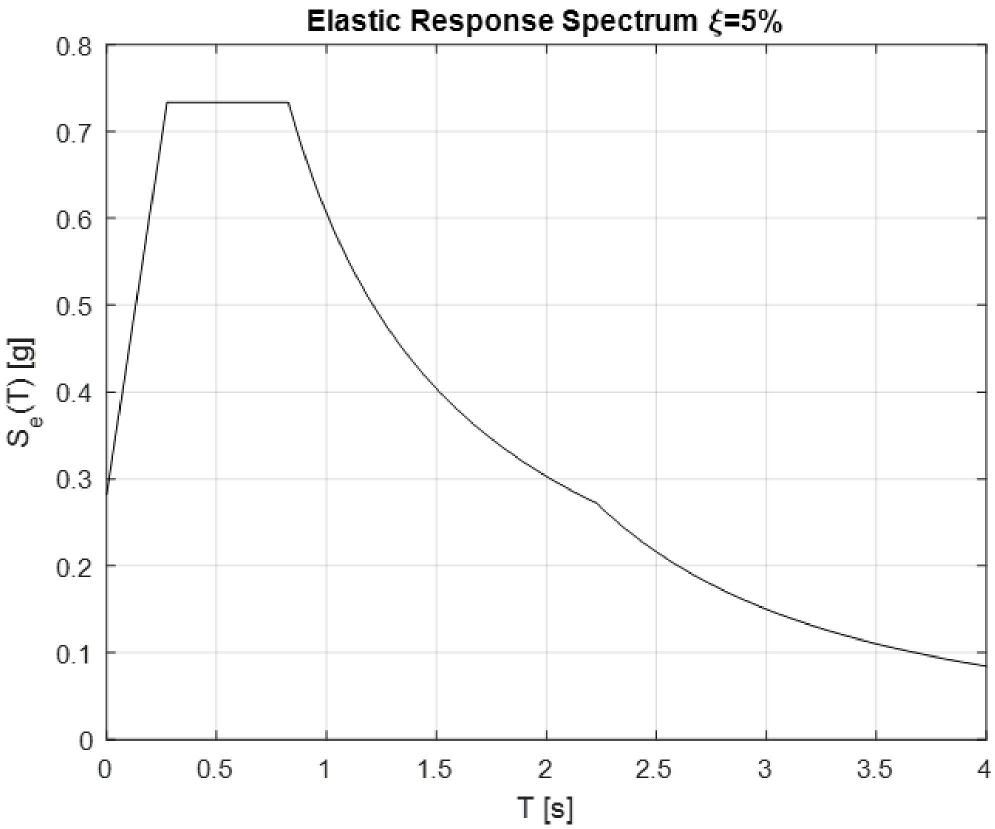

Figure 2.7: Elastic spectrum Foggia Airport

2.1.2 Historical – critical analysis

The research of the historical materials that support the calculation design of the structure were performed by a company of the region. The original drawings of the structure were given by the administration of the airport in DWG format, this company double checked the information provided to extend the level of detail that such drawings have.

The company detected several discrepancies between the given information and the original drawings. Therefore, to evaluate the real situation of the building the final as built drawings are the ones that command the modelling phase. The inspection process was exhaustive and covered the critical areas where structural elements are located. The documentation and technical report were presented in 02/27/2021 and from this document we proceed with the primary source information concerned to the historical critical analysis.

In spite the document affirm that exist an extended survey we could notice that there are areas in which the physical inspection was impossible to perform, including foundation. Therefore, the level of knowledge assumed by the company in charge of this phase is L.C2

The document presents the following information:

• Architectural survey: Elevation view, top view of First, Second and Third storey

• Top view of Structural drawings: First, second and third floor

• Structural members detailings: Truss beams arrangement, truss beams detailing, columns detailing and slab detailing.

2.1.3 Geometric and physical survey

Due to the structural system, the success in this phase depends on a very well level of detail of the structural elements and laboratory test for representative samples of critical members. In addition, photographic inspection and measurement of the elements and spans are necessary to enhance the expected level of knowledge. Therefore, the cross matching of the photographic survey and the layout was fundamental to determine the area covered by the extended survey.

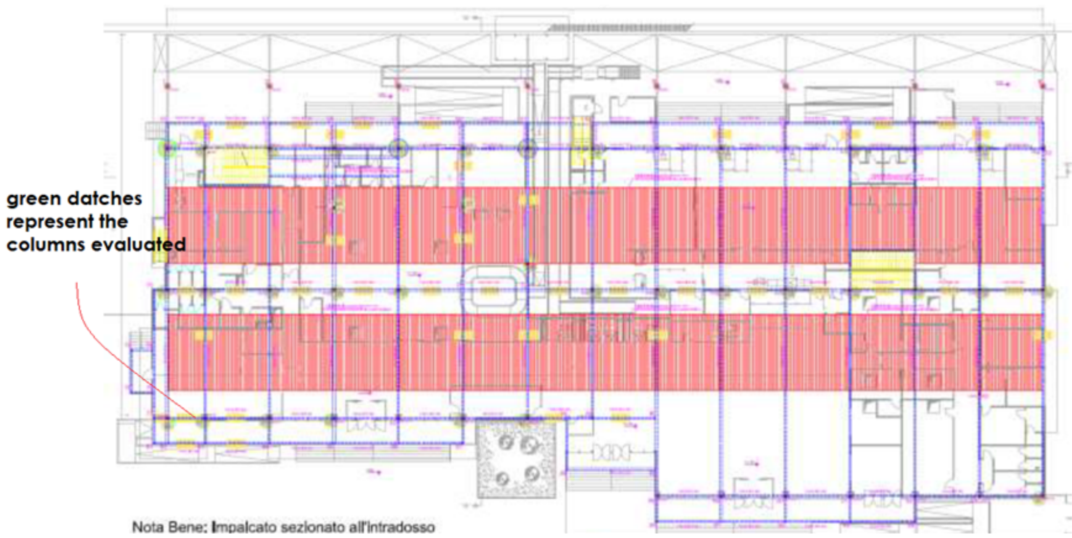

Figure 2.8: Raising floor and members evaluated by visual and physical measures

Figure 2.9: Discrepancies between record layouts and inspection survey. Column 51 and 48 in the records

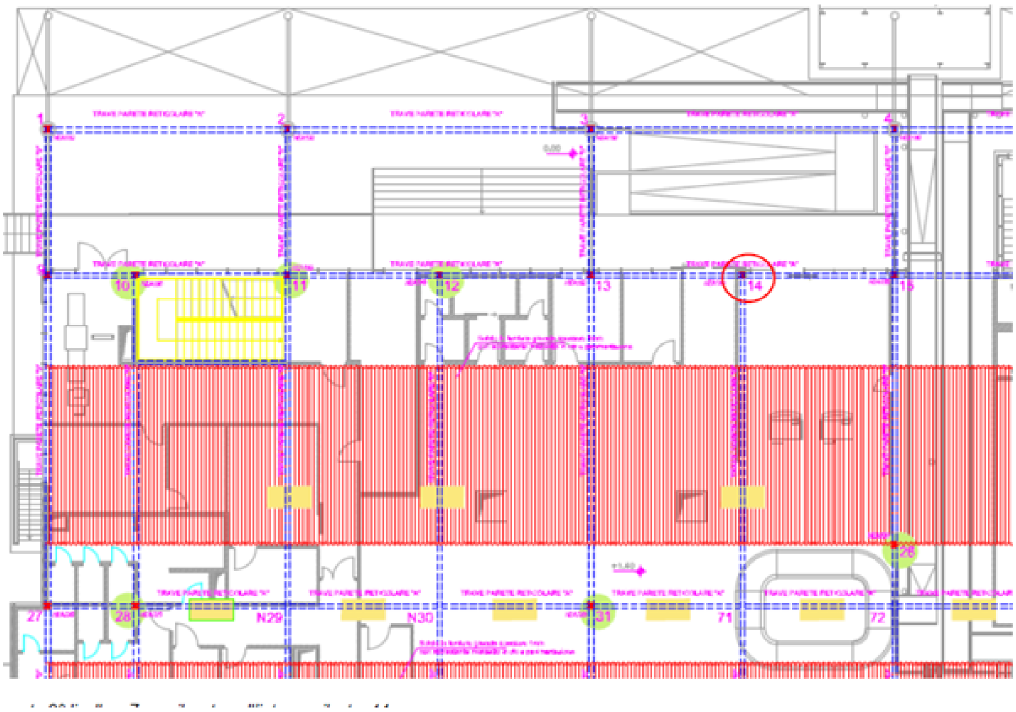

Figure 2.10: Discrepancies in the zone relevant to column 14

Figure 2.11: shape of a column HEA160 drawn as HEA 180

Figure 2.12: Hinged connection at the level of raising floor

Figure 2.13: Detail of a rigid connection at the truss main beams

Regarding the material properties an exhaustive survey was performed in the area demanded to achieve the extended survey category. The results presented a behaviour better of the technical drawing presented in average the yielding resistant of the steel members are in the order of 290 MPa. It means that the most representative type of steel in the European standards is S275. Even though, for the number of samples taken and tested and for the level of detail obtain in the technical drawings we could assume a Level of knowledge near to LC3 but following the recommendation of the technical reports we maintain the level of knowledge of LC2.

In fact according to the table C8.5.IV there are 3 criteria for steel structures to evaluate the level of knowledge (LC).

- The project possesses the original drawings and an extensive as built record drawings.
- Extensive survey of the elements and connections
- Exhaustive verification of the element's mechanical properties.

The NTC-2018 suggest a minimum of 3 samples per storey to be classified as extensive survey. For both Main elements and connections. Therefore, the quality of the survey could lead to Level of knowledge of LC3. The critical aspect that stopped the survey to suggest such level of knowledge is due to missing document related to the foundation drawings but mostly because the irregular typology of connections. Connections that are not technically classified at the level of the raising floor and roof level.

Tabella C8.5.IV – *Livelli di conoscenza in funzione dell'informazione disponibile e conseguenti metodi di analisi ammessi e valori dei fattori di confidenza, per edifici in calcestruzzo armato o in acciaio*

Livello di conoscenza	Geometrie (carpenterie)	Dettagli strutturali	Proprietà dei materiali	Metodi di analisi	FC (*)
LC1	Da disegni di carpenteria originali con rilievo visivo a campione; in alternativa rilievo completo ex-novo	Progetto simulato in accordo alle norme dell'epoca e ***indagini limitate*** in situ	Valori usuali per la pratica costruttiva dell'epoca e ***prove limitate*** in situ	Analisi lineare statica o dinamica	1,35
LC2		Elaborati progettuali incompleti con ***indagini limitate*** in situ; in alternativa ***indagini estese*** in situ	Dalle specifiche originali di progetto o dai certificati di prova originali, con ***prove limitate*** in situ; in alternativa da ***prove estese*** in situ	Tutti	1,20
LC3		Elaborati progettuali completi con ***indagini limitate*** in situ; in alternativa ***indagini esaustive*** in situ	Dai certificati di prova originali o dalle specifiche originali di progetto, con ***prove estese*** in situ; in alternativa da ***prove esaustive*** in situ	Tutti	1,00

Figure 2.14: Level of knowledge function of the survey quality[17]

To justify the quality of the survey the table C.8.5VI define the aspects that help us to distinguish between an exhaustive and extensive survey. They differ a lot with the standards that govern reinforced concrete structures.

Tabella C8.5.VI – *Definizione orientativa dei livelli di rilievo e prova per edifici di acciaio*

Livello di Indagini e Prove	Rilievo (dei collegamenti)[(a)]	Prove (sui materiali) [(b)(c)(d)]
	Per ogni elemento "primario" (trave, pilastro...)	
limitato	Le caratteristiche dei collegamenti sono verificate per almeno il 15% degli elementi	1 provino di acciaio per piano dell'edificio, 1 campione di bullone o chiodo per piano dell'edificio
esteso	Le caratteristiche dei collegamenti sono verificate per almeno il 35% degli elementi	2 provini di acciaio per piano dell'edificio, 2 campioni di bullone o chiodo per piano dell'edificio
esaustivo	Le caratteristiche dei collegamenti sono verificate per almeno il 50% degli elementi	3 provini di acciaio per piano dell'edificio, 3 campioni di bullone o chiodo per piano dell'edificio

Figure 2.15: quality of the survey [17]

Sigla	elemento	Elemento analizzato	Piano di appartenenza	Tensione di snervamento fy (N/mmq)	Tensione di rottura ft (N/mmq)
PB1	Pilastro 73 (ex51)	HEA 160	1^tesa	**265.0**	**381.8**
PB2	Pilastro 66 (ex60)	HEB 120	1^tesa	**320.3**	**425.0**
PB3	Pilastro 54 (ex40)	HEA 180	1^tesa	**303.0**	**418.0**
PB4	Trave 50-66 (ex60-61)	IPE 320	1°impalcato	**291.0**	**425.0**
PB5	Trave 51-67 (ex61-62)	IPE 320	1°mpalcato	**278.9**	**368.9**
PB6	Trave 59-m (ex45-m)	IPE 300	1° mpalcato	**310.0**	**394.0**
PB7	Trave trasversale sg1	L 50*50*4	2° mpalcato	**288.3**	**401.0**
PB8	Trave 28-42	L 75*75*5	2° mpalcato	**306.0**	**641.3**

Figure 2.16: results taken from the report presented to the airport

2.1.4 Materials and properties assumption

The obtention of the level of knowledge in the step before guided us to proceed with the final characteristics and properties that will be set in the further analysis. Therefore, and having considered the level of knowledge (LC2) we could set final mechanical characteristics of the structural elements. For a level of knowledge LC, the confidence factor FC must be 1.2.

$\mathrm{F}_{ym} = 275MPa$
$F_y = \frac{F_{ym}}{\gamma_{M1}} = \frac{275MPa}{1} = 275MPa according \quad to \quad E.C.3$
$F_{yd} = \frac{F_y}{FC} = \frac{275MPa}{1.2} = 229.16MPa(2.1)$

Concerning to the connections. The principal ones between the structural resistant system are welded. Welded plates were tested, and they shown a response of a steel S355.

2.1.5 Load evaluation

The load evaluation implemented in this case study considered the information of the technical survey and the parameters of the site. The evaluation was conducted in the most accurate way in correspondence with the current characteristics. It was split by stories and type of use. G2 was selected from the NTC-2018 in the chapter related to gravitational loads. There was no drilling core that could give us precision related to the materials that compose the slab. Therefore we took the recommendation of the italian code.

Table 2.2: Gravitational load evaluation. Raising Floor

FIRST FLOOR- RAISING FLOOR	
LOADS	kN/m2
G1	
Concrete Slab	1.466
G2	
Permanent non-structural loads	2
Q	
Airport traffic	5

Table 2.3: Gravitational load evaluation. Administrative offices

SECOND FLOOR - ADMINISTRATIVE OFFICES		
LOADS	kN/m2	kN/m2
G1		
Slab in concrete	1.25	1.466
corrugated deck	0.216	
G2		
Permanent non-structural loads		2
Q		
Airport offices non opened to the public		3

Table 2.4: Gravitational load evaluation. Roof top area

THIRD FLOOR - ROOF TOP AREA		
LOADS	kN/m2	kN/m2
G2		
Roof of concrete	1.25	1.466
corrugated deck	0.216	
Q		
Roof maintenance		3

Table 2.5: Wind analysis at Foggia airport

Wind Load Analysis		
Parameters for qb		
Air Density	1.25	kg/m3
ks	0.37	
a0	500	
vb,0	27	m
ca	1	m/s
vb	27	
ct	1	
vr	27	

Table 2.6: Wind pressure value

Wind Load Analysis		
Parameters for Ce		
kr	0.19	
z0	0.05	m
zmin	4	m
z	10.6	m
ce	791.659	
Cpe	0.4	
Cpe	0.8	
Cd	1	
Wind Pressure		
qb	0.456	kN/m2
Ce	2.390	
Cp	0.4	
Cd	1	
Cpe(0.4)	0.174	kN/m2
Cpe(0.8)	0.348	kN/m2

For evaluating the structure in its ultimate limit state (SLU) we took used the equation [2.5.1] of NTC 2018.

$\gamma_{G1}G_1 + \gamma_{G2}G_2 + \gamma_P P + \gamma_{Q1}Q_{k1} + \gamma_{Q2}\psi_{02}Q_{k2} + \gamma_{Q3}\psi_{03}Q_{k3} + \ldots$

For the seismic combination we use the equation [2.5.5]

$E + G_1 + G_2 + P + \psi_{21}Q_{k1} + \psi_{22}Q_{k2} \ldots$

2.1.6 Structural System

The system is considered a steel frame structure resistant to moment without lateral bracings [18]. This system is typified to experience high possible lateral displacement. The structure of the airport of Foggia is a flexible structure that could be described as 3-storey building with different mass arrangement per floors.

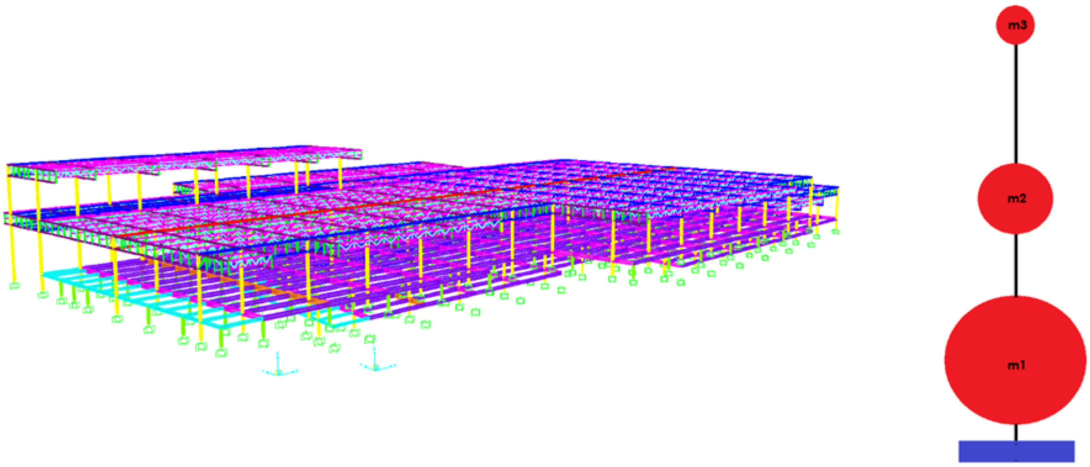

Figure 2.17: Structural setting of the case of study and distribution of masses representation

The mass arrangement of the building is heterogenic, the storeys have different magnitudes of masses in each level. And they could be represented as it is in the picture exposed above. The raising floor is heavily demanded in non-permanent loads and self weight in comparison to the rest of the structure.

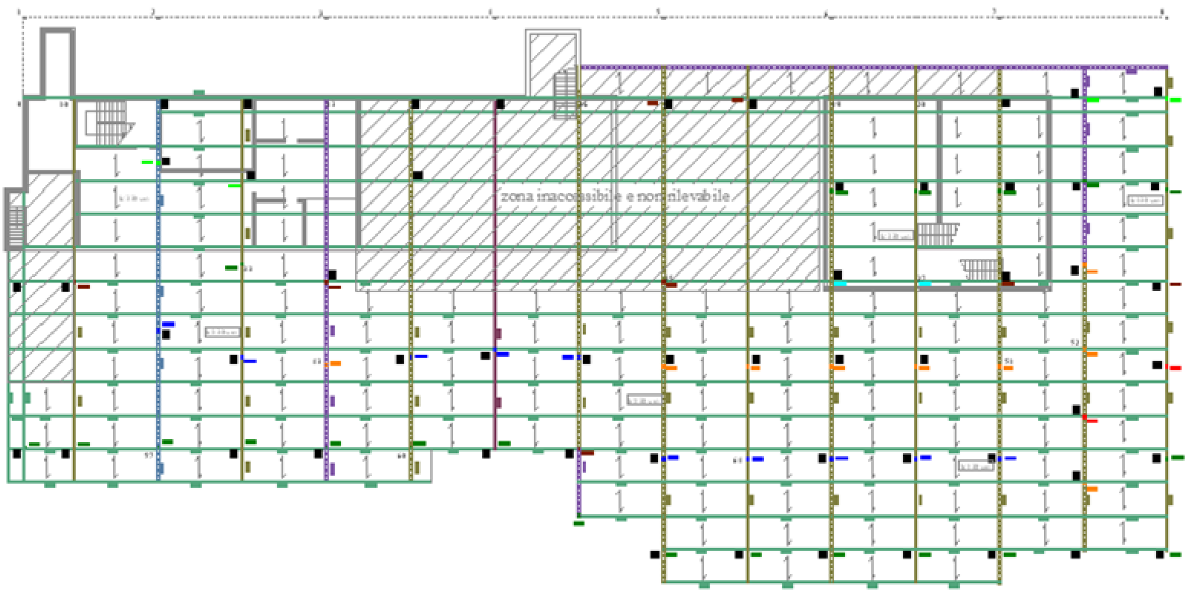

Figure 2.18: Raising Floor (+1.4m)

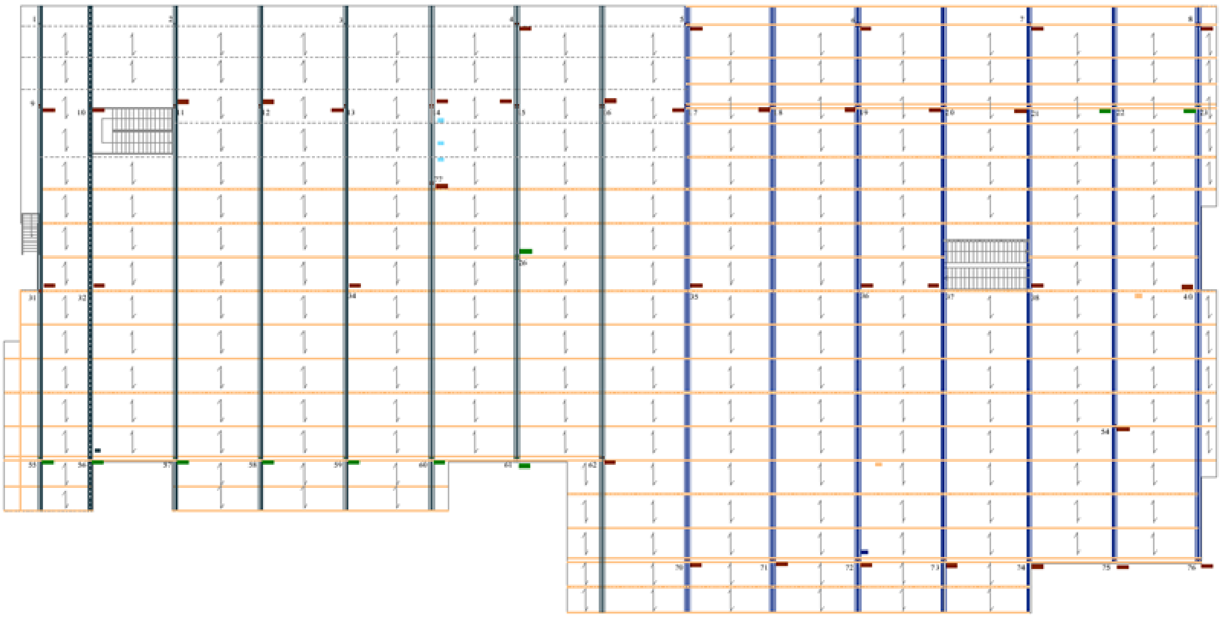

Figure 2.19: Second Storey (+6.15m)

The second storey of the building corresponds to an area partially covered by a roof made of a steel deck of 10cm poured with concrete and an area devoted to executive purposes.

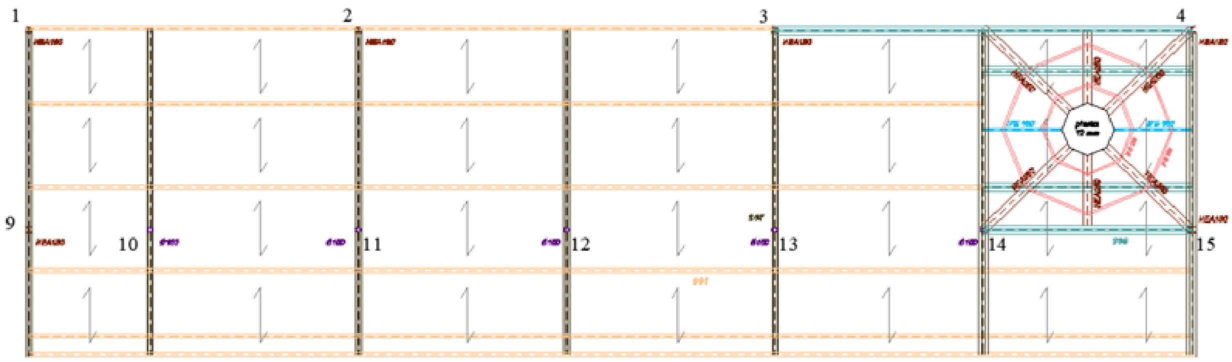

Figure 2.20: Third storey "Roof top" (+10.60m)

The third storey is composed by the roof of the executive offices. The imminent demolition of the tower is being considered in further investigation

One of the modeling hypotheses for our structure suggests not taking into account the control tower because it does not meet the life safety verification and is subject to constant vibrations. Historically, there was a regulation by the aviation authority that required the control tower to be located within the airport building. Not only does the tower fail to meet the life safety limit state, but it also has issues with the ultimate limit states of strength and comfort. The ENAC (Italian Civil Aviation Authority) recently issued a statement allowing airports to construct control towers outside the main airport building. This solution is the most advisable based on a recent study conducted. The structure has 15 setting of frames in Y direction and 17 setting of frames in X direction.

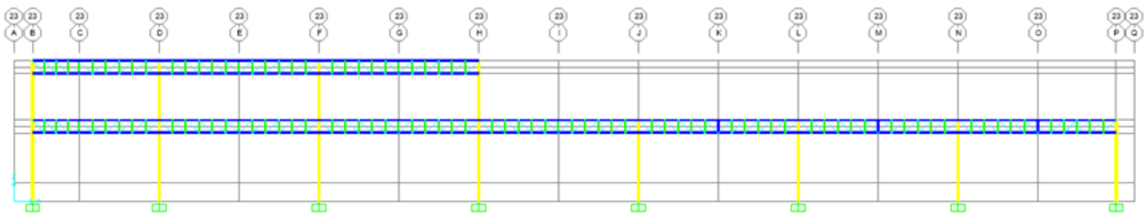

Figure 2.21: Representative Frame placed in X direction

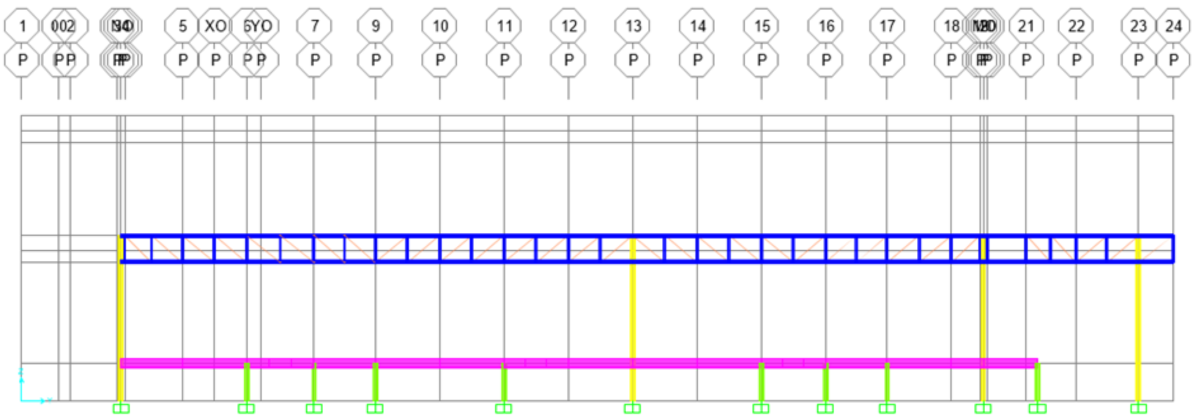

Figure 2.22: Representative frame in Y direction

2.2 Modelling strategies and assumptions

The structural FEM modelling of the existent structure should represent accurately the global characteristics of the structural system, the correct type of materials and the constitutive law of their behavior. It must present accurately the kinematic principles, internal restraints, and external boundary conditions. In addition, the precision of the response depends on the load assessment and the imposition of the loads. The current case of study presents a typology that does not address the behaviour of traditional structures. Therefore, we are obliged to describe the assumptions that justify our modelling.

2.2.1 Modelling of the columns

Starting from the ground, we could see from the survey that all the elements related to the foundation have a thick concrete cover that restraints the rotation. This might does not have the prequalified stiffeners of now days connections, but the thick cover of concrete adjusts the behaviour as a rigid one. Other aspects were evaluated in the survey and there is no evidence of corrosion in the elements.

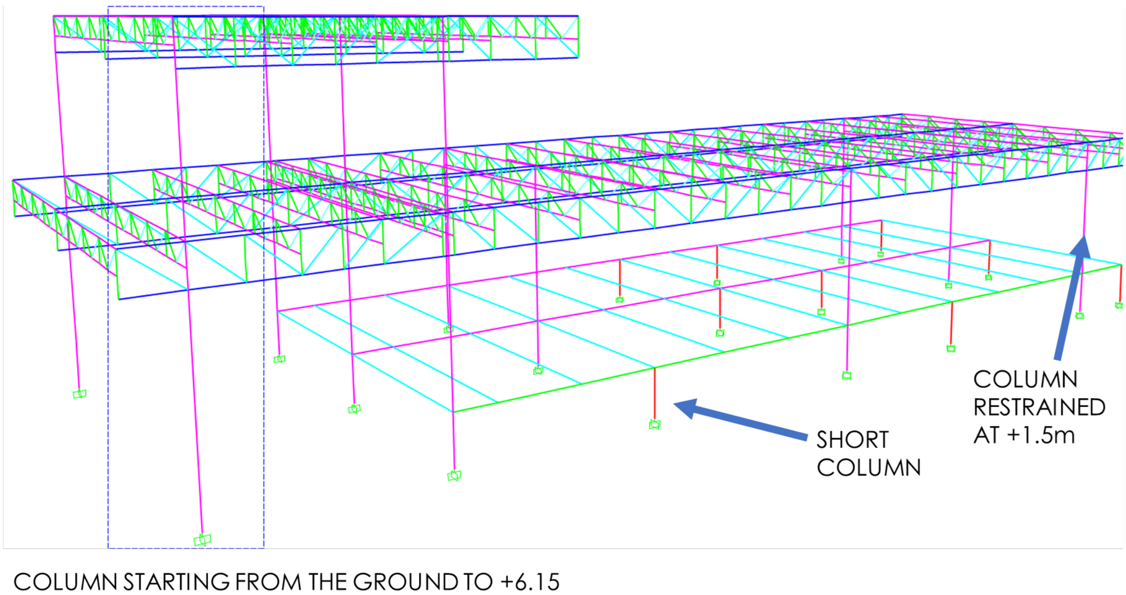

Figure 2.23: Columns scheme, section of the structure. Generic Frame (P)

The exhaustive survey performed in the current structures provided the dimensions and mechanical properties of the elements that are part of the seismic resistant structure. It was noticed that the structure is composed mainly by HEA 160 and HEA180 cross section columns.

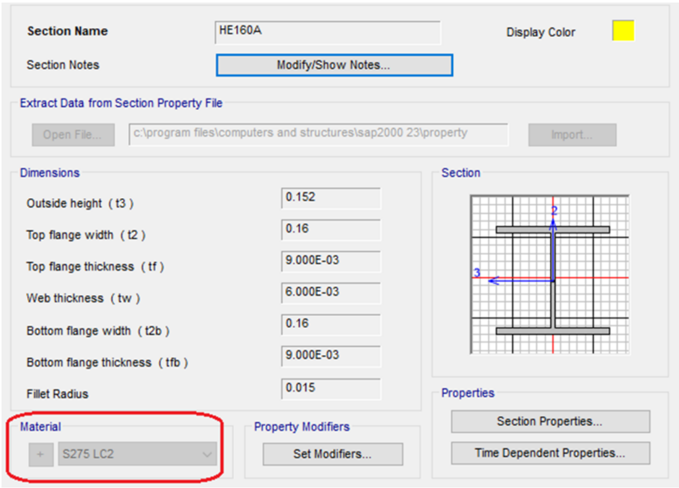

Figure 2.24: HEA 160 by default input

SAP2000 allows the user to import the default properties that comes from the Eurocode definition. All the geometric parameters are already defined according to the Europeans standards. The mechanical properties of the steel can be personalized by the user, SAP2000 also provides a library of materials. The confidence factor obtained from the specific level of knowledge must be considered by dividing the F_{yd} by default values times the confidence factor.

2.2.2 Truss Beams

One of the most critical points was the modelling of the truss beams. They are elements designed to work just in axial forces. In this case we could see that they not only work under axial loads. The connection to the columns is through stiff plates that helps to withstand bending moment in the connection, therefore we assumed that in the first elements of the truss beam they can withstand bending moment. The upper and lower rope are defined like (continuous elements) and the bracings are defined as (hinged elements). In Theory the upper rope and the lower rope must be also released from bending moment, but the manual of sap2000 warns you to do it because it creates instability in the model. The truss system is guaranteed just by releasing the internal elements from bending moment.

Figure 2.25: scheme of truss beams modelling

2.2.3 Raising floor Frame System

The raising floor is one of the most difficult parts of the building to model. The raising floor is built up as a deck composed by Gerber beams that aim to reduce the bending moment in the structural elements. Due to the configuration imposed by the original designer, it was noticed that potential high deflexions could appear. This design choice could be probably attributed to transportability issues of steel pieces during the construction stage for which steel beams were joined with bolded and welded connections in situ. Therefore, we could see that in some of the seated connections are presented modifications without any technicism. This kind of connections with weak welding supplementary plates was not taken into consideration for the modeling part. Due to the uncertainty of this behaviour, we modeled the deck by considering the Gerber connections in the scheme. Every frame has a different arrangement of seated connections, and they were assigned according to the last survey and the photographic support.

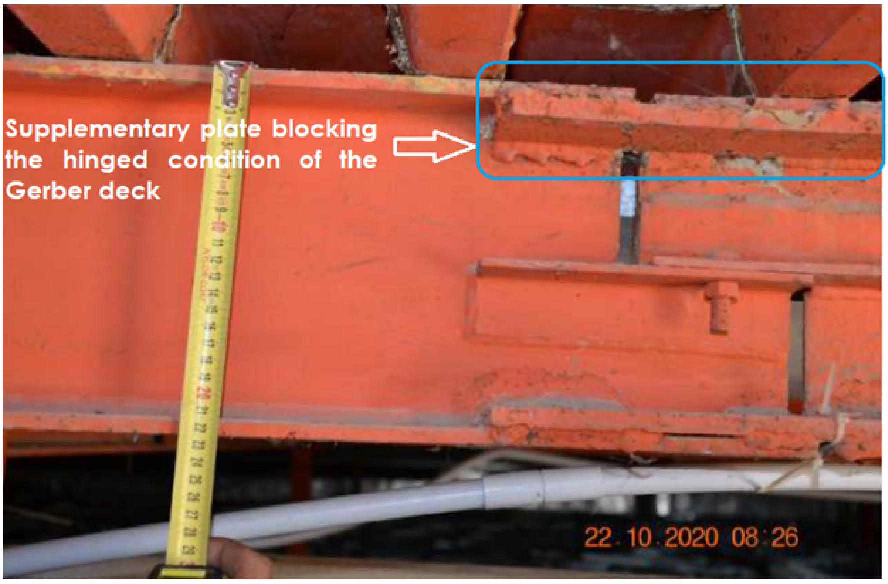

Figure 2.26: Modification of the Gerber scheme

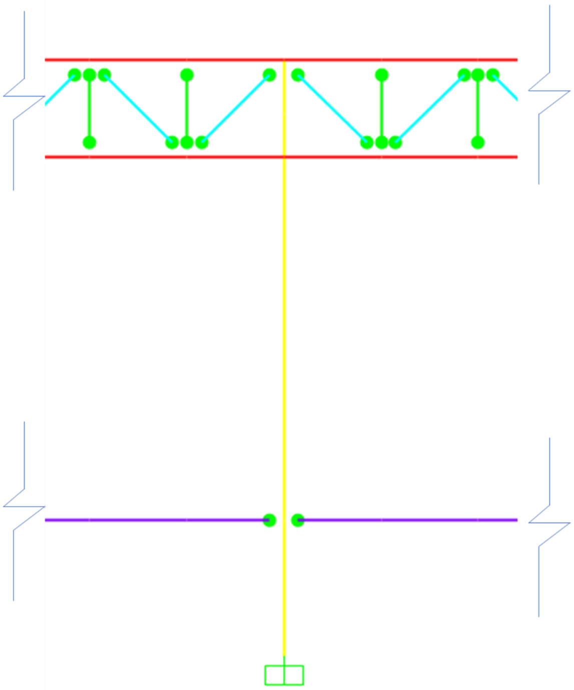

Figure 2.27: Representation of typical releases in the deck

2.2.4 Flexible behaviour of the storey levels Constrains at the storey levels

One of the differences between reinforced concrete structures and this typology of flexible steel structures is the global behaviour of the inter-story level. The assumption of diaphragmatic behavior in this system is a wrong approach and doesn't satisfy the minimum requirements of slab thickness equal to 12 cm provided by the NTC2018. More in detail, the story at the level +1.5 and +6.15, respectively, presents a clearly flexible behaviour due to the presence of a very slender slab realized by a corrugated sheet and a layer of concrete lower than 3cm. It means that we cannot assume a rigid body behaviour to simplify the eigenvalue analysis.

The software used to develop the model was SAP2000, it analyses the modal response of the structure based on the stiffness and the distribution of the masses. In This way the stiffness and mass matrices tend to be more complex. In consequence, we will experience more modes of vibrations to achieve a mass participation near to 85%. A considerable number of this modes of vibration don't show a global shape but show local response.

Another characteristic of the diaphragmatic behaviour is that the elements linked through a body constrain are immediately released of the axial problem. It means that the internal forces in the axial plane will be 0. This is a critical aspect because it is necessary to assess the internal axial forces in a truss beam. This aspect supports categorically the need of not using any body constrain.

2.2.5 Modelling of the static load patterns Loading imposition to the FEM model

The loading imposition to the FEM model structure was performed by adding load patterns directly to the elements that receive the solicitations from the slab. Due to missing information related to the connection between slab and beams, we cannot assume neither a diaphragmatic behavior nor composed action between slab and truss beams. In addition, for computing a static nonlinear analysis, shell elements reduce the efficiency of the software processing.

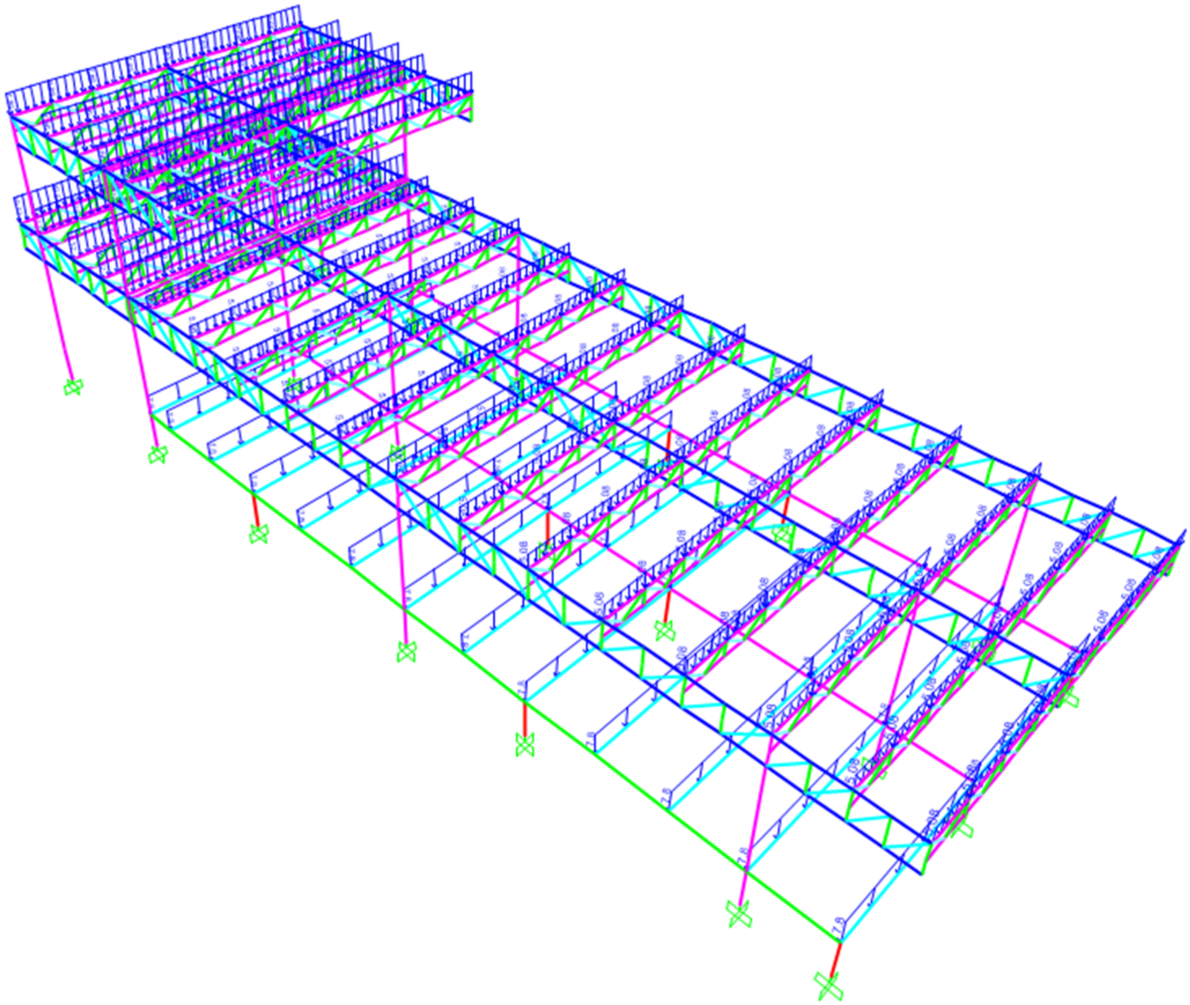

Figure 2.28: Static Load pattern configuration

The connection between area elements and frame elements presents some issues in mesh refinement. Mainly, because the length of the beams is not discretized in small elements that sometimes are not symmetric edge by edge. This random configuration present problem of connection between the nodes of area and frame elements. The refinement of the area element could be a solution but sometimes it presents a glitch that interferes with the stability of the model. In other words, the meshing of the area element doesn't coincide with the meshing of the frame element.

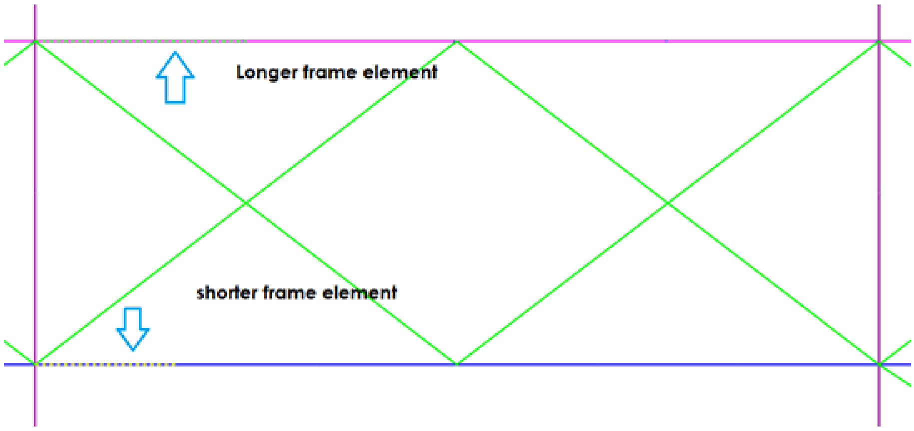

Figure 2.29: Top view of a deck section

For that reason, in this model, we decided to apply the equivalent loads to the frames avoiding stability problems and aiming more efficiency in the computational effort. Main and secondary beams were identified according to the warping of the corrugated sheet which represents the slender ground deck of the structure.

2.2.6 Techniques to avoid false buckling warning in truss elements

Usually, the connection between area elements like shells and frame elements create a scenario in which lateral buckling analysis is not critical. In our model the fact that we don't use the area elements to replicate the slabs lead to unrealistic warnings regarding to the failure of the frame elements due to lateral buckling.

For this reason, the implemented solution is to create frame elements that reproduce the portion of the slab and connect them. To not overestimate the model, we need to not consider the mass associated to that element. This connection should be a pinned connection to avoid the transmission of bending moment.

Another advantage of using this approach is that we reduce the number of numerical modes representative of local vibration modes related to single elements (like primary and secondary beams lie on the ground floor). By linking the truss beams we can experience a mayor mass participation in the modes with global shape. This is fundamental to predict a reliable analysis.

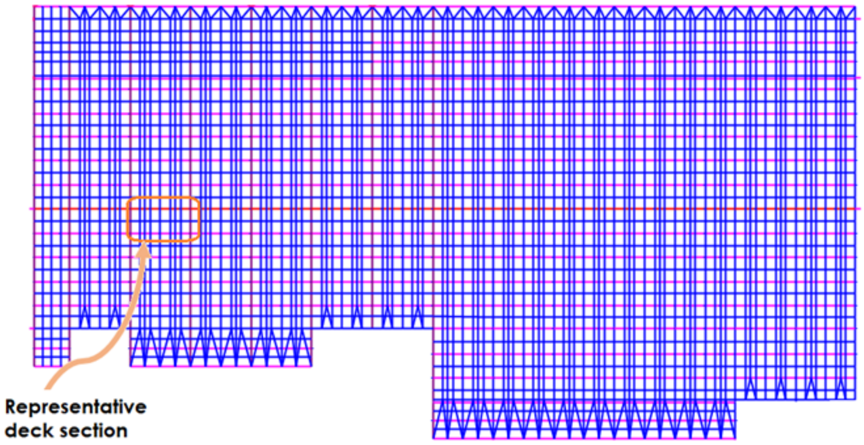

Figure 2.30: Top view of the storey +6.15m

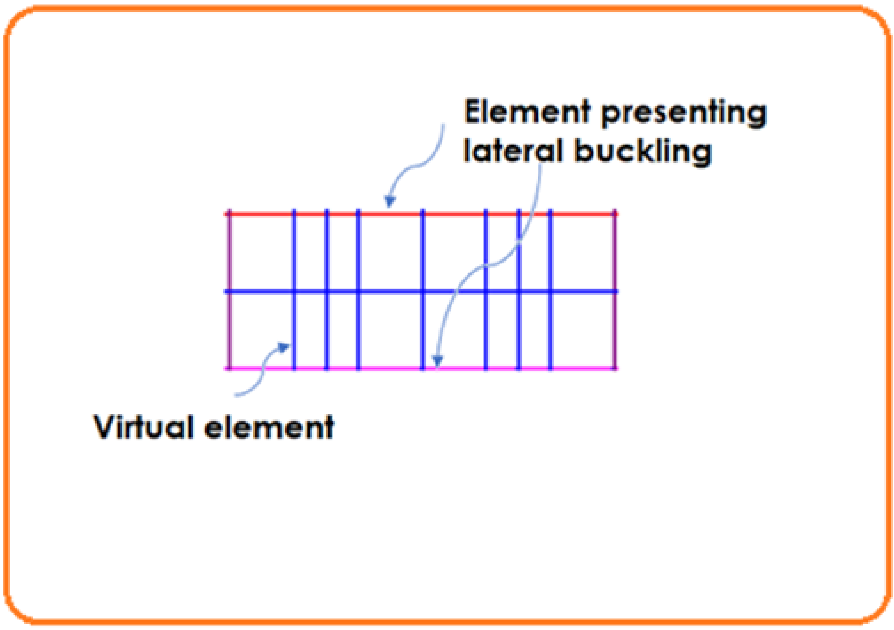

Figure 2.31: Representative Deck section

2.2.7 Plastic hinges

Equivalent force analysis and linear dynamic analysis the safety of the structure is guaranteed when the elements don´t reach the bearing capacity in its elastic field. Those procedures sometimes are very conservative, the ductility of the structure is never assessed through a mathematical computation but using a behavior factor that is considered to reduce the seismic demand in the response spectrum. Moreover, for this kind of structure, the equivalent force distribution is banned by the NTC2018 due to the lack of a unique fundamental mode of the structure.

Nonlinear analysis takes in consideration the plasticity of the elements, the redistribution of the action in the structure through the ongoing equilibrium scheme and global response. The formation of the plastic hinges under a monotonically increasing profile of forces changes the global equilibrium scheme, the plasticity of the structure is related to the number of plastic hinges that could be formed following the hierarchy of importance. It is expected to have plastic hinges in the ending-starting zone of the beams and lastly in the level of the column. In addition, the constitutive law that rules the behaviour of the plastic hinge should be coherent with the real response of the structure. For example, we cannot define the activation of a plastic hinge in steel structure with the constitutive law of a concrete material.

SAP 2000 has a predefined library of plastic hinges based on FEMA-356 regulations and ASCE 41-13 standards for the case of steel structures. Our analysis of nonlinearity will adopt the constitutive law proposed by ASCE 41-13 for steel members.

Hinge Length: Sap2000 defined hinges as discrete points, all deformation, either displacement or rotation occurs within that point. This mean that the user should assume the length for the hinge where the plastic strain and plastic curvature is presented. Neither FEMA-356 and ASCE 41-13 stablish a way to derive the length of the plastic hinge but usually this is assumed as the depth of the cross section. [4]

P**lastic deformation curve:**

The curve A-B-C-D-E reproduces the yield values and plastic deformation in a moment rotation curve. This state could be applied to any degree of freedom, the software allows you to use a symmetric curve or one that differs in the positive and negative direction.

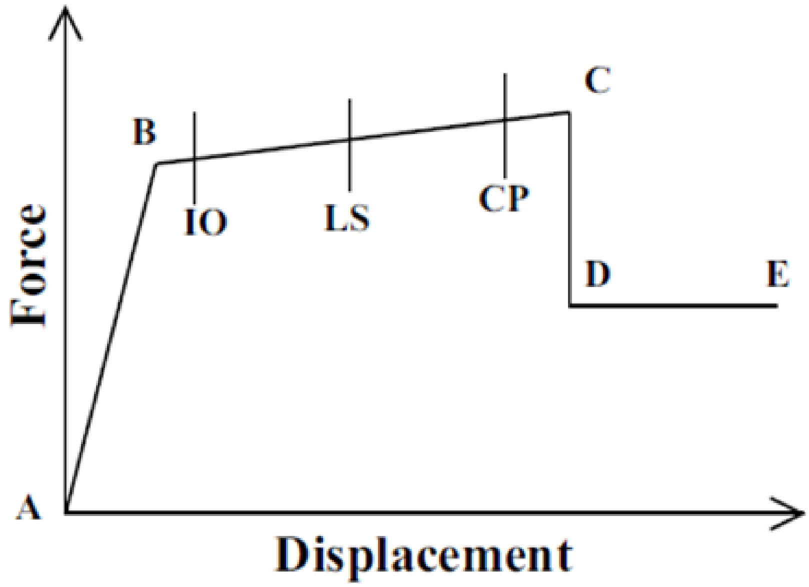

Figure 2.32: (Force or moment) Vs Displacement curve [4]

Point A represents the origin, point B represents the yielding point. From A to B there is no plastic deformation in the element. Point C represent the ultimate capacity that could achieve the element for the pushover analysis. Point D represent a residual strength. Point E represent a total failure of the element, from point E the hinge will drop the load down.

There are additional deformation measures between point B and C. IO represents (immediate occupancy), LS (life safety), CP (collapse prevention). This information is only useful for a performance-based design.

- **Beams**

Before assigning a specific property to a Frame element. We need to understand how the structure behave. The beams of this structure are composed by frame elements with double T section and truss beams.

Raising floor: Our case of study shows that beams at the level of the raising floor already possess a mechanism of releasing bending moment. Therefore, the creation of a specific property to evaluate the formation of a plastic hinge is useless. All the connections at the level of raising floor are free to rotate.

First floor and Roof: As we described before, the main truss beams were considered with a rigid connection to the columns. This assumption enforces us to put in the model properties of hinges subjected to bending moments. The properties were assumed by using FEAM 5-6 table. They were automatically generated by the software, and the generation of the moment rotation diagram was compared to one performed by hand for one element to check the accuracy in SAP2000. Additionally, the presence of plastic hinges at the edge of each single element results in being useless due to the fact that, during the Pushover analysis, we are focused on detecting the global failure of the structure mainly related to plastic hinges at the level of the column-beam connections.

Table 5-6 Modeling Parameters and Acceptance Criteria for Nonlinear Procedures—Structural Steel Components

	Modeling Parameters			Acceptance Criteria				
	Plastic Rotation Angle, Radians		Residual Strength Ratio	Plastic Rotation Angle, Radians				
					Primary		Secondary	
Component/Action	**a**	**b**	**c**	**IO**	**LS**	**CP**	**LS**	**CP**
Beams—flexure								
a. $\frac{b_f}{2t_f} \le \frac{52}{\sqrt{F_{ye}}}$ and $\frac{h}{t_w} \le \frac{418}{\sqrt{F_{ye}}}$	$9\theta_y$	$11\theta_y$	0.6	$1\theta_y$	$6\theta_y$	$8\theta_y$	$9\theta_y$	$11\theta_y$
b. $\frac{b_f}{2t_f} \ge \frac{65}{\sqrt{F_{ye}}}$ or $\frac{h}{t_w} \ge \frac{640}{\sqrt{F_{ye}}}$	$4\theta_y$	$6\theta_y$	0.2	$0.25\theta_y$	$2\theta_y$	$3\theta_y$	$3\theta_y$	$4\theta_y$
c. Other	Linear interpolation between the values on lines a and b for both flange slenderness (first term) and web slenderness (second term) shall be performed, and the lowest resulting value shall be used							

Table 2.7: Modelling parameters of plastic rotations-angle for elements under flexure actions[1]

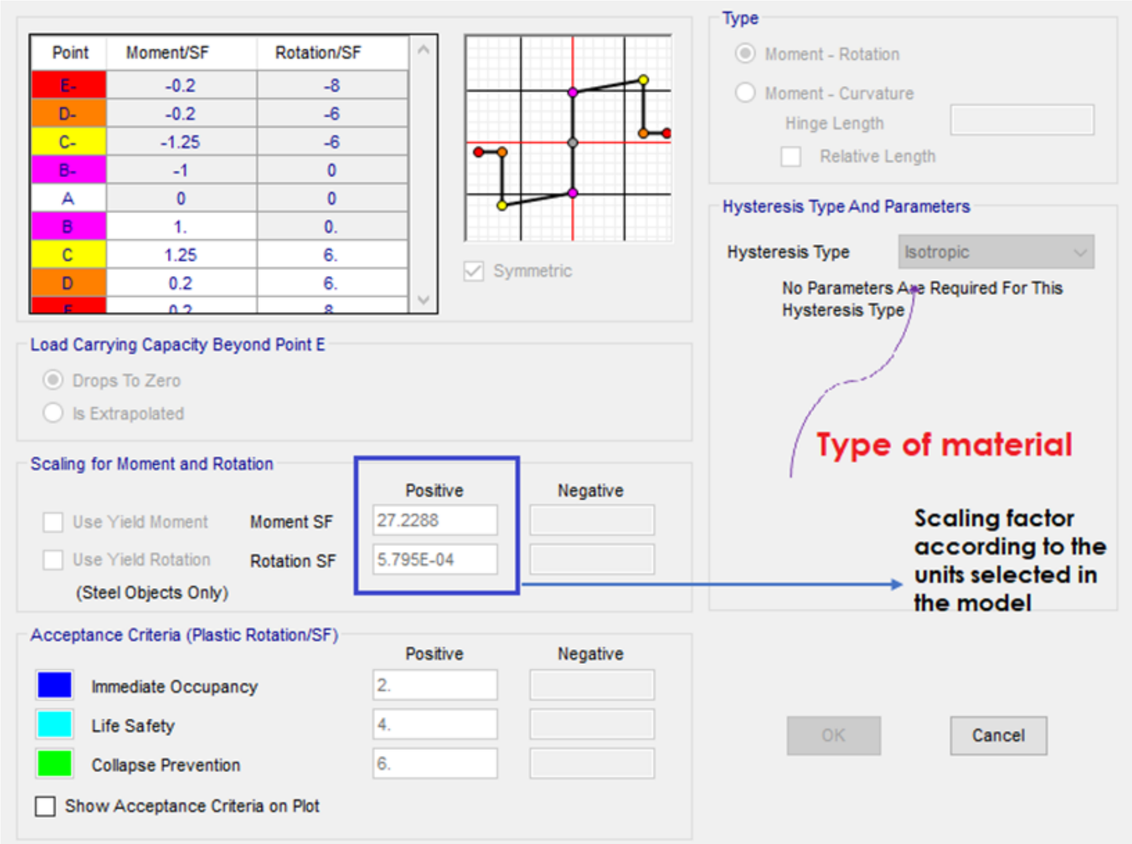

Figure 2.33: Hinge property data example for an element capable to resist bending moment action. Image taken from the software SAP 2000

- **Columns**

The properties that rule the column hinges must consider the main actions that undergo in the column, Axial and bending moment. By adding the actions of the axial forces, the diagram of moment rotation experiences a significant change. This hinge property is the most important to define in our study case. Due to the typology of our structure we expected to activate more hinges in the columns. As we did with the beams, we used the tables of FEMA 356 to adopt the constitutive law that govern the hinges.

Table 5-6 ***Modeling Parameters and Acceptance Criteria for Nonlinear Procedures—Structural Steel Components***

	Modeling Parameters			Acceptance Criteria				
	Plastic Rotation Angle, Radians		Residual Strength Ratio	Plastic Rotation Angle, Radians				
					Primary		Secondary	
Component/Action	**a**	**b**	**c**	**IO**	**LS**	**CP**	**LS**	**CP**
Columns—flexure [2, 7]								
For $P/P_{CL} < 0.20$								
a. $\frac{b_f}{2t_f} \le \frac{52}{\sqrt{F_{ye}}}$ and $\frac{h}{t_w} \le \frac{300}{\sqrt{F_{ye}}}$	$9\theta_y$	$11\theta_y$	0.6	$1\theta_y$	$6\theta_y$	$8\theta_y$	$9\theta_y$	$11\theta_y$
b. $d\,\frac{b_f}{2t_f} \ge \frac{65}{\sqrt{F_{ye}}}$ or $\frac{h}{t_w} \ge \frac{460}{\sqrt{F_{ye}}}$	$4\theta_y$	$6\theta_y$	0.2	$0.25\theta_y$	$2\theta_y$	$3\theta_y$	$3\theta_y$	$4\theta_y$
c. Other	Linear interpolation between the values on lines a and b for both flange slenderness (first term) and web slenderness (second term) shall be performed, and the lowest resulting value shall be used							
For $0.2 < P/P_{CL} < 0.50$								
a. $\frac{b_f}{2t_f} \le \frac{52}{\sqrt{F_{ye}}}$ and $\frac{h}{t_w} \le \frac{260}{\sqrt{F_{ye}}}$	—[3]	—[4]	0.2	$0.25\theta_y$	—[5]	—[3]	—[6]	—[4]
b. $\frac{b_f}{2t_f} \ge \frac{65}{\sqrt{F_{ye}}}$ or $\frac{h}{t_w} \ge \frac{400}{\sqrt{F_{ye}}}$	$1\theta_y$	$1.5\theta_y$	0.2	$0.25\theta_y$	$0.5\theta_y$	$0.8\theta_y$	$1.2\theta_y$	$1.2\theta_y$

Table 2.8: Modelling parameters of plastic rotations-angle for elements under flexion-axial actions[1]

The parameters a,b,c represents measurements in the ABCDE scaled curve. And they are very intuitive to derive based on the table 5-6 of FEMA-356.

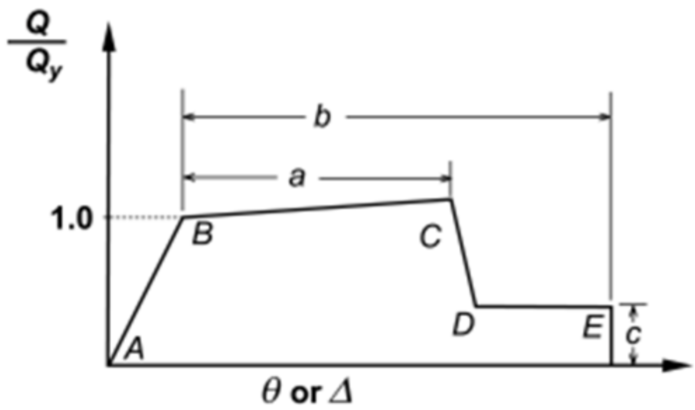

Figure 2.34: Generalized- force deformation relations. [1]

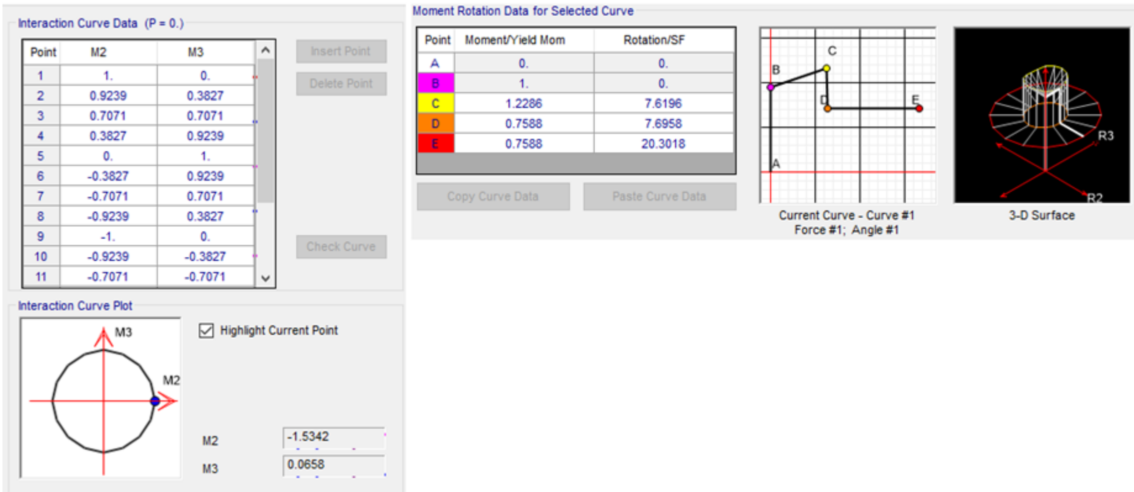

Figure 2.35: ABCDE curve Moment- rotation of a representative column and interaction curve

Since we are working in a tridimensional space. We need to consider the interaction of both planes. For a case in which the axial load is 0 we can observe the relationship between the two planes. The software also allows to work with only one plane but the level of accuracy decreases.

Sap2000 present two options for considering the plastic hinges with isotropic behaviour. Interactive M2-M3 and P-M2-M3, the difference is that the first one gives you the chance of not taking in consideration the axial forces or allows you to select the nonlinear case from which you can obtain the axial force. On the other hand, the P-M2-M3 automatically assign the permanent load case. To be more precise it is recommendable to use the first option and create a nonlinear combination of loads from which the software would assign the most accurate hypothesis of vertical load. In our case was 100% of G1 and G2 and the 30% of the non permanent load.

Finally, this approach leads to a realistic failure scenario in which the critical failure will be achieved when kinematics are provided by the proper plastic-hinges configurations at the level of columns.

2.3 Model Validation and Nonlinear parameters settings

Before conducting the imposition of nonlinear load cases to perform the pushover analysis and obtaining the capacity curve in a MDOF. There were 3 criteria sensible for the accuracy of results:

- Position of application of the seismic load profile;
- the type of load case;
- the software solution scheme.

SAP2000 is very open to modify user preference regarding to the behavior of the imposition of nonlinear load cases. The fact that users can modify multiple parameters could lead to crucial mistakes if there is no expertise in the global settings of the model. The case study was evaluated following the guidelines of the manual and evaluating the variation of the response by modifying certain parameters.

One of the goals of this evaluation was to manage an accurate way to impose the nonlinear load cases. SAP 2000 manage to provide three distributions of forces for the nonlinear static analysis. Specifically, NTC2018 suggests the following load profile modelling:

- The unimodal distribution;
- The uniform distribution proportional to story mass;
- the customized option to assign random force distribution by increasing the magnitudes in the degree of freedom selected.

Due to the nature of our problem, it was necessary to explore the third option to provide an accurate force distribution of the seismic action.

In a first stage, we evaluated the response of a representative portion of the building to check the behavior of the structure regarding to modal and gravitational scheme. Then we proceeded to apply the non-linear parameters of the possible plastic hinges that could be formed.

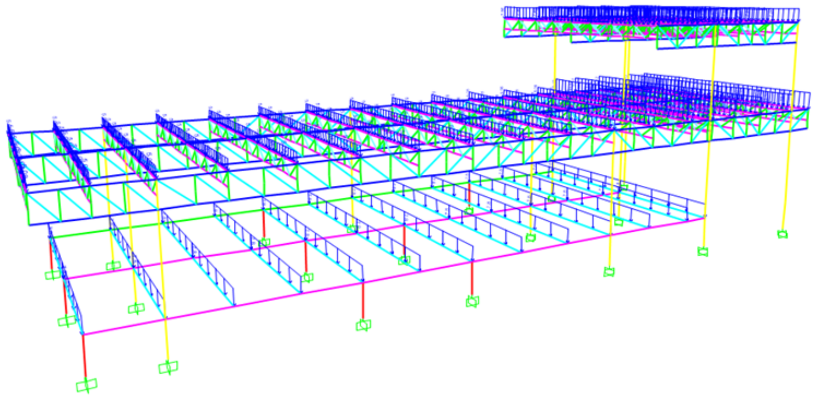

Figure 2.36: Reduce model for validation purposes

The outcome of this model by assessing the nonlinear behaviour outcast a non ductile capacity curve. Therefore, we needed to refine our analysis to check the accuracy of our inputs. This time we used a bi-dimensional frame with different cross sections but using the same parameters.

Bidimensional calibration model to assess nonlinear parameters.

The aim of this calibration exercise was to check if the parameters used to describe the capacity curve of the previous model could reproduce the behavior of the structure in the nonlinear field. The structure subjected to this study was simpler to obtain faster and conclusive response.

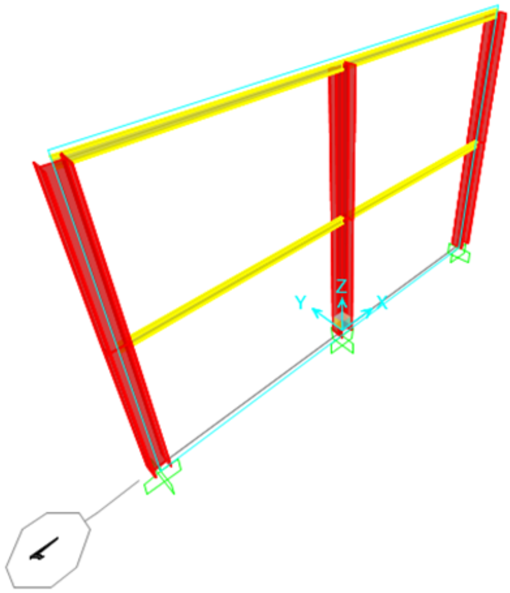

Figure 2.37: Bidimensional two story plane frame for calibration purposes

This frame is composed by columns of cross sections HEA320 and beams IPE140. Fully connected and clamped. The plastic formation of hinges was determined according to the automatic setting for steel structures of SAP2000 that are based on the guidelines of FEMA 356.

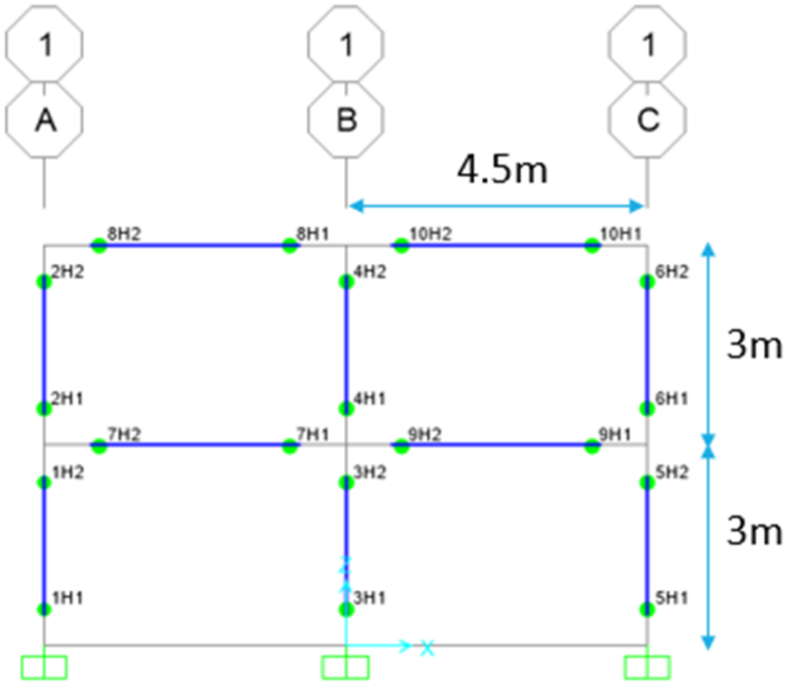

Figure 2.38: Frame dimensions and possible plastic hinges formation

To perform the nonlinear analysis, we proceed with:

• **Creation of the non-linear gravitational load case:** It involves all the permanent and the 30% of the non permanent ones. The initial condition of the structure and the type of analysis which is nonlinear.

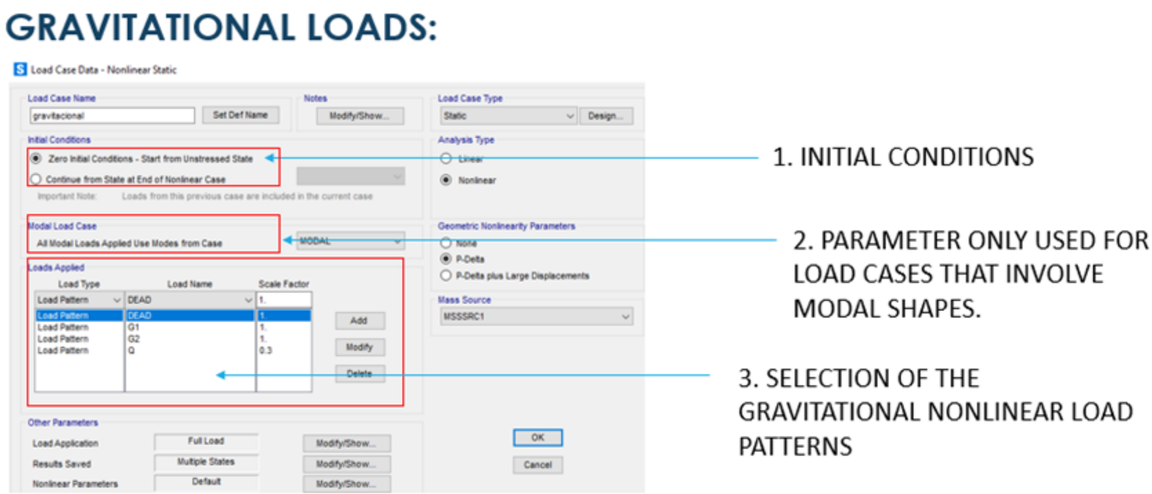

Figure 2.39: Main display dialog for Non-linear gravitational load case

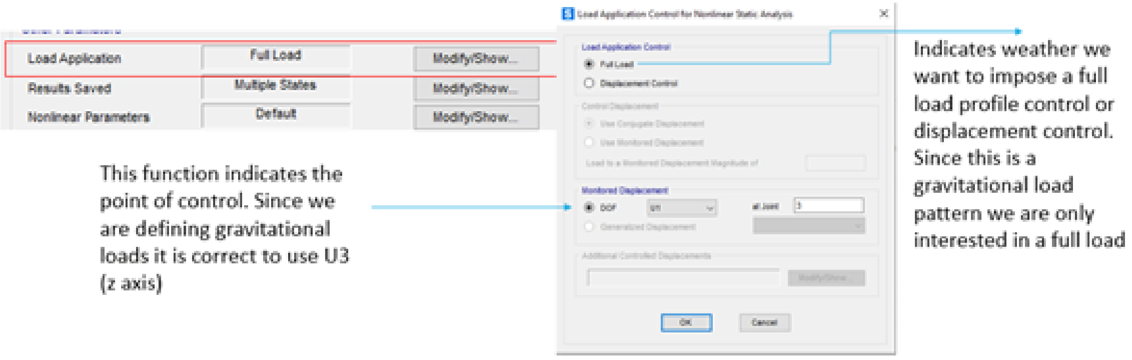

Figure 2.40: Display dialog for load application parameters

- **Creation of the static nonlinear load**

The static nonlinear load case is the load profile that will increase monotonically until the end of the global resistance in the plastic field. Sap 2000 provides 3 types of options for building the load case. One that considers the modal shape, another one that consider the mass of the structure to create a uniform distribution and the third one that considers a random profile.

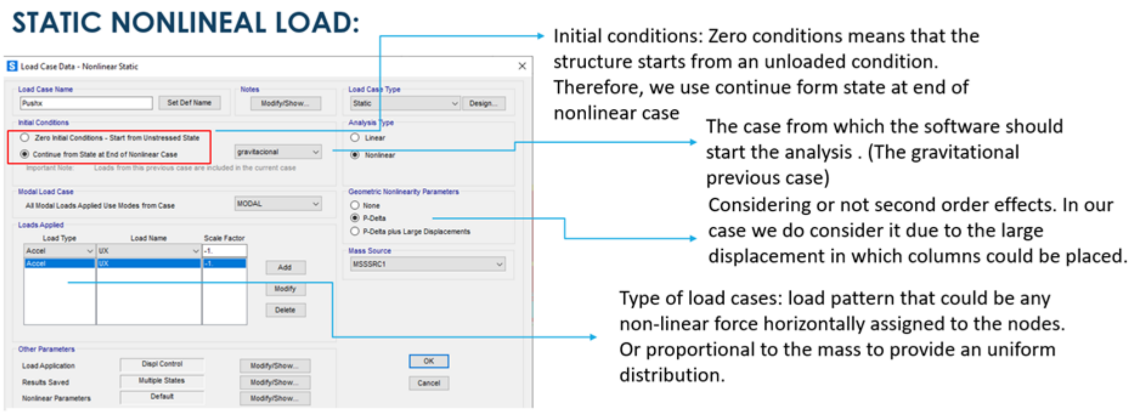

Figure 2.41: Static nonlinear case

After the final settings performed in the two load cases fundamental for the non-linear analysis. We proceed to run the model and obtaining the results of the pushover with a distribution of the first mode of vibration. The outcome of the analysis exposes a considerable ductility before the failure of the structure. This proof that the software can assess very well the load pattern imposed and it can plot the non-linear behavior of it.

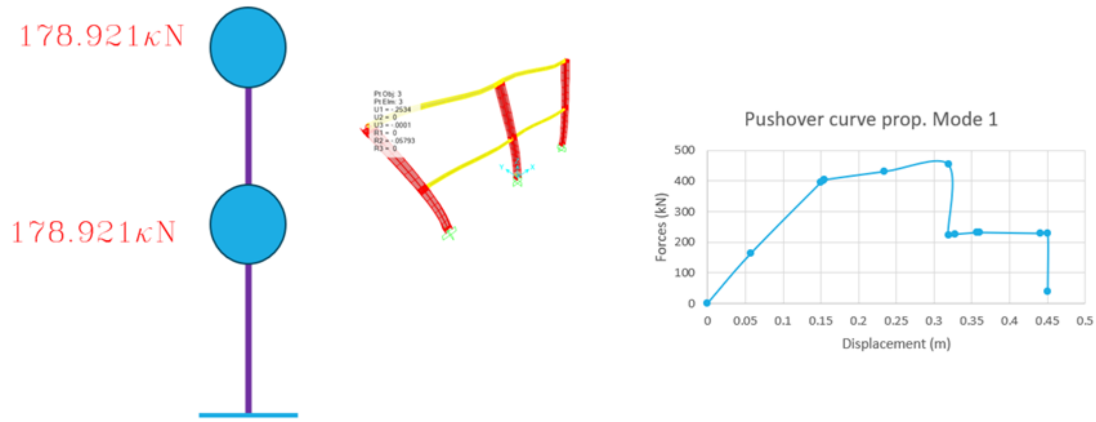

Figure 2.42: Capacity curve obtained form the calibration

The pushover exhibits a ductile behaviour that is in accordance with the constitutive law adopted from FEMA 356. This validation demonstrates the feasibility of the non-linearity behavior modeling adopted for our purposes and allows us to use the same approach also for a more complex model in which the entire structure will be modeled.

2.4 Stability assessment under gravitational actions

The purpose of this analysis is to verify the behavior of the structure under gravitational actions. To do this, we use the fundamental equation for the ultimate limit state that involves only the gravitational scheme. This assessment helps us to identify local issues regarded to elements that could not bear a critical arrangement of forces.

The safety assessment of the structures based on non-linear methodologies does not enforce the compliance of the fundamental equation for ULS. Due to the importance of the structure, we imposed these criteria as the minimum basic standard for the structural behavior.

Equation [2.5.1] of NTC 2018.

$\gamma_{G1}G_1 + \gamma_{G2}G_2 + \gamma_P P + \gamma_{Q1}Q_{k1} + \gamma_{Q2}\psi_{02}Q_{k2} + \gamma_{Q3}\psi_{03}Q_{k3} + \ldots$

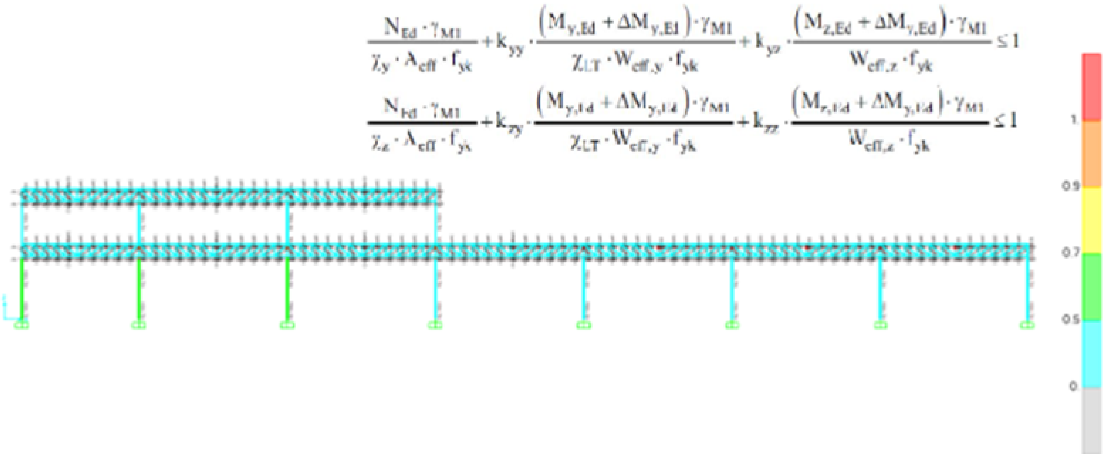

Figure 2.43: Typical frame in X dir. analyzed by SAP2000 check option

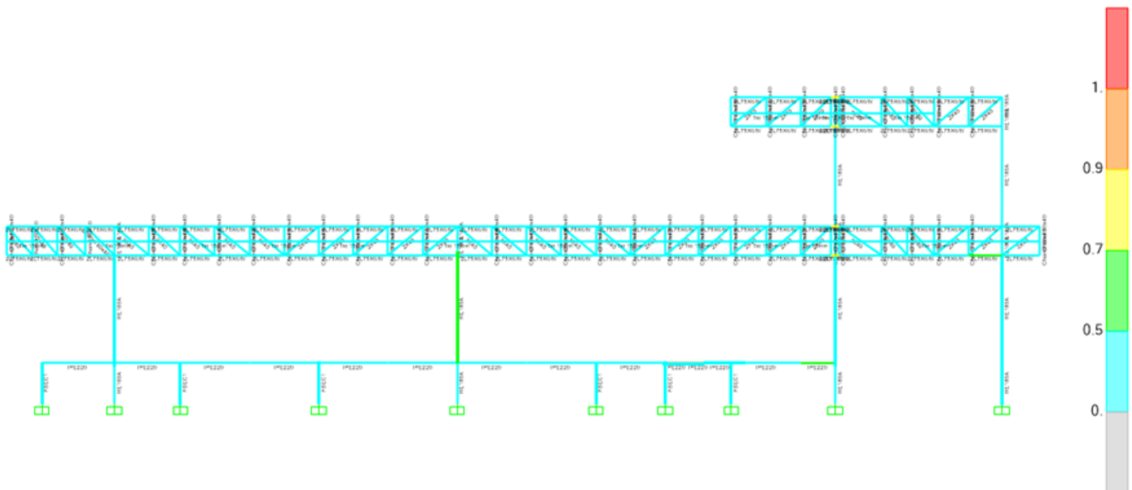

Figure 2.44: Typical frame in Y dir. analyzed by SAP2000 check option

The equations that evaluate the ULS for are based on:

- Calculation of axial area (NTC § 4.2.4.1.2.1)
- Design for axial tension (NTC § 4.2.4.1.2.1)
  - Design for axial compression (NTC § 4.2.4.1.2.2)
  - Design for axial buckling (NTC § 4.2.4.1.3.1)
  - Design for bending moment (NTC § 4.2.4.1.2.3 and § 4.2.4.1.2.6)
  - Design for lateral-torsional buckling (NTC § 4.2.4.1.3.2)

- Calculation of shear area (NTC § 4.2.4.1.2.4)
- Design for shear (NTC § 4.2.4.1.2.4)
- Design for shear buckling (NTC § C4.2.4.1.3.4)
- Analysis of torsion related stresses (SCI Publication 385)
- Design for shear in presence of torsion (EC3 6.2.7)
- Design for combined actions (EC3 6.2.1(7), 6.2.9.1(6), 6.2.9.3(2), Annex A of BS EN 1993-6)

This preliminary assessment aims the detection of critical zones that might present deficiencies. Not always they are related to a real failure for instance Design or check lateral-torsional buckling (NTC § 4.2.4.1.3.2) might present issues like plots warnings in elements that are virtually not constrain. The area elements that connect trusses in real life prevent the element of lateral buckling, therefore we are forced to use virtual of null mass and equivalent stiffness to avoid false warnings. More over Buckling in general doesn't work very well in structures with considerable stiffness like trusses. The software considers the bottom cord as beams and axial buckling analysis (NTC § 4.2.4.1.3.1) is severely castigated.

2.5 LINEAR DYNAMIC ANALYSIS

The typology of the building and the observed characteristic of the case study expose a predictable flexible behavior. The linear dynamic analysis is developed to assess buildings with a strong hypothesis of residual ductility exhibited by the structure. Nowadays regulations establish certain parameters to guarantee global ductility and to ensure the workability of each member in its linear field to bear the limit state demand. It is very common to see old structures with deficiencies related to horizontal actions.

By adopting this analysis, the critical event for which the structure can be considered unsafe is obtained by a multiple scaling procedure of the elastic spectrum. In this way, the first failure configuration can be identified and the corresponding demand spectrum is wrongly determined.

The vulnerability index measured by this method depends on the sensitivity of the engineer. It is possible that some elements would not resist in linear field the demand imposed by the seismic actions. This method does not consider:

- Non-linear behaviour of the elements
- Redistribution of stresses due to plastic hinges formation in the structure
- Critical mechanism of failure

Another aspect that is fundamental to consider is that the ductility can't be assumed by considering the behavior factor, q. The behavior factor could be applied under certain conditions in which we assume that connections, structural system, foundation, and regularity are coherent with the hypothesis of ductility.

The structure of Foggia was not considered with the criteria of dissipation of energy. On the other hand, the Italian regulation accept a minimum of 1.5 ratio for the behavior factor. In sometimes this hypothesis could be very optimistic if the structure cannot provide any ductility in the system.

The seismic equation used was based on NTC-2018 for evaluating seismic actions. SAP2000 also allows us to use different arrangements to consider the direction of the seismic actions. For instance, we created 8 Seismic combinations to assess the 100% of the force in a specific direction and the 30% in the other. The 8 combinations are created to consider the possible combinations of the direction of the seismic actions. The 8 combinations were expanded 4 times to consider the accidental torsional action due to the uncertainty of the loads. Finally, SAP2000 evaluates 32 different combinations.

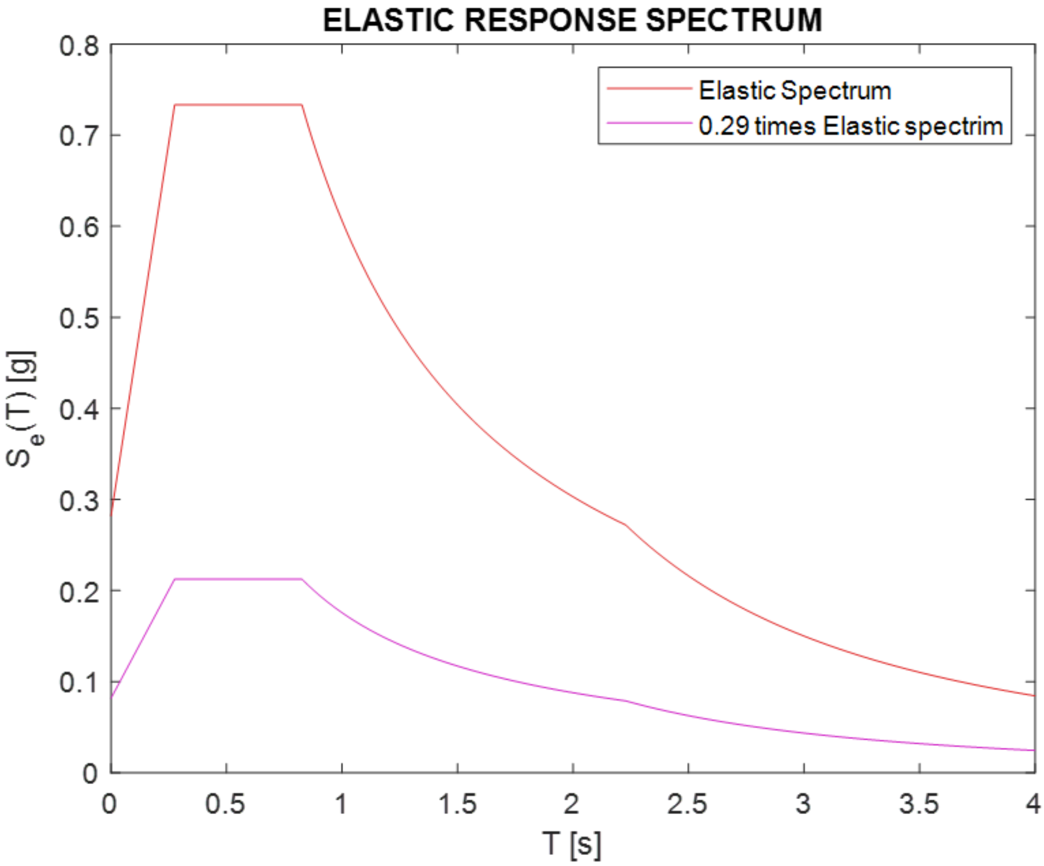

Figure 2.45: Elastic Spectrum that induce the Limit state in the case study

The complete mechanism of failure was observed to appear when the elastic spectrum is 0.29 times the magnitude of the reference elastic spectrum. It was observed in different iterations that some critical elements started to fail in the elastic field when the seismic action is only 10% in the reference spectrum.

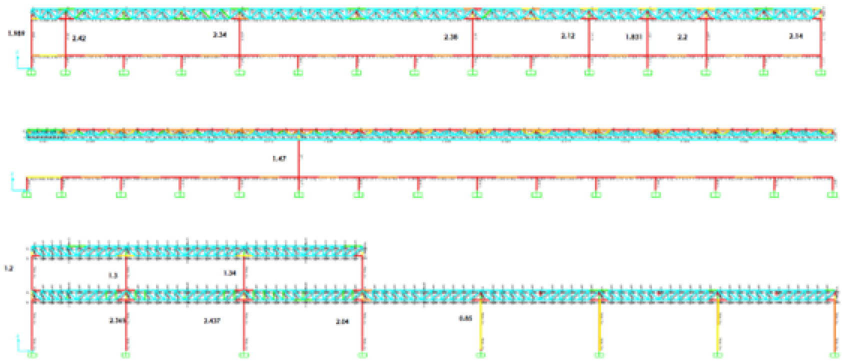

Figure 2.46: Failing elements in frames 13, 16 and 23

By using the solver, we can deduce that the vulnerability index of the structure is near to 0.29 times the elastic spectrum. In this analysis we could appreciate that the software doesn't consider the redistribution of the actions and it just evaluate the internal forces in the linear range of the elements. Therefore, assessing the vulnerability index through this method could be very subjective.

2.6 STATIC NON-LINEAR ANALYSIS

The non-linear static analysis aims that a tridimensional structure that is subjected to a seismic evaluation could receive a monotonically and unidirectional increasing force distribution to obtain a response beyond the linear field. The increasing force (pushing force) could undergo until the failure of the structure or stop at a determined control point[19].

The analysis starts by applying a horizontal load that is scaled from the maximum peak value of the distribution. The structure is getting measured in terms of relative displacement (control point) and Resultant force (shear at the base). The control point that we define is usually a representative point in which the structure could reach the maximum global displacement. Usually, it could be the center of mass of the top floor when the slab has a diaphragmatic behavior, or it could be the point of maximum displacement in flexible slab.

Regarding to the horizontal distribution of forces the disposition of NTC-2018 at 7.3.42 requires two distributions in each direction. One should be adopted from group 1 and the other adopted from group 2.

Group 1 defines:

• Only if the mass participation factor of the fundamental mode could reach the 75% of the global mass in the selected direction. It could be adopted a distribution proportional to the static forces.

• Only if the mass participation factor of the fundamental mode could reach the 75% of the global mass in the selected direction. A distribution corresponding to an acceleration trend proportional to the shape of the fundamental mode of vibration.

• A distribution corresponding to the trend of the storey equivalent forces acting in both directions that comes from the selection of the modes that reach at least the 85% of the mass participation factor. Such values could be obtained from the linear dynamic analysis.

Group 2 defines:

• A distribution of forces as a trend of uniform accelerations along the height of the building

• Adaptative distribution

• A multi-modal distribution, considering at least no.6 different fundamental modes to which significant mass participation factors are associated.

Our case study presents a topology that doesn't match with the average and usual buildings. To fulfill the requirements demanded by the NTC-2018. We need to select two distributions, one principal from the first group and the secondary adopted from the second group.

We assumed as a principal configuration:

I. A distribution equivalent to the storey forces by selecting the modes with the highest mass participation factor which sum is at least the 85% of the total mass participation. Any fundamental mode with a participation factor higher than 5% has been founded.

We assumed as a secondary distribution:

II. A distribution of uniform acceleration. This distribution could be perceived in such a way when the storey masses are similar along the building height.

2.6.1 Modal shapes and mass participation factors

According to the most important guidelines that rule Italy, NTC-2018 and Eurocode. To assess properly a linear dynamic analysis, there are certain criteria that we need to respect. One of them is that the procedure must capture at least more than the 85% of the mass participation. It totally makes sense; the statistical modal combination should combine a representative number of modes that capture almost the totality of the mass. As we deduced in our analysis, the hypothesis imposed in our model rejects, in this preliminary stage, a diaphragmatic condition that doesn't exist. Though the computational effort of the modal analysis is significantly increased when a huge number of vibration modes is considered, it was preferred to remove the hypothesis of the rigid floor. However, a certain stiffness was considered due to the presence of virtual elements, see Figure 2.31 that constraint beams at the level of the ground and the roof of the structure.

We proceed to assess the mass participation ratios with translational component:
$r_{xn} = \frac{\Gamma^2}{M_x}$
where Γ is the participation factor and Mx is the unrestrained mass acting in X direction. In the same way we can also analyse the mas participation ratio in Y direction.
$r_{yn} = \frac{\Gamma^2}{M_y}$

Table 2.9: Mass Participation ratio X direction

TABLE: Modal Participating Mass Ratios Xdir				
CASE	MODE	MODE NUMBER	Period	XDIR
MODAL	Mode	1	2.145436	0.26064
MODAL	Mode	21	0.803036	0.14229
MODAL	Mode	26	0.684622	0.14088
MODAL	Mode	28	0.585776	0.09213
MODAL	Mode	2	1.757164	0.08648
MODAL	Mode	36	0.429789	0.04222
MODAL	Mode	32	0.470633	0.03081
MODAL	Mode	29	0.572045	0.0305
MODAL	Mode	24	0.732817	0.02155
MODAL	Mode	38	0.427591	0.01945
				86.6%

Table 2.10: Modal Participating Mass Ratios Y direction

TABLE: Modal Participating Mass Ratios Ydir				
CASE	MODE	MODE NUMBER	Period (s)	YDIR
MODAL	Mode	5	1.166847	0.22409
MODAL	Mode	6	0.948274	0.17614
MODAL	Mode	8	0.85172	0.15622
MODAL	Mode	12	0.839336	0.10364
MODAL	Mode	7	0.873345	0.05823
MODAL	Mode	10	0.846739	0.0564
MODAL	Mode	13	0.838047	0.0262
MODAL	Mode	20	0.812106	0.01765
MODAL	Mode	31	0.501061	0.0168
MODAL	Mode	4	1.183392	0.013
MODAL	Mode	11	0.841662	0.00942
				85.8%

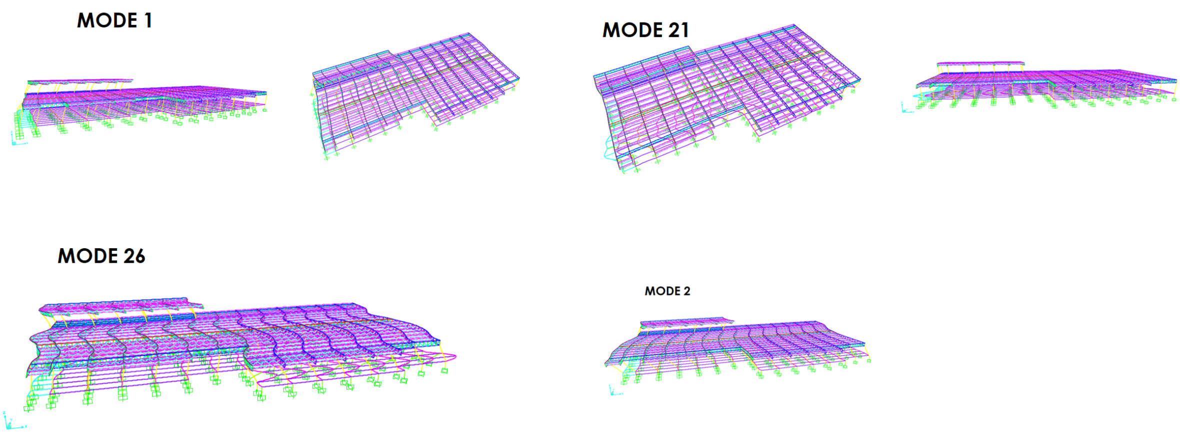

Figure 2.47: Shape forms X dir

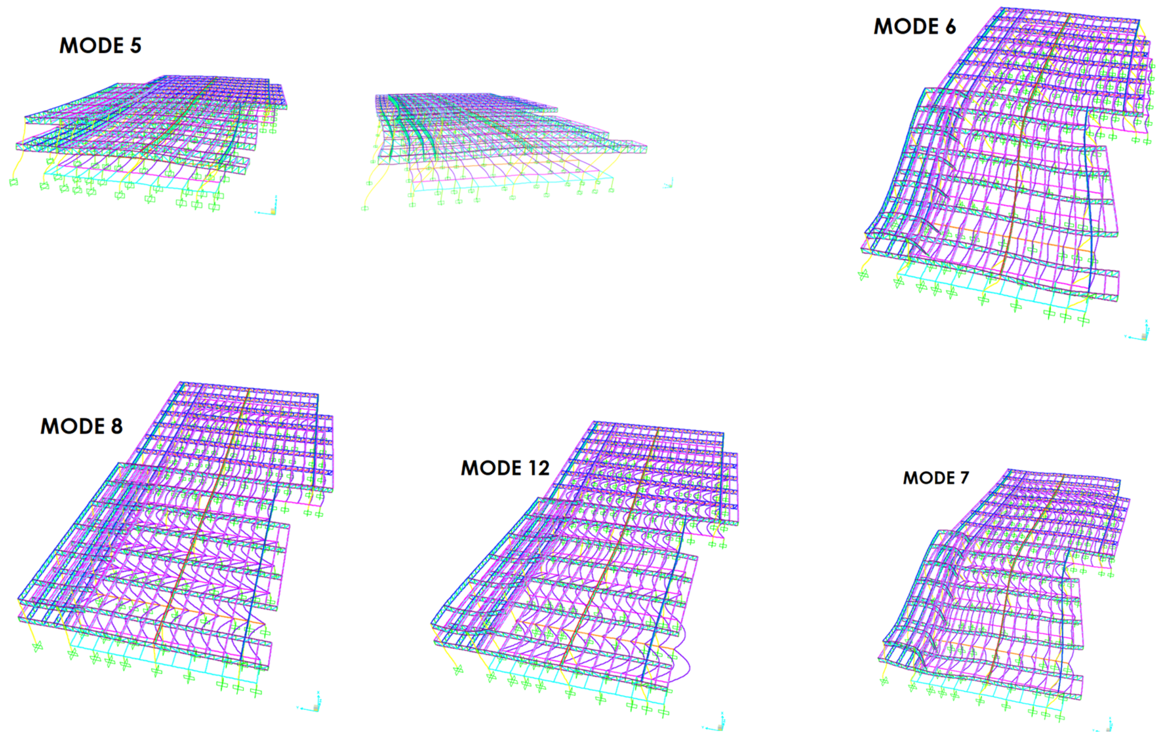

Figure 2.48: Shape forms Y dir

2.6.2 Assessment of the Group 1- Load profile: equivalent to the storey forces

The first distribution is based on the outcome obtained from the linear dynamic analysis. The shape forms with greatest representation of mass participation ratio are selected to be combined with a statistical principle that in this case is the square root of the sum of the squares SRSS to obtain a final representative distribution of forces.

From the classical linear dynamic analysis, we know that either SRSS or CQC are two procedures adopted to assess the final outputs of the internal forces of the represented modes of vibration. Specifically, the statistical combinations of the structural effect (e.g. axial, shear, bending, and displacement) obtained by performing a linear dynamic analysis mode-by-mode could lead to overestimating the seismic demand due to the superposition of seismic action which does not occur at the same time. In this case in which a Pushover analysis is conducted, a unidirectional and monotonically increased load distribution is applied step-by-step. Such distribution is proportional to the equivalent forces that induce the modal shapes[7]. To achieve a load distribution representative of all the fundamental modes, a statistical combination is suggested by the NTC2018 Chapter 7.3.4.2 in which the SRSS or CQC is encouraged to combine the input load profile derived by each mode. The validity of this procedure is accepted in the NTC-2018 and several authors [19] [3] use the method to illustrate examples.

Now we proceed to determine the distribution starting from the equation of motion from a multiple degree of freedom system.

$m\ddot{u} + cu + ku = -mi\ddot{u}_g(t)$

where m, c, and k are mass, damping, and stiffness matrices of structure, respectively, and i is the unit vector. The right hand side of the previous equation represents the effective earthquake forces, p_{eff}, and can be written as[2]:

$p_{eff}(t) = -mi\ddot{u}_g(t) = -s\ddot{u}_g(t)$

$$s = mi = \sum_{n=1}^{N} s_n = \sum_{n=1}^{N} \Gamma_n m \Phi_n$$

$$u(t) = \sum_{n=1}^{N} \boldsymbol{\Phi}_n q_n(t)$$

$$\ddot{q}_n + 2\zeta_n \omega_n \dot{q}_n + \omega_n^2 q_n = -\Gamma_n \ddot{u}_g(t)$$

$$\Gamma_n = \frac{\Phi_n^T \boldsymbol{mi}}{\Phi_n^T \boldsymbol{m} \Phi_n}$$

$$q_n(t) = \Gamma_n D_n(t)$$

• where (s) is the distribution of effective earthquake forces over building's height

• where, Γ n is the nth **modal participating factor** and ϕn is the corresponding mode shape. This parameter Γ will pay a significant role in the upcoming discussion.

• $q_n(t)$ is the modal coordinate

By posing we could obtain the formulation of the Equivalent storey force:

$F_{mi} = \Gamma_m \phi_{mi} m_i S_a^{(m)}$

Once obtained all the equivalent storey forces related to each mode. We proceed to apply the SRSS to finally obtain the representative distribution of this group[19].

$$\Psi_i = \sqrt{\sum_{m=1}^{N_m} F_{mi}^2} = \sqrt{\sum_{m=1}^{N_m} \left(\Gamma_m \phi_{mi} m_i S_a^{(m)}\right)^2}$$

Table 2.11: distribution equivalent to the storey forces,Xdir

Distribution $\sqrt{\sum_{m=1}^{N_m}\left(\Gamma_m\phi_{mi}m_iS_a^{(m)}\right)^2}$		
FRAME 00	Final Force Distribution profile (N)	Unscaled Force Vector
Ground Floor	8143.953248	0.000291777
FRAME NO		
First Floor	7479050.348	0.2679554
Ground Floor	2035062.413	0.072911123
FRAME 6		
Ground Floor	6263562.245	0.224407545
FRAME 7		
First Floor	4650793.218	0.166626122
Ground Floor	4639181.754	0.166210113
FRAME 9		
First Floor	1109522.045	0.03975136
Ground Floor	17298868.56	0.619774574
FRAME 11		
Ground Floor	27911549.3	1
FRAME 13		
First Floor	12408517.61	0.444565706
Ground Floor	5621777.192	0.201414014
FRAME 14		
First Floor	661719.2222	0.023707721
Ground Floor	4391544.032	0.157337881
FRAME 15		
Ground Floor	12648575.53	0.453166372
FRAME 16		
First Floor	887116.2025	0.031783123
Ground Floor	7901043.478	0.283074343
FRAME 17		
Ground Floor	16091390.12	0.576513684
FRAME MO		
Roof	2950634.899	0.105713763
First Floor	3975867.724	0.142445254
Ground Floor	1572944.463	0.05635461
FRAME 21		
Ground Floor	4857149.22	0.174019334
FRAME 23		
Roof	456919.0543	0.016370251
First Floor	4695923.54	0.168243027

Table 2.12: distribution equivalent to the storey forces, Ydir (PART 1)

$\sqrt{\sum_{m=1}^{N_m}\left(\Gamma_m \phi_{mi} m_i S_a^{(m)}\right)^2}$		
FRAME B	Final F.D	Unscaled
-	profile (N)	Force Vector
Roof	391107.1947	0.084826414
First floor	886022.0267	0.192167448
Ground Floor	257928.4903	0.055941566
FRAME C		
Roof	666263.2302	0.144504426
First floor	2971296.001	0.644438119
Ground Floor	2767920.624	0.600328463
FRAME D		
Roof	648348.5323	0.140618945
First Floor	1620140.34	0.351388819
Ground Floor	4011758.027	0.870101732
FRAME E		
Roof	268800.5525	0.058299585
First Floor	573291.0472	0.124339885
Ground Floor	2558216.827	0.554846249
FRAME F		
Roof	1003803.281	0.217712775
First Floor	3715107.807	0.805761892
Ground Floor	3534806.488	0.766656719
FRAME G		
Roof	1016713.71	0.220512891
First Floor	2139938.3	0.464126702
Ground Floor	3512795.513	0.761882806
FRAME H		
Roof	847113.0007	0.183728551
First Floor	4015248.98	0.870858878
Ground Floor	2748768.429	0.596174584
FRAME I		
First Floor	1633488.33	0.354283837
Ground Floor	4425091.325	0.959748719
FRAME J		
First Floor	2628706.2	0.57013454
Ground Floor	2448059.042	0.530954359

Table 2.13: distribution equivalent to the storey forces, Ydir (PART 2)

$\sqrt{\sum_{m=1}^{N_m}\left(\Gamma_m\phi_{mi}m_iS_a^{(m)}\right)^2}$		
FRAME K	FINAL F.D	Unscaled
-	profile (N)	Force Vector
First Floor	613047.7092	0.132962624
Ground Floor	2510591.902	0.544516979
FRAME L		
First Floor	2086871.858	0.452617233
Ground Floor	4610676.98	1
FRAME M		
First Floor	2184152.86	0.473716304
Ground Floor	3601619.403	0.781147632
FRAME N		
First Floor	3767868.367	0.817205019
Ground Floor	1037869.956	0.225101424
FRAME O		
First Floor	2378667.922	0.515904266
Ground Floor	2548134.818	0.552659583
FRAME P		
First Floor	1957573.279	0.424573937
Ground Floor	368046.7813	0.07982489

2.6.3 Assessment of the Group 2-Load profile: Uniform acceleration

The present distribution is usually called simply "uniform" because of the shape of this distribution in regular buildings. It does not mean that this distribution needs to adopt literally the expected shape. Our case study has different arrangement of masses in all 3 storeys. This is why it is better to call this distribution as it is mentioned in the codes, distribution of uniform acceleration.

The need to apply two different typology of force distributions lies in the necessity to capture the response that could be obtained in a more sophisticated and precise nonlinear dynamic analysis. The static nonlinear analysis stablishes a lower and upper limit by using two different distributions. Distribution of forces proportional to the mode of vibration tend to capture the dynamic response better if the structure remains in the elastic range. On the other hand, structures with large deformation are better represented by distribution proportional to forces with uniform distribution [19].

By adopting these two distributions we could predict a realistic behavior of a structure in both limits. Of course, one is more suitable than the other depending on the failure mechanism of the structure.

$F_i = m_i$

Table 2.14: Distribution of uniform acceleration. X.Dir

D. UNIFORM	acc / X.dir	Acc (m/s2)	9.81	
FRAME 00	mass kN	mass kG	Force Profile (N)	Unscaled Distribution
Ground Floor	273.433	27872.88481	273433	0.086751305
FRAME NO				
First Floor	775.018	79002.85423	775018	0.245887742
Ground Floor	953.14	97160.04077	953140	0.302399999
FRAME 6				
Ground Floor	1716.067	174930.3772	1716067	0.544451664
FRAME 7				
First Floor	627.739	63989.70438	627739	0.199160955
Ground Floor	843.981	86032.72171	843981	0.267767436
FRAME 9				
First Floor	140.471	14319.16412	140471	0.044566832
Ground Floor	2413.118	245985.525	2413118	0.765603039
FRAME 11				
Ground Floor	3151.918	321296.4322	3151918	1
FRAME 13				
First Floor	1776.625	181103.4659	1776625	0.563664727
Ground Floor	2596.874	264717.0234	2596874	0.823902779
FRAME 14				
First Floor	183.49	18704.38328	183490	0.058215347
Ground Floor	1047.679	106797.0438	1047679	0.332394117
FRAME 15				
Ground Floor	2478.687	252669.419	2478687	0.786405928
FRAME 16				
First Floor	69.805	7115.698267	69805	0.022146833
Ground Floor	929.844	94785.3211	929844	0.295008944
FRAME 17				
Ground Floor	2298.94	234346.5851	2298940	0.729378112
FRAME MO				
Roof	543.184	55370.43833	543184	0.172334433
First Floor	1814.216	184935.3721	1814216	0.575591116
Ground Floor	1047.679	106797.0438	1047679	0.332394117
FRAME 21				
Ground Floor	513.538	52348.41998	513538	0.162928731
FRAME 23				
Roof	134.691	13729.96942	134691	0.042733028
First Floor	892.931	91022.52803	892931	0.283297662

Table 2.15: Distribution of uniform acceleration. Y.Dir (PART 1)

D. UNIFORM	acc / Y.dir	Acc (m/s2)	9.81	
FRAME B	mass kN	mass kG	Force Profile (N)	Unscaled Distribution
Roof	46.179	4707.33945	46179	0.0284
First floor	128.865	13136.08563	128865	0.0792
Ground Floor	372.221	37943.01733	372221	0.2289
FRAME C	-	-		
Roof	77.516	7901.732926	77516	0.0477
First floor	473.058	48222.01835	473058	0.2909
Ground Floor	1001.579	102097.7574	1001579	0.6158
FRAME D	-	-		
Roof	142.507	14526.70744	142507	0.0876
First Floor	473.037	48219.87768	473037	0.2908
Ground Floor	1268.546	129311.5189	1268546	0.7800
FRAME E	-	-		
Roof	95.627	9747.910296	95627	0.0588
First Floor	304.191	31008.25688	304191	0.1870
Ground Floor	1265.267	128977.2681	1265267	0.7779
FRAME F	-	-		
Roof	149.763	15266.36086	149763	0.0921
First Floor	816.122	83192.86442	816122	0.5018
Ground Floor	1265.324	128983.0785	1265324	0.7780
FRAME G	-	-		
Roof	96.754	9862.793068	96754	0.0595
First Floor	294.543	30024.77064	294543	0.1811
Ground Floor	1224.29	124800.2039	1224290	0.7527
FRAME H	-	-		
Roof	69.529	7087.56371	69529	0.0427
First Floor	511.405	52130.98879	511405	0.3144
Ground Floor	1181.936	120482.7727	1181936	0.7267
FRAME I	-	-		
First Floor	251.522	25639.3476	251522	0.1546
Ground Floor	1406.722	143396.738	1406722	0.8649

Table 2.16: Distribution of uniform acceleration. Y.Dir (PART 2)

D. UNIFORM	acc / Y.dir	Acc (m/s2)	9.81	
FRAME J	mass kN	mass kG	Force Profile (N)	Unscaled Distribution
First Floor	667.643	68057.39042	667643	0.4105
Ground Floor	1626.434	165793.476	1626434	1.0000
FRAME K	-	-		
First Floor	259.119	26413.76147	259119	0.1593
Ground Floor	1624.517	165598.0632	1624517	0.9988
FRAME L	-	-		
First Floor	588.086	59947.60449	588086	0.3616
Ground Floor	1626.433	165793.3741	1626433	1.0000
FRAME M	-	-		
First Floor	399.153	40688.3792	399153	0.2454
Ground Floor	1625.291	165676.9623	1625291	0.9993
FRAME N	-	-		
First Floor	533.763	54410.09174	533763	0.3282
Ground Floor	1599.726	163070.948	1599726	0.9836
FRAME O	-	-		
First Floor	320.274	32647.70642	320274	0.1969
Ground Floor	1555.668	158579.8165	1555668	0.9565
FRAME P	-	-		
First Floor	259.514	26454.0265	259514	0.1596
Ground Floor	783.038	79820.38736	783038	0.4814

2.7 CAPACITY CURVES IN A MDOF

Using the FEM software sap2000 we proceeded to apply the previous force distributions to the model to obtain the capacity curve. This curve plots the maximum displacement of the structure against the final force that induce such event. Since there is a load distribution along the model the final force could be understood as the shear at the base. This capacity curve is referred to a multiple degree of freedom system.

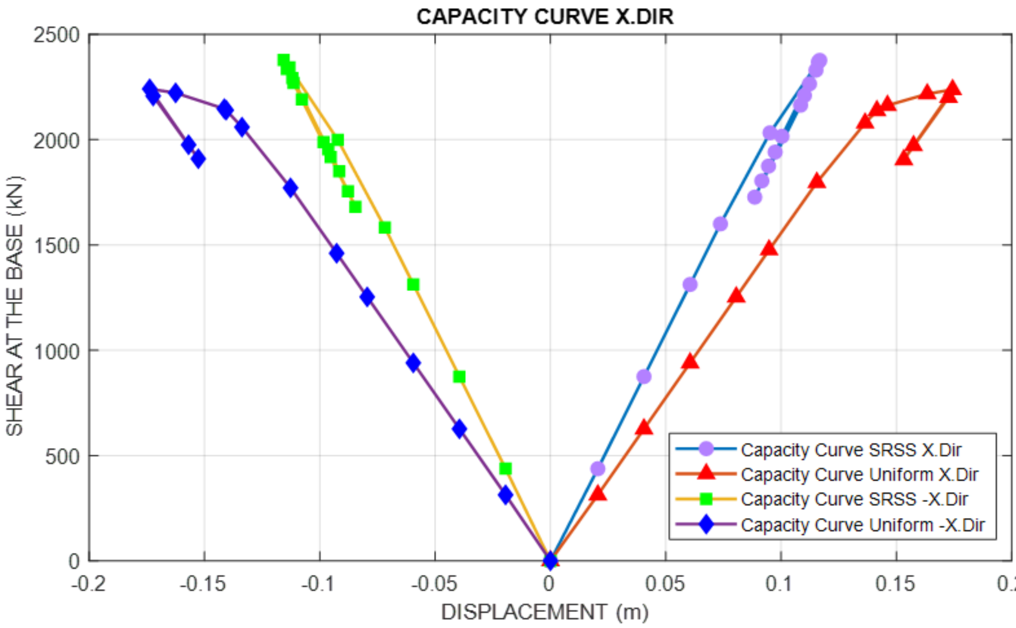

Figure 2.49: Capacity Curves Reference Model X.DIR

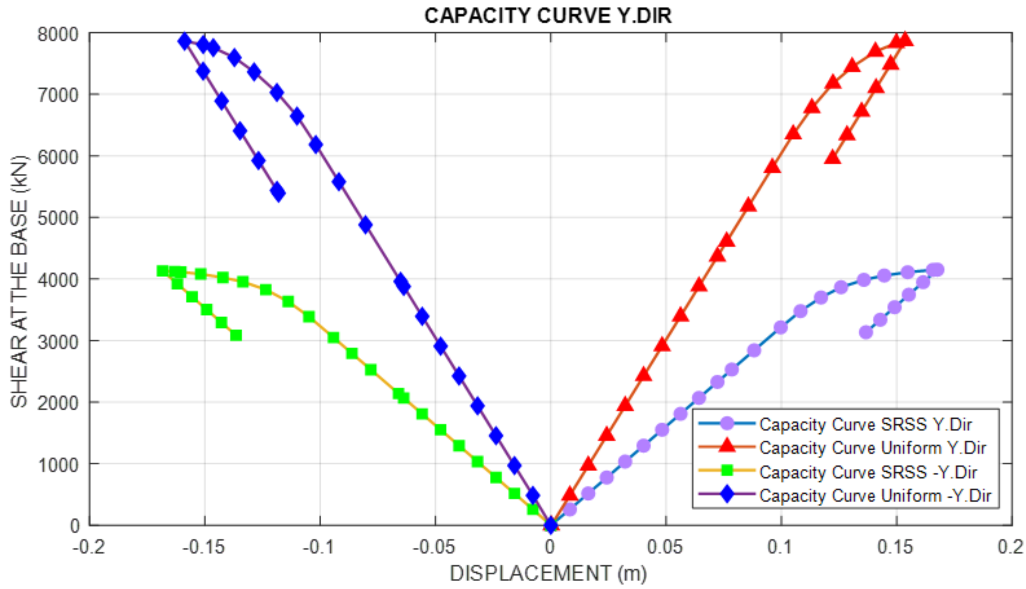

Figure 2.50: Capacity Curves Reference Model Y.DIR

As we can see the response of the system that is expected to work mainly with elastic behaviour and low permanent deformation before the collapse presents the lower criteria of capacity evaluated through the shear at the base.

In reinforced concrete structures the distribution that induces the most unfavorable scenario is the "uniform" distribution. Our case study provides a typology in which the biggest concentration of the mass occurs in the lowest level and the two upper storeys present a mass that is not even half of the rising floor. In table 2.15 we can appreciate the length of the vector of forces, our second group distribution in other words is not a classical uniform distribution. Therefore the outcome of our results doesn't represent the traditional upper limit boundary [19] because the forces in the upper levels are not maintained, but reduced. The upper levels don't experience a pushing force that induce a considerable damage in the lowest storey.

2.8 COMPARISONS BETWEEN DIFFERENT APPROACHES FOR ASSESSING THE TRANSFORMATION FACTOR Γ

One of the most interesting aspects is that there is no official information or clear procedures suggested by the Italian Standard Regulation for assessing the Transformation Factor Γ when, passing from a multiple degree of freedom to a single degree of freedom system, more than one mode is considered.

The transformation factor Γ is usually obtained by considering the participation factor of the only first mode of vibration when the eigenvector is normalized to the maximum storey displacement. This approach is feasible when a specific building provides a representative mode of vibration that captures at least 75% of the mass participation ratio or, when, at least one mode can be associated with significant mass mobilization of the structure [19]. On the other hand, structures with a debatable representative modal shape could address missing information by using just one participation factor.

Our approach is based on a basic structural principle which is the relationship between masses mobilized and modal shapes. The participation factor is a term that is entirely linked to a specific modal shape. Now we have a distribution that comes from a statistical combination, we can establish a relationship that could lead to a new transformation factor.

Different statistical and practical approaches are widely used to obtain a single-degree Pushover curve:

1. SRSS or CQC combination of all the transformation factor obtained for each mode
2. the weighted average of all the transformation factor obtained for each mode
3. the mathematical average of all the transformation factor obtained for each mode
4. Adopting the Transformation factor related to the first vibration mode only

All this approaches lack of validity and present a theoretical problem because they don't consider the final shape and the respective mass.

The solution presented in this document derives the transformation factor using the relationship of the shape and the mass. The procedure starts:

- To impose the load distribution and provoke a deformation in the linear field.

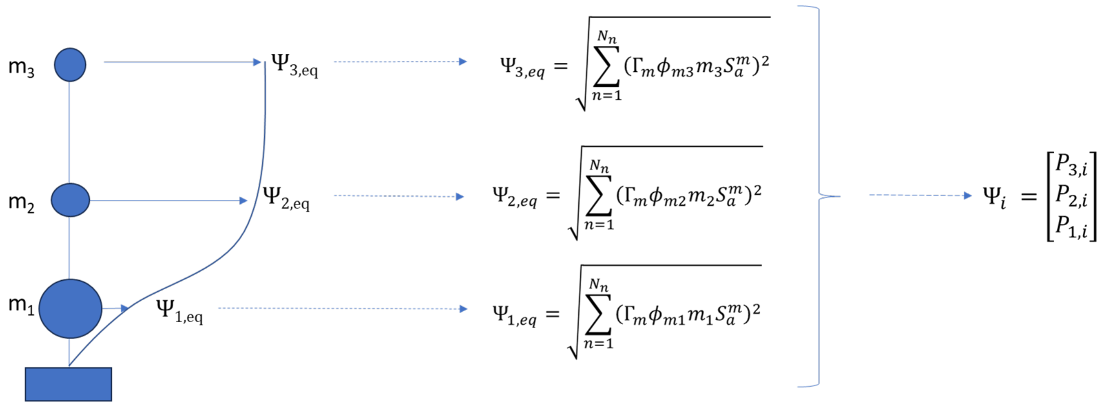

Figure 2.51: Scheme Imposition of the final distribution

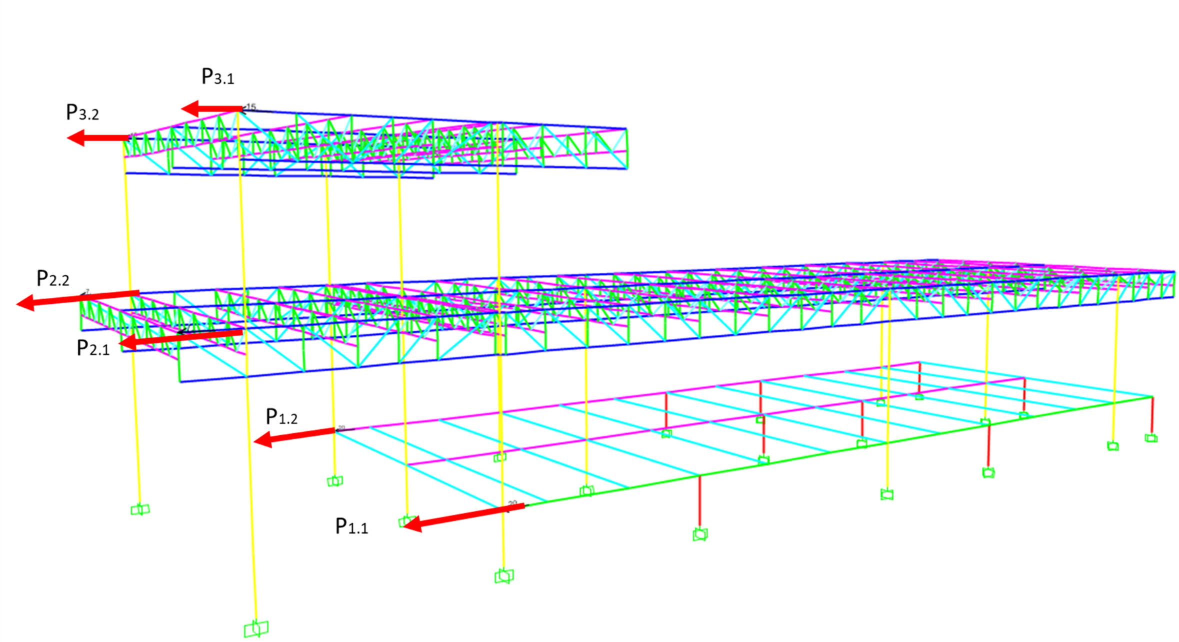

Figure 2.52: At FEM:Imposition of the final distribution

- The deformation let us measure the displacement in the center of mass of each storey, or we could use the average displacement among the nodes that are part of the storey.

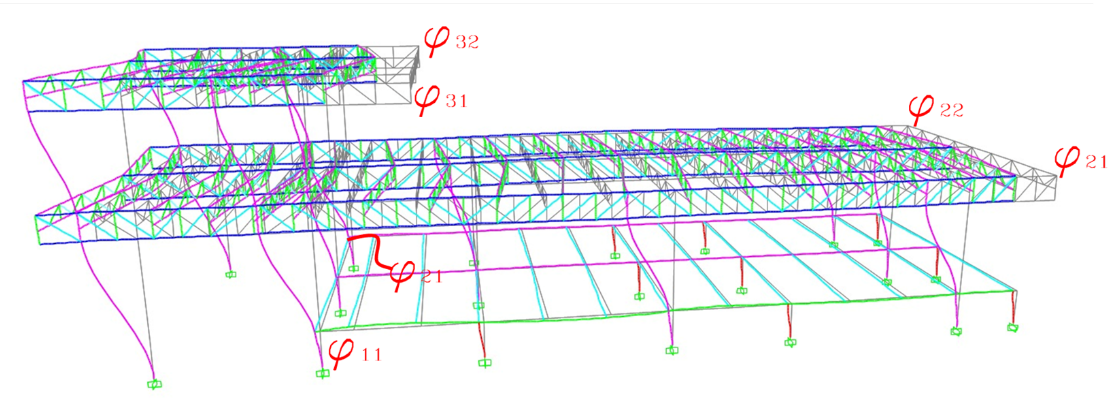

Figure 2.53: At FEM:Shape of the imposed distribution

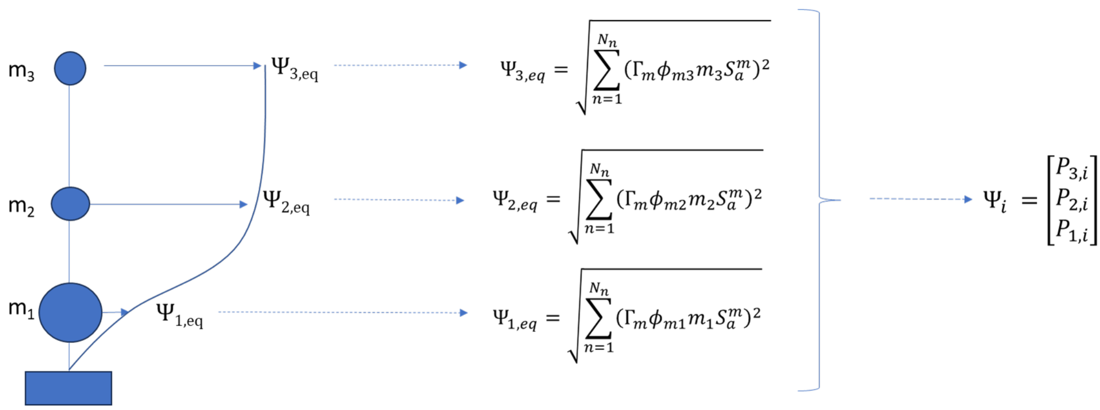

Figure 2.54: Scheme:Shape of the imposed distribution and obtained Vector

- A new vector is formed by using this simple principle. This vector doesn't come from the eigenvalue problem but is loyal to the load distribution that is used for the pushover procedure.

$$\Gamma = \frac{\phi^T\ M\ \tau}{\phi^T\ M\ \phi} = \frac{\sum m_{storey}\ \phi_{storey}}{\sum m_{storey}\ \phi^2{}_{storey}}$$

- By considering the mass of each storey we can use the transformation factor equation and the new value is completely representative to the load distribution that is imposed.

This transformation factor is based in the equations of equilibrium when the new load distribution doesn't appear from the eigenvalue problem.

Table 2.17: Transformation factor comparison

T. FACTOR DUE TO THE LOAD DISTRIBUTION	1.4250711
T. FACTOR SRSS of PARTICIPATIONS FACTORS	5.80414652
T. FACTOR W.AVERAGE of PARTICIPATION FACTOR	1.71648762
T. FACTOR W.AVERAGE of PARTICIPATION FACTOR	1.608
T. FACTOR DUE TO FIRST MODE	2.1079084

As we could see the transformation factors obtained by using statistical approaches do not provide a realistic value. For instance, the SRSS provides a nonsense value that could punish the capacity curve of the building represented in a single degree of freedom system. On the other hand, using the first mode of vibration as the reference of the final response make the system loose important information that reduce considerably the capacity curve represented in SDOF. The weighted average capture closely the expected response but its acceptance as a reliable method depends on a extended survey.

2.9 Safety Assessment and Evaluation of Demand

The safety assessment of the structure is performed by employing a procedure in which we need to convert our capacity curve from a multiple degree of freedom system in a one degree of freedom system. By doing this previous step we can compare the response of the building with the response spectra.

As we know the response spectra of pseudo acceleration is expressed in function of the period (T) and pseudo-accelerations. The comparison of the demand and capacity could be done in a more intuitive way by using the ADRS (accelerations-displacement response spectrum). Forces and acceleration are proportional, the fact that we are using a representative single degree of freedom system allow us to express the capacity curve which is in terms of forces and displacement and passing to a capacity curve in terms of acceleration and displacement. In other words, we can obtain a visual representation of the demand and capacity.

The solutions are presented also in this way[5]

$$F_{bu}^{*} = \frac{F_{bu}}{\Gamma_l}$$

$$d^{*} = \frac{d_u}{\Gamma_l}$$

$$k^{*} = \frac{F_y^{*}}{d_y^{*}}$$

$$m^{*} = \boldsymbol{\Phi}_l^T \boldsymbol{M} \tau$$

$$T^{*} = 2\pi \sqrt{\frac{m^{*}}{k^{*}}}$$

$$F_E = F_E^{*} = S_e\left(T^{*}\right) m^{*}$$

$$F_y = F_y^{*}$$

$$q^{*} = \frac{F_E^{*}}{F_y^{*}} = \frac{S_e\left(T^{*}\right) m^{*}}{F_y^{*}}$$

$$\mu_d = \left(q^{*} - 1\right) \frac{T_c}{T^{*}} + 1 \quad \left(T^{*} < T_C\right)$$

$$\mu_{\max}^{*} = \frac{d_{\max}^{*}}{d_y^{*}}$$

$$d_{\max}^{*} = \frac{d_{e,\max}^{*}}{q^{*}} \left[\left(q^{*} - 1\right) \frac{T_c}{T^{*}} + 1\right] \left(T^{*} < T_C\right)$$

$$For\left(T^{*} > T_C\right)$$

$$\mu_d = q^{*}$$

$$d_m^{*}ax = d_(^{*}e, max)$$

- The * is referred to point out that we are referring to a single degree of freedom system.

- Fbu is the peak force in the capacity curve.

- d is the displacement measure in the capacity curve

- k* is the stiffness of associated to the single degree of freedom system.

- m* is the mass associated to the single degree of freedom system.

- T* is the fundamental period of the single degree of freedom system

- Fe is the Elastic force that is obtained by multiplying the pseudo-acceleration of a specific period times the mass of the system.

- q is the reduction factor

- μ is the ductility of the system

Finally, the vulnerability index ζ_E could be obtained through this reasoning:
$\zeta_E = \frac{PGA\ capacity}{PGA\ demand} \approx \frac{S_a cap\ (T*)}{S_a dem\ (T*)} = \frac{d_{max} cap}{d_{max} dem}$

2.9.1 Safety check X direction. SRSS distribution

Table 2.18: Vulnerability index SRSS Distribution X.DIR

MODAL X		**Vulnerability**	
T [s]	1.333	de,max [m]	0.201
m*	976.514	du* [m]	0.082
Say [m/s2]	1.627	dy* [m]	0.073
Say [g]	0.166	μc	1.118
Sae [g]	0.455	q∼*	1.118
q*	2.744	de,max∼* [m]	0.082
μd	2.744	ζ_E	0.409

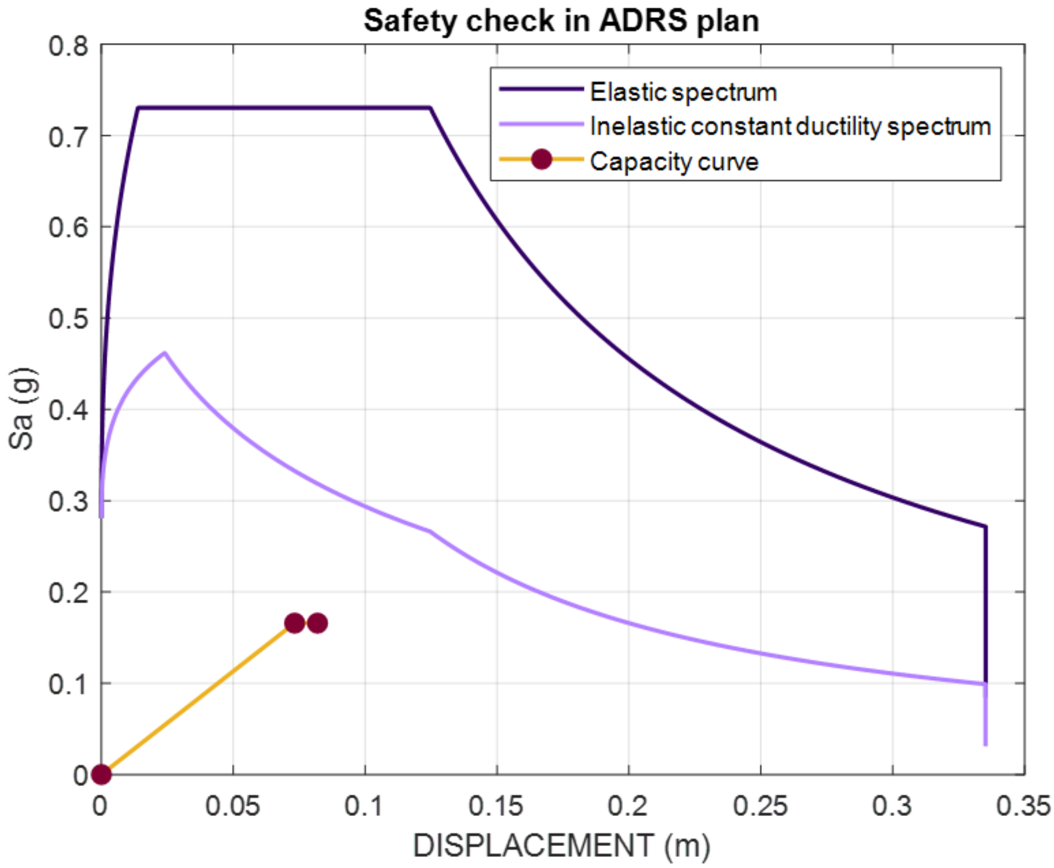

Figure 2.55: Safety check X.DIR SRSS Distribution

2.9.2 Safety check X direction. uniform distribution

Table 2.19: Vulnerability index Uniform Distribution X.DIR

MASS X		Vulnerability	
T [s]	1.392	de,max [m]	0.209
m*	763.747	du* [m]	0.101
Say [m/s2]	1.644	dy* [m]	0.081
Say [g]	0.168	μc	1.253
Sae [g]	0.435	q∼*	1.253
q*	2.599	de,max∼* [m]	0.101
μd	2.599	ζ_E	0.483

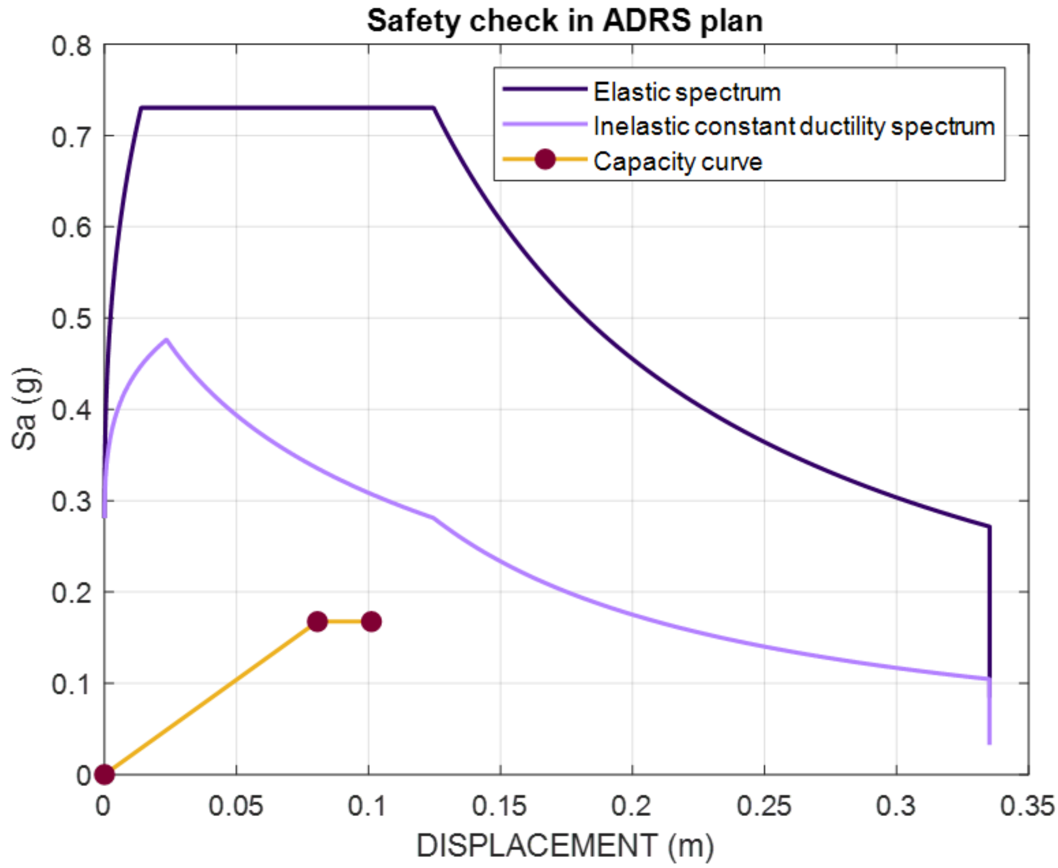

Figure 2.56: Safety check X.DIR Uniform Distribution

2.9.3 Safety check Y direction. SRSS distribution

Table 2.20: Vulnerability index SRSS Distribution Y.DIR

MODAL Y		Vulnerability	
T [s]	0.86	de,max [m]	0.12
m*	608.23	du* [m]	0.10
Say [m/s2]	4.09	dy* [m]	0.077
Say [g]	0.41	μc	1.4
Sae [g]	0.70	q∼*	1.391
q*	1.68	de,max∼* [m]	0.10
μd	1.686	ζ_E	0.832

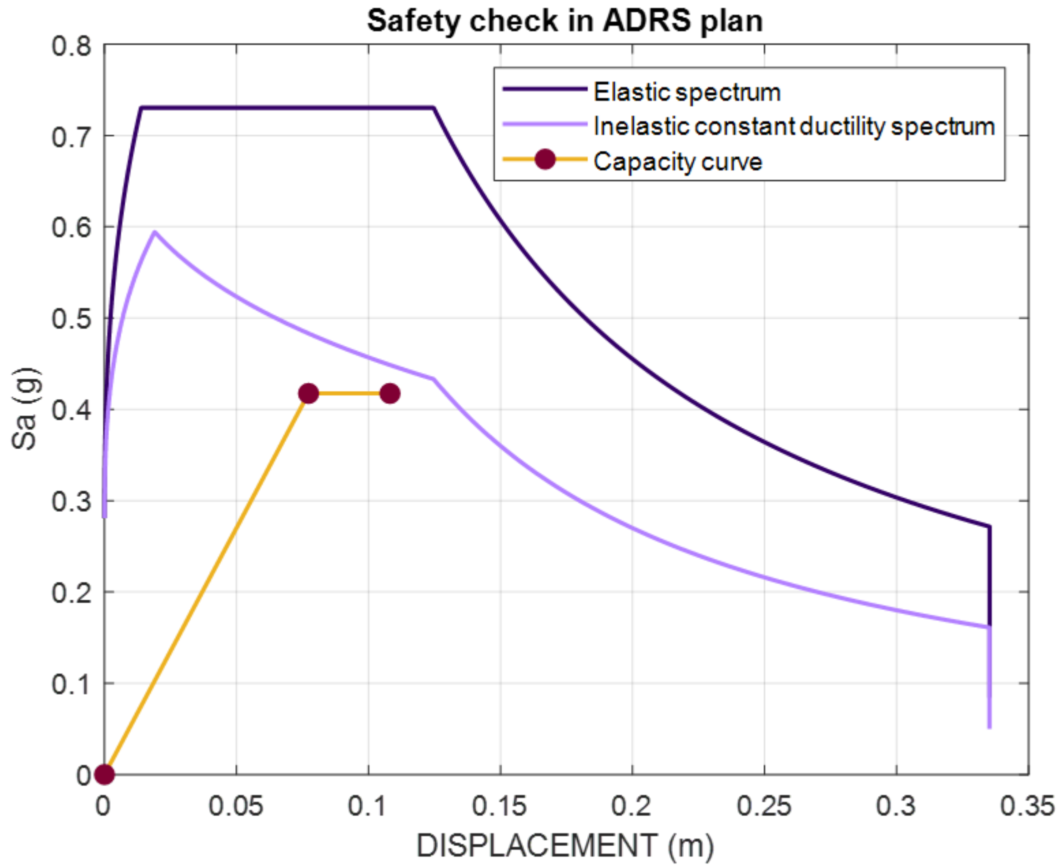

Figure 2.57: Safety check Y.DIR SRSS Distribution

2.9.4 Safety check Y direction. Uniform distribution

Table 2.21: Vulnerability index Uniform Distribution Y.DIR

MASS Y		Vulnerability	
T [s]	0.664	de,max [m]	0.080
m*	675.563	du* [m]	0.091
Say [m/s2]	6.530	dy* [m]	0.073
Say [g]	0.666	μc	1.241
Sae [g]	0.730	q∼*	1.193
q*	1.097	de,max∼* [m]	0.087
μd	1.121	ζ_E	1.088

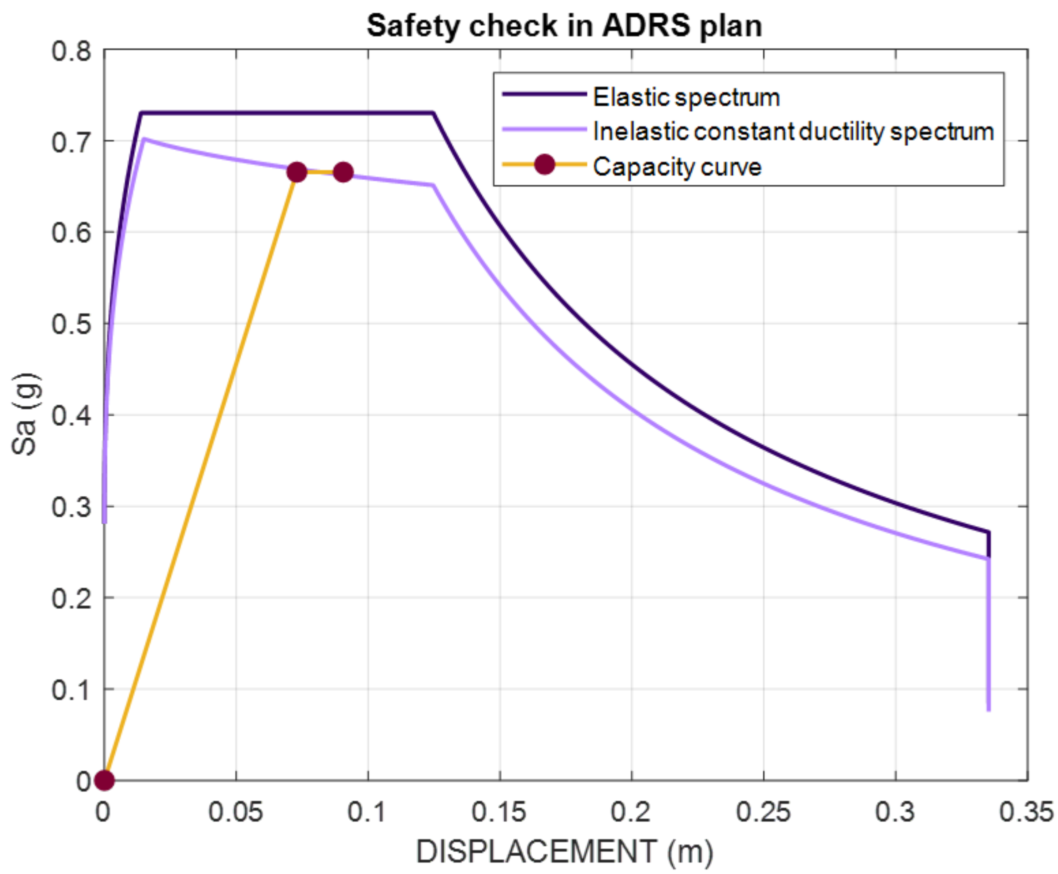

Figure 2.58: Safety check Y.DIR Uniform Distribution

2.9.5 Safety check -X direction. SRSS distribution

Table 2.22: Vulnerability index SRSS Distribution -X.DIR

MODAL X		Vulnerability	
T [s]	1.32	de,max [m]	0.199
m*	976.51	du* [m]	0.081
Say [m/s2]	1.6272	dy* [m]	0.072
Say [g]	0.1659	μc	1.126
Sae [g]	0.4551	q∼*	1.126
q*	2.7438	de,max∼* [m]	0.081
μd	2.7438	ζ_E	0.408

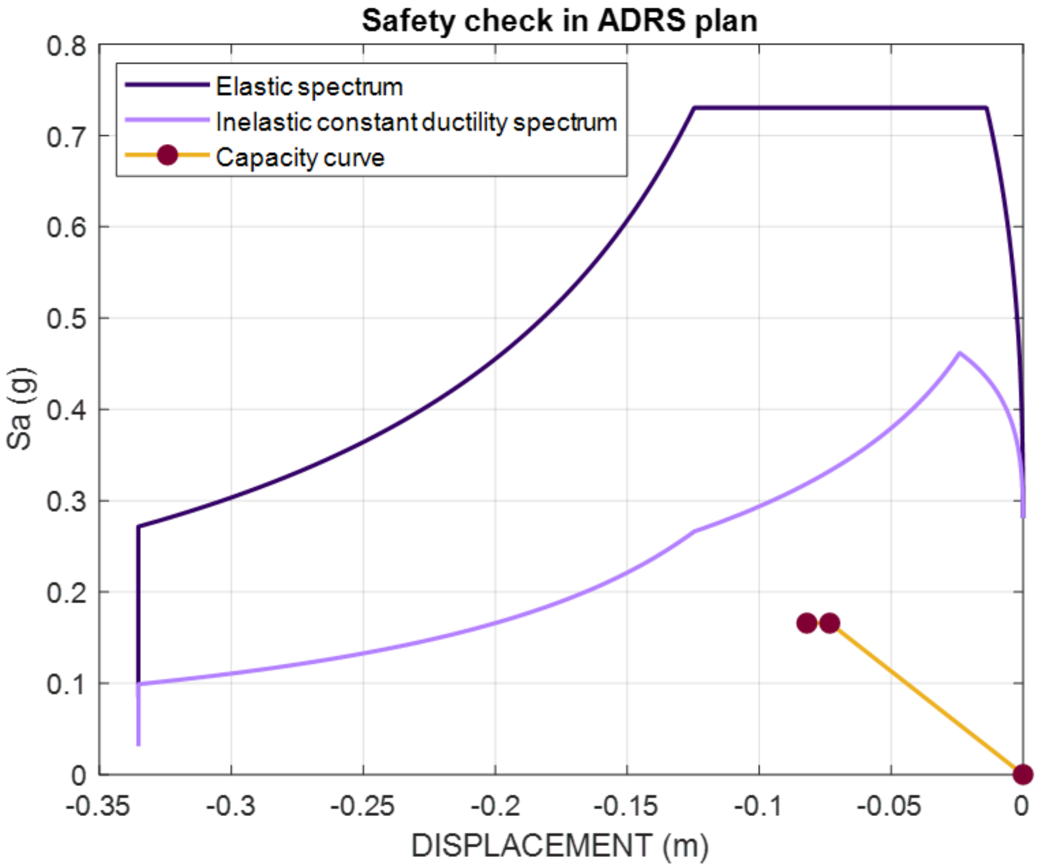

Figure 2.59: Safety check -X.DIR SRSS Distribution

2.9.6 Safety check -X direction. uniform distribution

Table 2.23: Vulnerability index Uniform Distribution -X.DIR

MASS X		Vulnerability	
T [s]	1.38	de,max [m]	0.208
m*	763.75	du* [m]	0.101
Say [m/s2]	1.6437	dy* [m]	0.080
Say [g]	0.1676	μc	1.265
Sae [g]	0.4355	q∼*	1.265
q*	2.5990	de,max∼* [m]	0.101
μd	2.5990	ζ_E	0.484

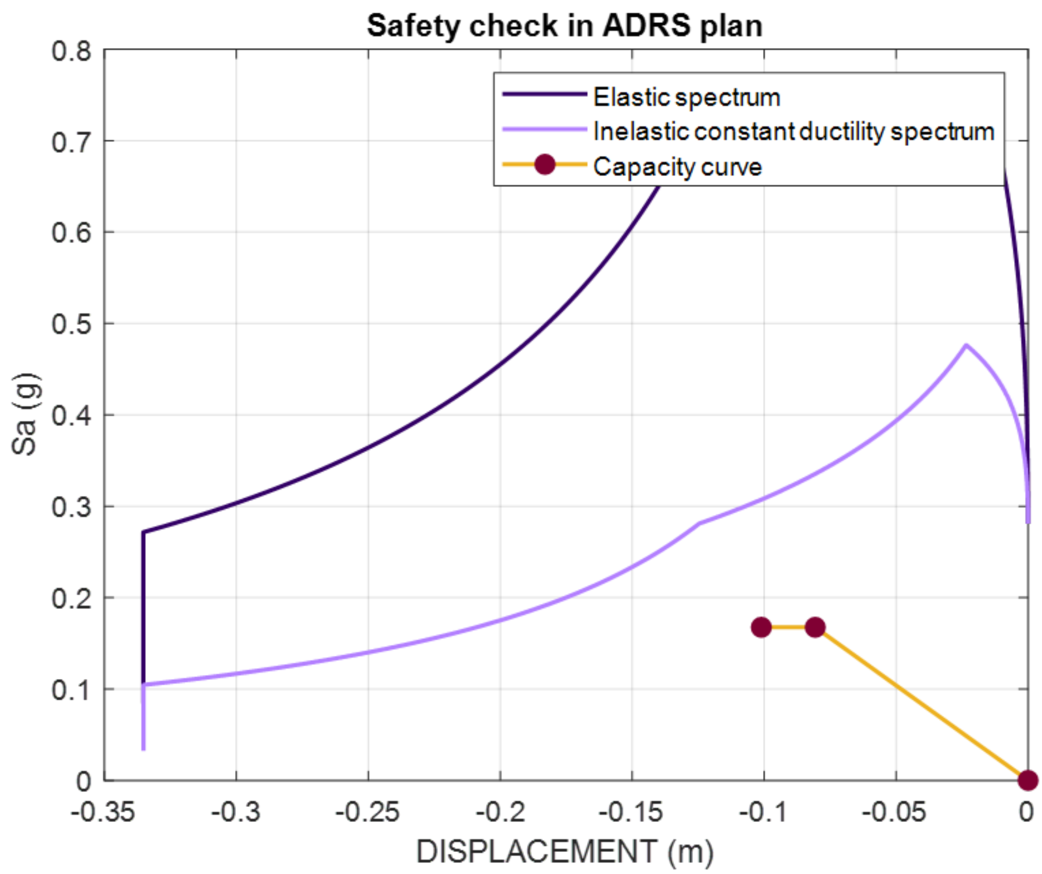

Figure 2.60: Safety check -X.DIR Uniform Distribution

2.9.7 Safety check -Y direction. SRSS distribution

Table 2.24: Vulnerability index SRSS Distribution -Y.DIR

MODAL Y		Vulnerability	
T [s]	0.86	de,max [m]	0.129
m*	608.24	du* [m]	0.093
Say [m/s2]	4.0949	dy* [m]	0.077
Say [g]	0.4174	μc	1.209
Sae [g]	0.7038	q∼*	1.209
q*	1.6861	de,max∼* [m]	0.093
μd	1.6861	ζ_E	0.718

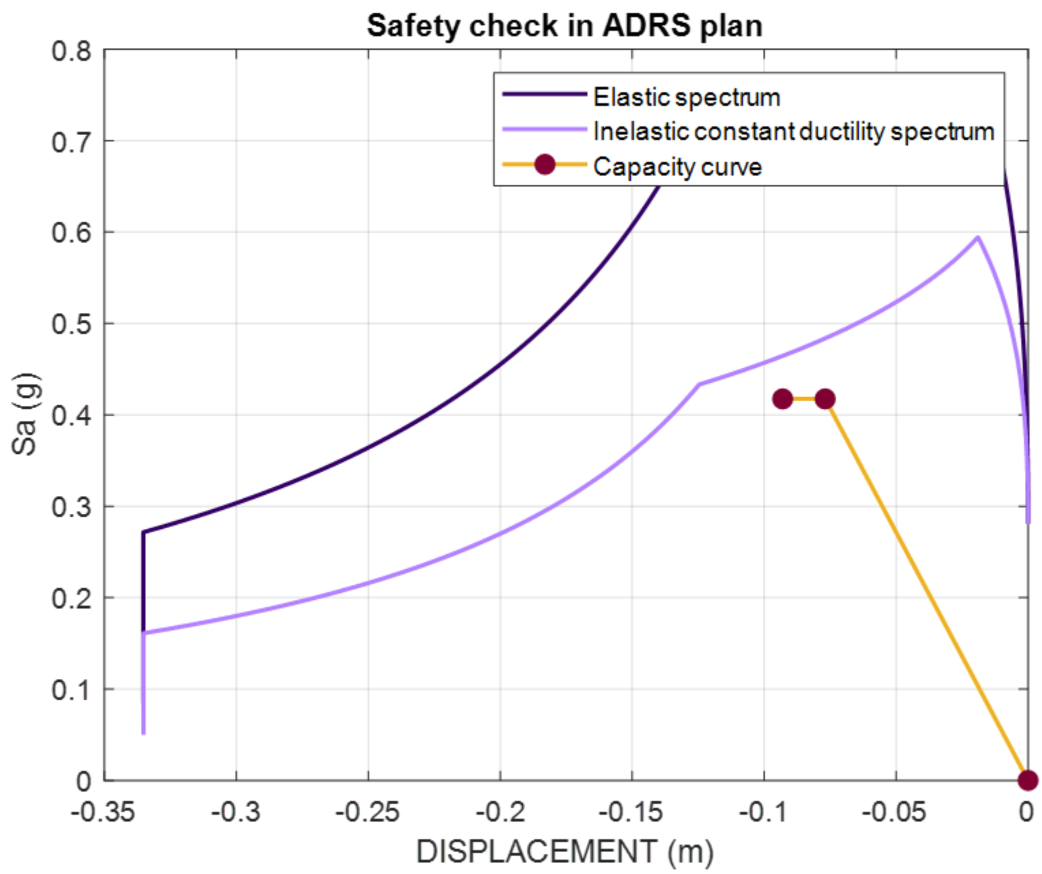

Figure 2.61: Safety check -Y.DIR Uniform Distribution

2.9.8 Safety check -Y direction. Uniform distribution

Table 2.25: Vulnerability index Uniform Distribution -Y.DIR

MASS Y		Vulnerability	
T [s]	0.66	de,max [m]	0.080
m*	675.56	du* [m]	0.094
Say [m/s2]	6.5296	dy* [m]	0.073
Say [g]	0.6656	μc	1.290
Sae [g]	0.7304	q∼*	1.232
q*	1.0973	de,max∼* [m]	0.089
μd	1.1217	ζ_E	1.122

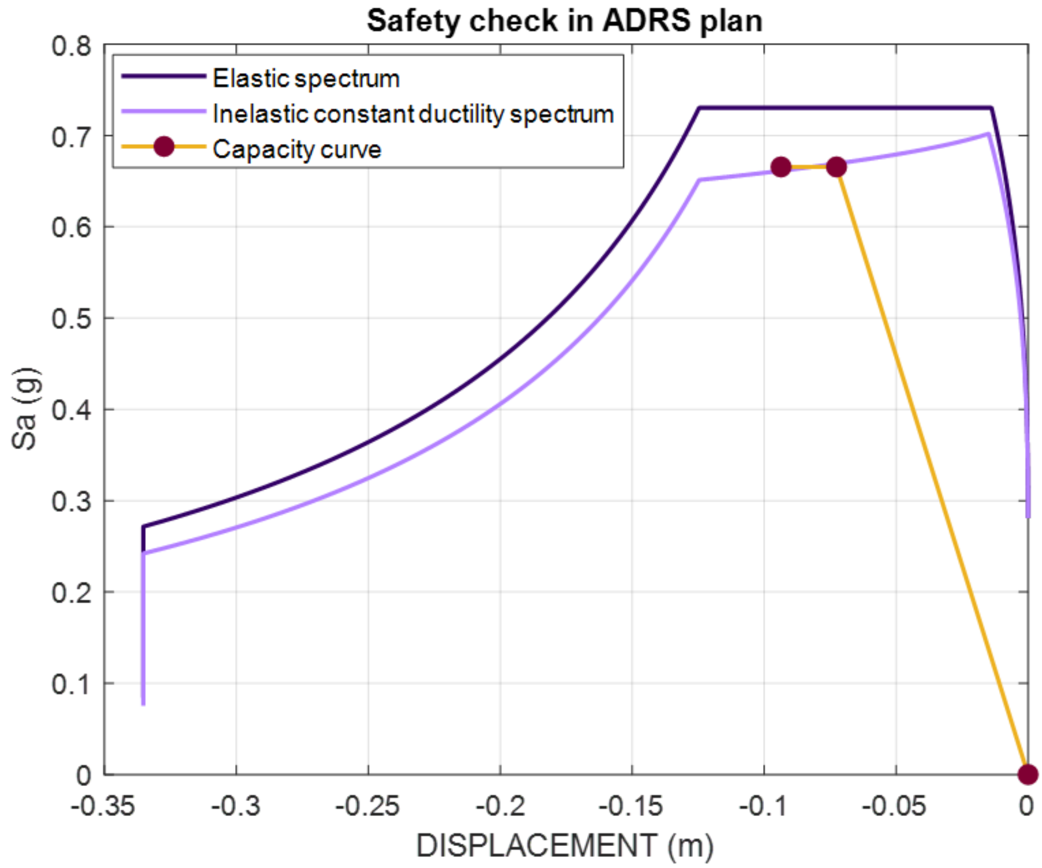

Figure 2.62: Safety check -Y.DIR Uniform Distribution

2.10 SAFETY ASSESSMENT SUMMARY

Table 2.26: Values of ζ_E considering the Distribution Equivalent to the storey Forces

Distribution	Direction	ζ_E
Equivalent	X+	0.409
to the Storey	X-	0.408
Forces	Y+	0.832
(SRSS)	Y-	0.718

We could summarize the safety assessment of this structure by saying that neither X nor Y direction full fill the minimum requirement to guarantee the safety condition. The building exposes a very weak behavior in X direction. In Y direction the lower limit suggests us that the building is vulnerable, not at the same level of

Table 2.27: Values of ζ_E considering the Distribution of uniform accelerations

Distribution	Direction	Zeta
Uniform	X+	0.483
Accelerations	X-	0.484
(Uniform)	Y+	1.088
	Y-	1.122

X direction but still far away from our target. The reality show us that we need to intervene the structure to guarantee its functionality.

Chapter 3

SEISMIC REHABILITATION OF FOGGIA AIRPORT: A INNOVATIVE 3D ARCH EXOSKELETON

Before selecting the most suitable structural retrofitting system, certain criteria were considered by the airport administration, extending beyond technical aspects. The structural response in a nonlinear analysis also provided insights into potential effective techniques. This chapter specifically addresses the type of intervention, the reasons behind its selection, the retrofitting strategy, and its final configuration, preceding the safety assessment of the ultimate structure.

3.1 NONLINEAR RESPONSE OF THE REFERENCE STRUCTURE

As we could observe in the Figures 2.55 2.59, the behavior of the structure is consistently non-dissipative. Nearly all seismic intervention strategies focus on localized improvement, providing better performance within the plastic range. This allows regions prone to early failure to perform better in the plastic range. Our proposal challenges the paradigm of this concept by suggesting a solution that keeps the base structure within the elastic range, while an external structure absorbs the majority of the seismic forces.

The response obtained in our nonlinear analysis demonstrates that our structure will always remain within in elastic range. The design of the truss beams prevents the formation of plastic hinges, directing all energy dissipation to the column level. This situation is reflected in the structural response of our nonlinear analysis, resulting in a curve with predominantly linear behavior and minimal plasticity.

The use of an externally rigid structure provides an opportunity to transfer horizontal forces from the base structure to the one with greater structural rigidity. The type of connection plays a crucial role in determining whether a dissipative behavior is desired or a rigid connection that improves lateral force dissipation without reducing the overall demand.

Under the previously discussed condition, we will proceed to evaluate other aspects that influence the final solution type. As we explored in the first chapter, different categories of external structures offer an optimal response for specific cases. As for the performance of our structure within a non-linear range, it serves as the basis for proposing a methodical and efficient alternative that aligns with the problem at hand.

3.2 NON TECHNICAL CONSTRAINS THAT AFFECT THE SOLUTION

One of the factors that determine the final solution for structural intervention pertains to the structure's functionality. Foggia Airport provides uninterrupted service, which is beneficial to the residents of the nearby regions. Therefore, any invasive intervention within this structure is not considered a feasible option.

In addition, it is essential to adhere to the guidelines provided by the airport administration, specifically in preserving the facades of the main entrances and the bus arrival area, which transports passengers from neighboring areas to the runways. These conditions must be respected as part of the overall considerations.

Figure 3.1: Top view Foggia Airport, zones of principal constrains

These limitations will directly determine the type of structural intervention. The rear area, as depicted in Figure 3.1, refers to the vehicular access point where users are picked up or dropped off. The front area, as shown, is the airport's main entrance.

3.3 THEORETICAL FRAMEWORK FOR DETERMINING STRUCTURAL INTERVENTION STRATEGIES

As demonstrated in the preceding sections of this chapter, our case study initially exhibits elastic behavior with limited energy dissipation prior to the potential structural collapse. Furthermore, the airport administration deems it unfeasible to implement an invasive intervention that would affect the entire building's perimeter facades.

Considering the available information and an extensive review of the existing literature, it is apparent that the most suitable seismic intervention approach is of an external nature, one that effectively maintains the entire base structure within an elastic range prior to the initiation of structural failure. This implies that our base structure must remain within the elastic range until the first plastic hinge forms within the external structure.

In light of this, we present three potential alternatives that could provide viable solutions for our case study:

Parallel Exoskeleton: This structural solution is designed to proficiently control lateral displacement of the base structure, enhancing its torsional behavior. It absorbs a portion of the seismic forces, standardizes the global behavior of the structure, and ensures that it exhibits its anticipated primary modal shapes.

Perpendicular Exoskeleton or Shear Wall: This form of structure reinforces specific connection nodes, drawing a significant share of seismic forces. However, it operates unidirectionally and may be susceptible to torsional damage. Additionally, it alters the modal analysis of the combined structure by introducing local modes.

Three-Dimensional Exoskeleton: This particular exoskeleton design amalgamates elements from both of the previous solutions. It becomes an optimal choice when there is a need to disrupt the continuity of the appendix structure. However, it does not achieve complete regularization of the base structure, requiring efficient placement for an improved global response. This design diverts lateral forces from the structure in a primary plane, akin to the perpendicular exoskeleton, while also mitigating them in the opposite direction on a smaller scale, without introducing torsional weaknesses.

Given the distinct characteristics of our base structure, the decision was made to implement a three-dimensional exoskeleton system. The vast perimeter of the Foggia airport site led us to forgo the idea of completely enveloping the base structure to enhance the final response, as this could result in an overdimensioned intervention. Therefore, we opted for a system of three-dimensional exoskeletons.

3.4 CHARACTERISTICS OF THE SELECTED COUPLED SYSTEM

The selection of three-dimensional exoskeletons was based on a theoretical approach aimed at achieving maximum stiffness in minimal space. This approach involved considering a hyperstatic structure known for its high rigidity and minimal displacement in the primary plane of action. In the domain of structural engineering, it is evident that spherical structures exhibit substantial rigidity and tend to transmit forces axially.

The integration of a series of exoskeletons placed strategically around the base structure's perimeter allows for precise control of the structure's displacements. The inclusion of a limited number of exoskeletons can effectively mitigate torsional effects and enhance the structure's seismic performance. Conversely, the incorporation of an extensive number of exoskeletons positions the entire system within the range of short periods, thus altering the ductility assumptions and causing the structure to fall below the limits of Tc.

Our base structure consists of a framework that offers attachment points for exoskeletons at beam-column connections. The exoskeletons are expected to be placed over a foundation system separate from the base structure. It is imperative to emphasize that energy dissipation is not a significant factor in our theoretical framework; as such, our connection is designed to be rigid.

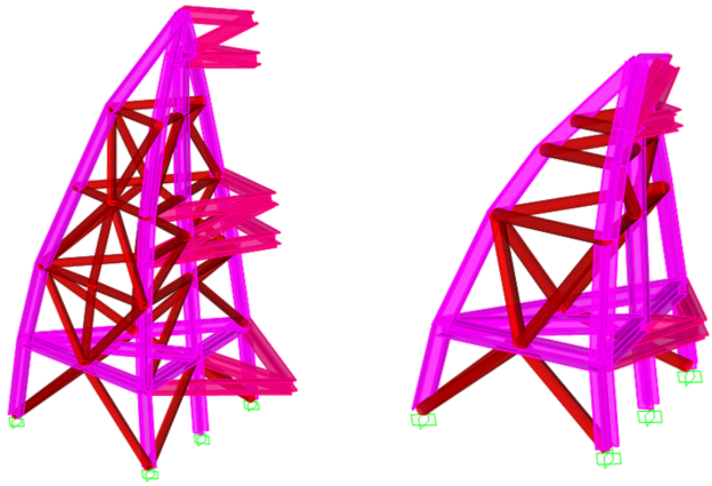

Figure 3.2: Non-scaled three-dimensional exoskeletons

3.4.1 Geometry of exoskeletons

Having established the seismic intervention criteria, we now proceed to define the morphology of our three-dimensional exoskeletons, which are crucial components of the structural retrofitting. Our approach involves precise engineering calculations without unnecessary abstraction.

As a primary consideration, the depth and width of the exoskeleton are directly tied to the height of the building under consideration. In practical terms:

The depth is constrained by a simple 1/2 ratio with respect to the building's height.

The width varies according to the size of the exoskeleton. For smaller exoskeletons, it is set at a 2/3 ratio to the building's height. In the case of larger exoskeletons, a 1/2 ratio is applied to avoid any overlap between neighboring exoskeletons.

When determining the radius of the arches within the exoskeleton structure, we didn't rely on a direct geometric guideline but instead tested their performance concerning the axial forces they could sustain.

Given the specific building height of 10.60 meters in our case, we established that the radius should be approximately four times the exoskeleton's depth. Smaller-radius arches might exhibit superior performance but would necessitate a greater exoskeleton depth, potentially resulting in an oversized retrofitting structure. The Figure 3.3

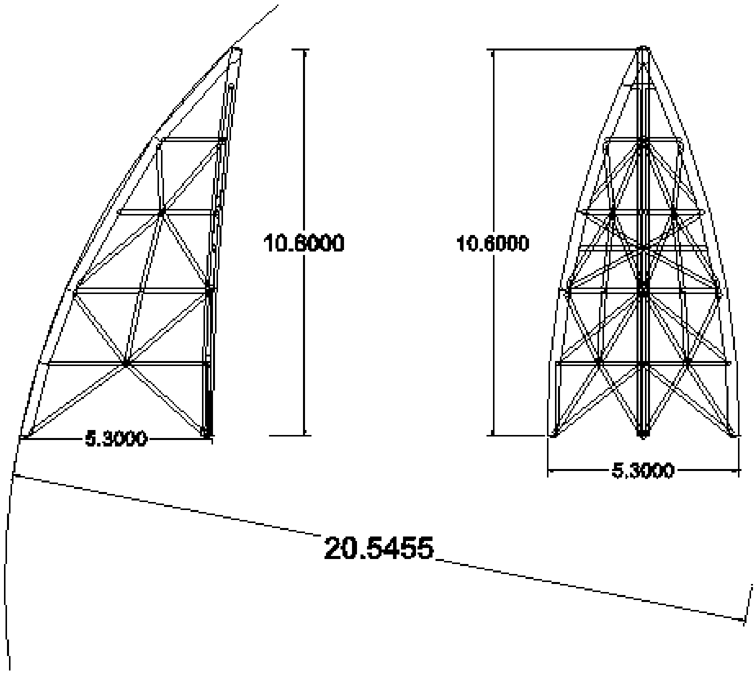

Figure 3.3: Scheme of the geometry of exoskeletons

3.4.2 Initial Placement of Exoskeletons

Initially, the exoskeletons were arranged alternately along the primary axes of the frames. This initial configuration necessitates the development of a strategy aimed at utilizing the fewest possible exoskeletons while ensuring structural stability.

Furthermore, it's important to note that exoskeletons, on their own, do not constitute the entire structural intervention strategy. Complementary horizontal bracings play a vital role by connecting the slab, enabling it to behave as a rigid body. This intervention is minimally invasive and is essential to maximize the efficiency of the exoskeletons while significantly reducing the number of local modes within the base structure.

The specific positioning of each exoskeleton with respect to the reference structure is influenced by non-structural elements that prohibit close proximity. Consequently, the dimensions of the rigid connections are designed with substantial inertia.

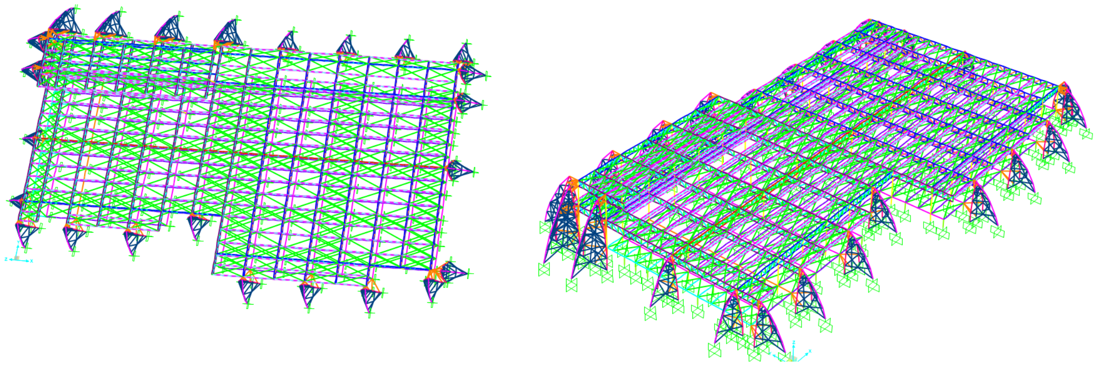

Figure 3.4: Initial placement of exoskeletons

3.4.3 Connection of Horizontal Bracing at Slab Level

One of the initial deficiencies we identified during our survey was the absence of a horizontal bracing system in the slabs. This absence prevents us from assuming rigid body behavior in the slabs within our structural analysis, thus leading to localized issues within the building. The use of horizontal bracing becomes an imperative necessity for slabs lacking a monolithic system, especially in the context of roof structures constructed with truss beams. This strategic addition serves to uphold the structural shape and integrity.

A structural modeling exercise was performed with the objective of reducing the mass participation ratio in localized vibration modes. The results of this exercise have demonstrated the potential to capture 85% of the mass participation factor in the X direction with just three vibration modes and 85% in the Y direction with only five vibration modes. These results signify a substantial improvement compared to the base scenario.

In the case of the raised floor, it was necessary to incorporate a considerable number of bracings with exceptional efficiency, effectively achieving behavior closely resembling that of a rigid body. A comparative analysis between scenarios involving a rigid diaphragm and those without indicated that the number of modes exhibiting the highest modal participation was consistent between them, with only a minor variance in the Y direction.

This exercise has been instrumental in determining the most optimal bracing configuration for minimizing the number of vibration modes within the structure.

The subsequent figure visually illustrates the variation in some horizontal bracing configurations until arriving at the most optimal solution.

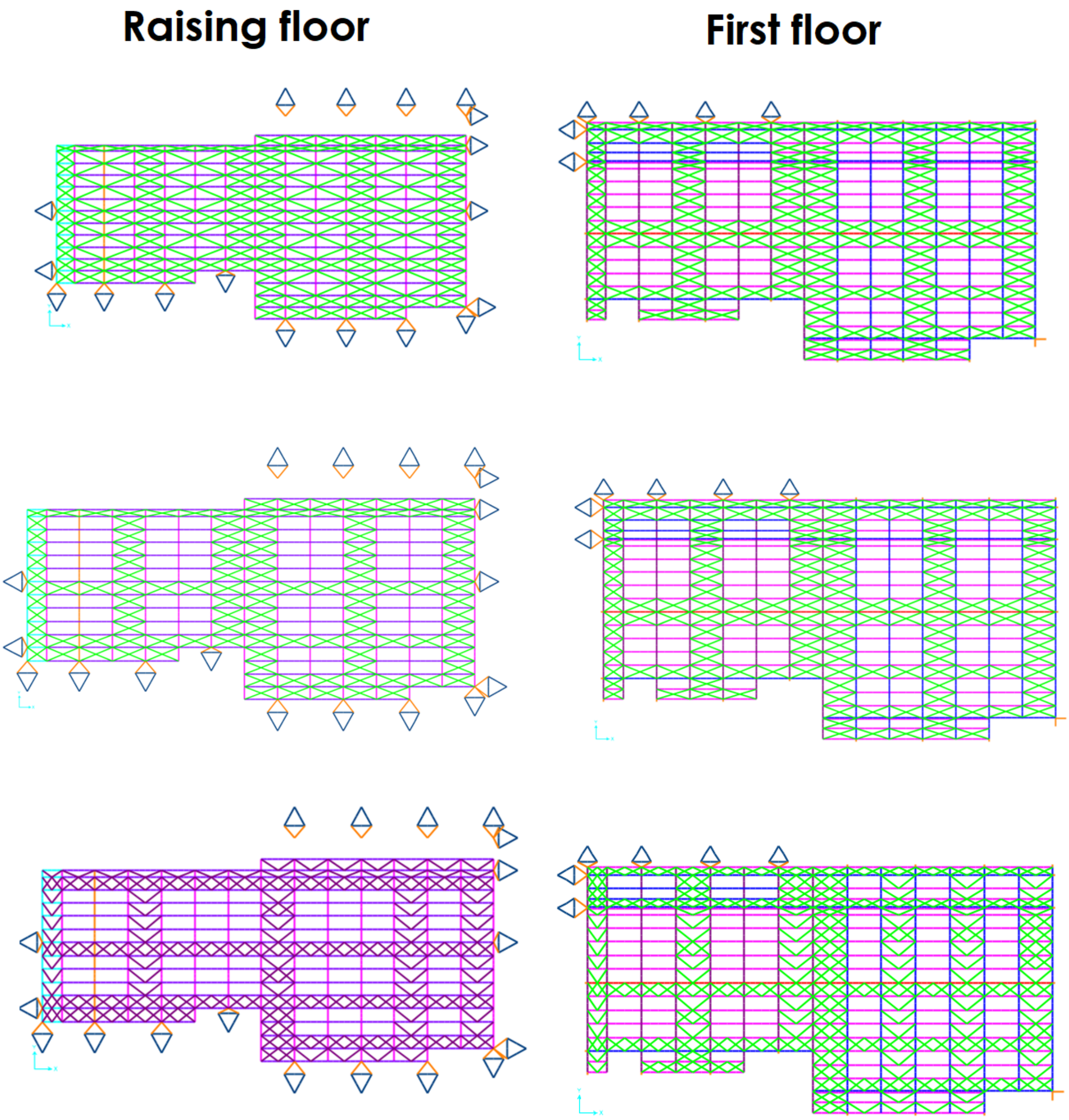

Figure 3.5: Bracing configuration

Table 3.1: Bracing arrangement N°27. Mass participation factor X.dir

Trial 27 - Mass participation factor X.dir		
Mode	**Period (s)**	**UX (unitless)**
1	0.3056	0.683
36	0.2536	0.103
18	0.2682	0.082
-	-	86.80%

Table 3.2: Bracing arrangement N°27. Mass participation factor Y.dir

Trial 27 - Mass participation factor Y.dir		
Mode	**Period (s)**	**UY (unitless)**
208	0.16425	0.506
40	0.250952	0.21217
190	0.193584	0.07509
170	0.215141	0.0457
169	0.216226	0.04006
-	-	87.90%

3.5 ASSESSMENT OF THE FINAL EXOSKELETON CONFIGURATION

The final configuration scheme for the exoskeletons is not determined through a specific method or standardized process but rather evolves through an iterative procedure. This process takes into account variables such as the quantity of exoskeletons, their positioning, and the cross-sectional element dimensions.

In our analysis, the initial criterion is the seismic vulnerability coefficient, obtained from a nonlinear analysis. While our regulations stipulate a minimum criterion that the structure must meet, it proves insufficient for our specific case. Our structure must demonstrate its capability to remain within an elastic range under the seismic demand. Moreover, it is crucial to ensure that the exoskeletons are functioning efficiently.

Recent research on exoskeletons [14] [15] [8] suggests that they should substantially reduce the shear forces at the base of the reference structure, preventing it from reaching a failure condition that would necessitate retrofitting.

The moment we observe a reduction in the final demand on the reference structure, we can infer that the reference structure is being laterally unloaded. This criterion is not arbitrary; it is based on the understanding that the failure mechanism of the structure is not energy-dissipative, and a sudden failure poses a significant risk to occupants.

Our objective is to ensure that, under all circumstances, the structure remains within an elastic range before the coupled system undergoes permanent deformations. In essence, we aim to force the failure within the exoskeletons, ensuring that the base structure never reaches a state of plastic deformation.

Nonlinear analysis provides us with a continuous perspective in which we can observe the development of plastic hinges during the distribution of forces.

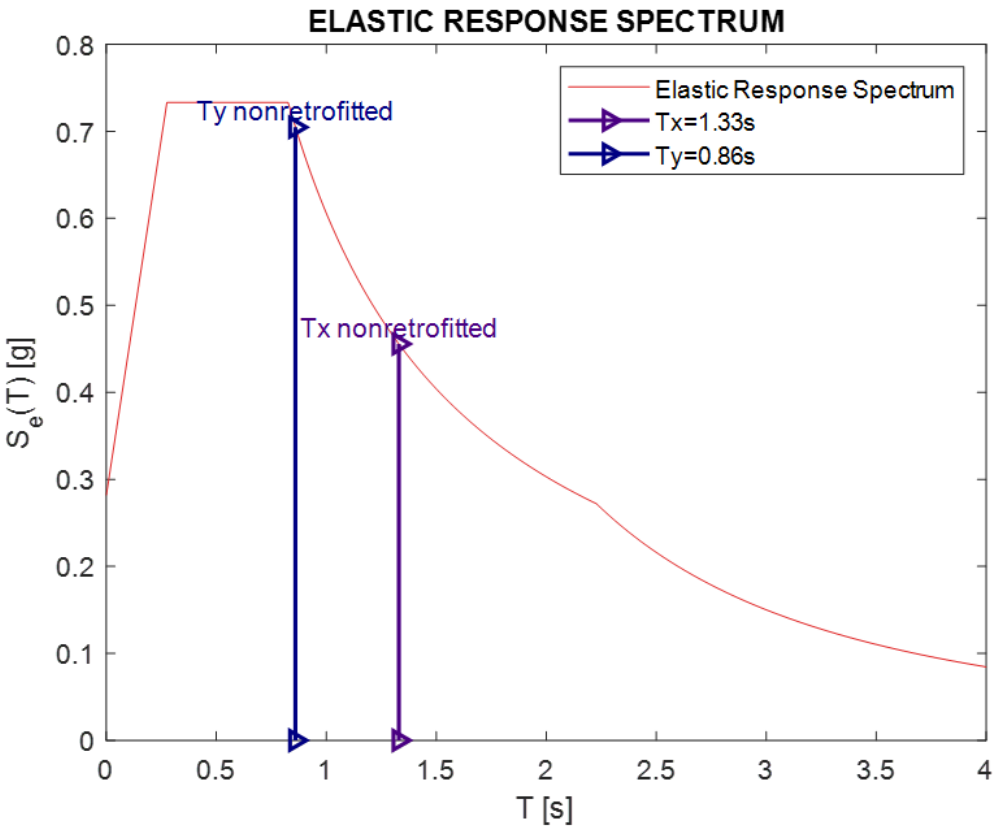

Figure 3.6: Non-retrofitted fundamental periods Xdir Ydir

3.5.1 First Strategy

Bringing the structure's periods in the descendent side of Tc and minimizing the number with a total mass participation ratio of at least 85

The initial strategy, carried out before we begin a nonlinear analysis, involves two key goals:

1. Avoiding the region in the response spectrum where strong accelerations occur, precisely the plateau. In our specific study, the challenge arises because our structure is highly flexible and not very rigid. This means it easily operates in the zone of longer periods. Exoskeletons add extra stiffness, which could push the structure into the plateau, where seismic responses reach their highest accelerations. This challenges our initial design idea.

1. Reducing the number of vibration modes so that their total mass participation ratio stays at or above 85%. This approach is based on the concept of regularity, where we assume that a structure's main mode in the analytical direction has the highest mass participation ratio and displays translational movement.

Table 3.3: Exoskeletons in all the perimeter

INITIAL CONFIGURATION			
Y dir	T(s)	acc (g)	UY
Mode 208	0.164	0.548	0.504
Mode 40	0.251	0.689	0.212
Mode 190	0.194	0.595	0.075
Mode 170	0.215	0.631	0.046
Mode 169	0.216	0.632	0.040
-	-	-	-
Xdir	T(s)	acc (g)	UX
Mode 1	0.306	0.730	0.683
Mode 36	0.254	0.694	0.104
Mode 18	0.268	0.717	0.080

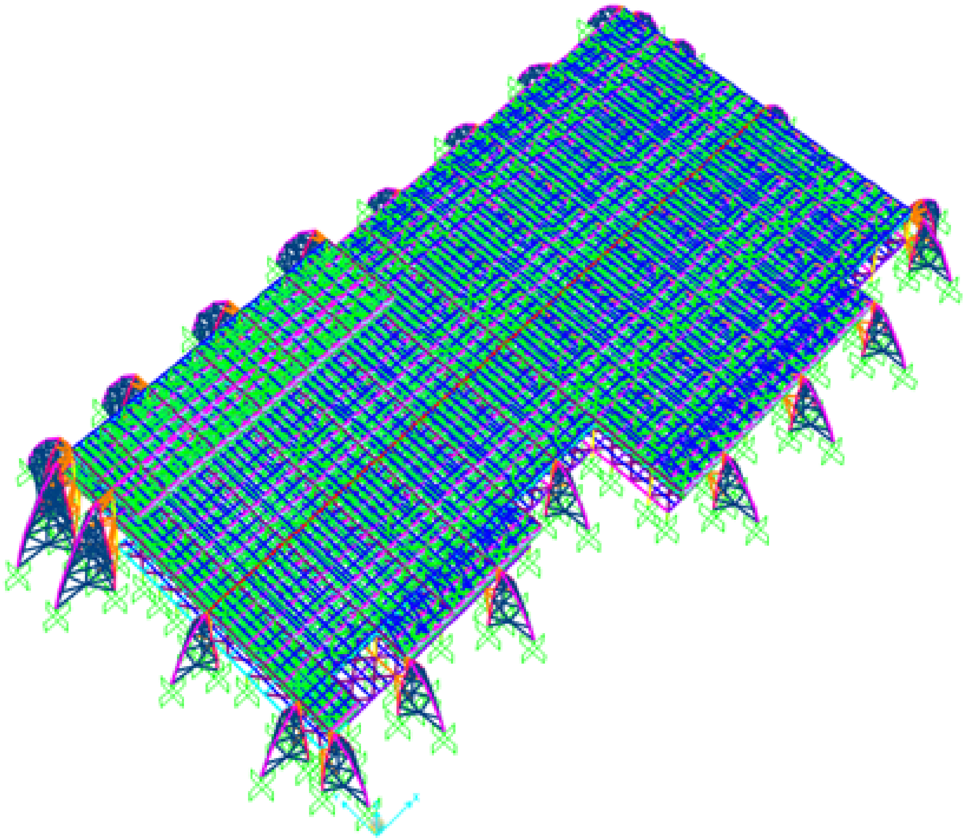

Figure 3.7: Layout initial configuration

Table 3.4: Second configuration, 14 exoskeletons

Second Configuration			
Y dir	T(s)	acc (g)	UY
Mode 210	0.167642	0.5525929	0.40865
Mode 4	0.296667	0.73035707	0.20715
Mode 209	0.168782	0.55584689	0.06208
Mode 2	0.35379	0.73035707	0.03957
Mode 218	0.150443	0.52493401	0.03894
Mode 138	0.23613	0.66485546	0.03848
Mode 211	0.165098	0.54933891	0.02625
Mode 23	0.267446	0.71529226	0.02385
Mode 204	0.169856	0.55747388	0.0238
X dir	T(s)	acc (g)	UX
Mode 1	0.401914	0.73035707	0.62163
Mode 3	0.3216	0.73035707	0.26966

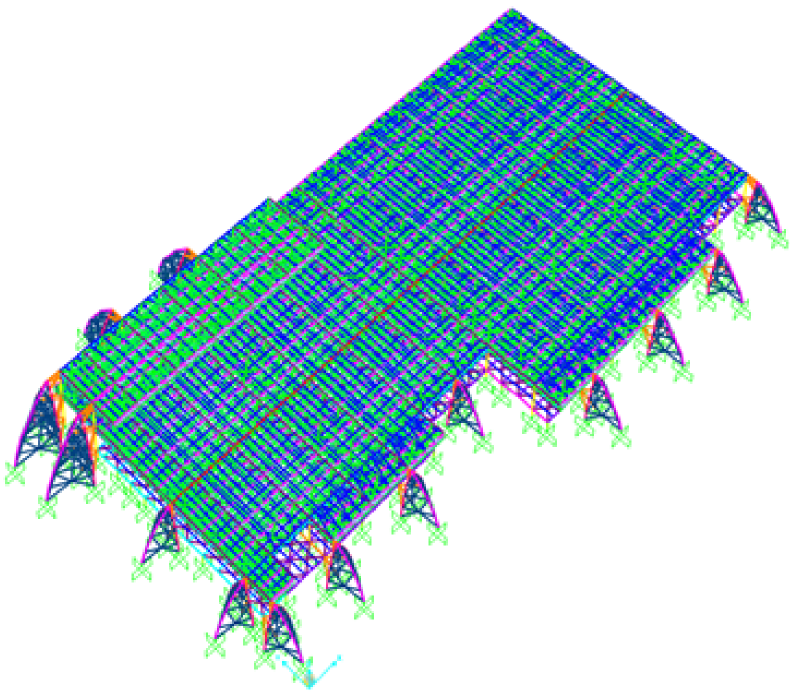

Figure 3.8: Layout Second configuration of Exoskeletons

Table 3.5: Third Configuration: 12 Exoskeletons

Third Configuration			
Y dir	T(s)	acc (g)	UY
Mode 203	0.174	0.564	0.375
Mode 4	0.314	0.730	0.144
Mode 2	0.366	0.730	0.108
Mode 204	0.174	0.562	0.101
Mode 211	0.167	0.551	0.044
Mode 5	0.292	0.730	0.042
Mode 202	0.175	0.566	0.032
Mode 201	0.176	0.567	0.031
X dir	T(s)	acc (g)	UX
Mode 1	0.407	0.730	0.611
Mode 3	0.324	0.730	0.272

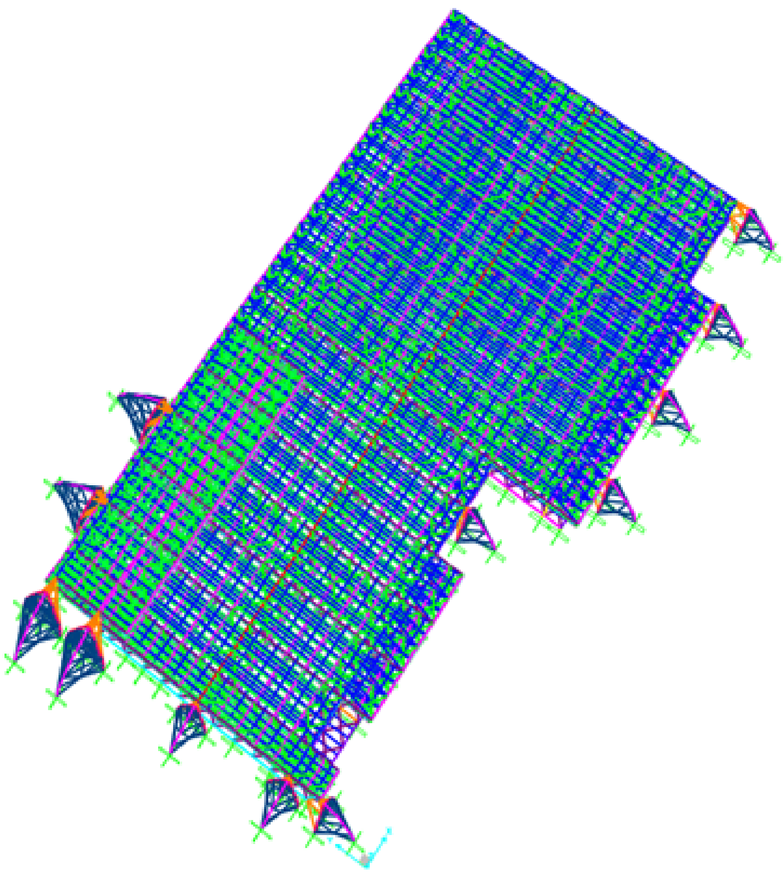

Figure 3.9: Layout Third configuration of Exoskeletons

Table 3.6: Fourth Configuration: 14 Exoskeletons

Fourth Configuration			
Y dir	T(s)	acc (g)	UY
Mode 201	0.174	0.564	0.413
Mode 3	0.313	0.730	0.246
Mode 202	0.174	0.564	0.117
Mode 199	0.176	0.567	0.031
Mode 6	0.289	0.730	0.030
Mode 209	0.166	0.551	0.023
X dir	T(s)	acc (g)	UX
Mode 1	0.390	0.730	0.695
Mode 2	0.318	0.730	0.205

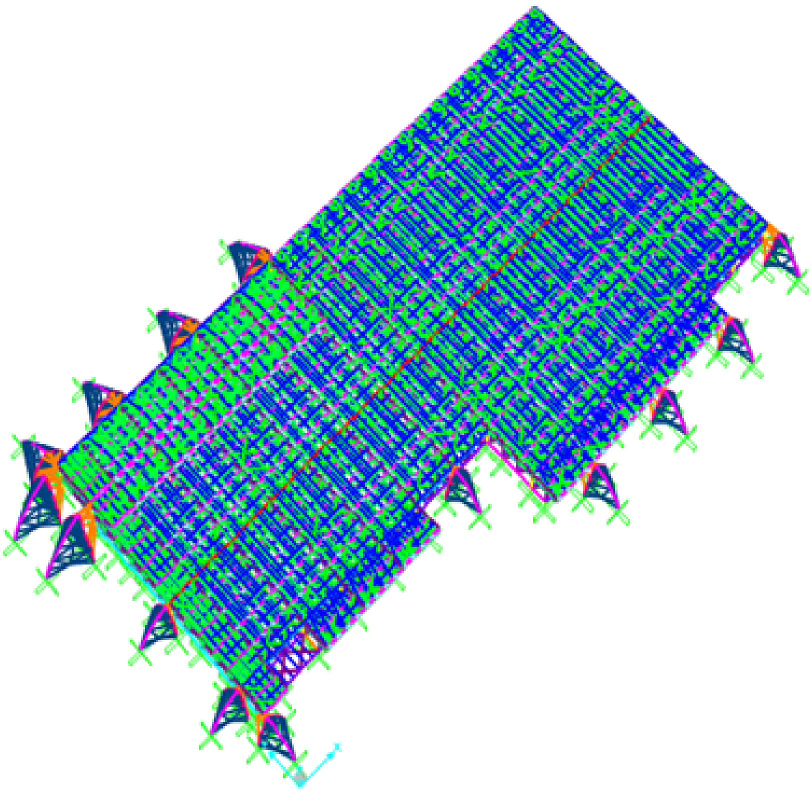

Figure 3.10: Layout Fourth configuration of Exoskeletons

Table 3.7: Fifth Configuration: 12 Exoskeletons

Fifth Configuration			
Y dir	T(s)	acc (g)	UY
Mode 2	0.338	0.730	0.257
Mode 210	0.166	0.551	0.214
Mode 195	0.189	0.588	0.188
Mode 179	0.211	0.623	0.095
Mode 4	0.292	0.730	0.038
Mode 191	0.196	0.600	0.029
Mode 193	0.193	0.595	0.027
X dir	T(s)	acc (g)	UX
Mode 1	0.399	0.730	0.647
Mode 3	0.323	0.730	0.261

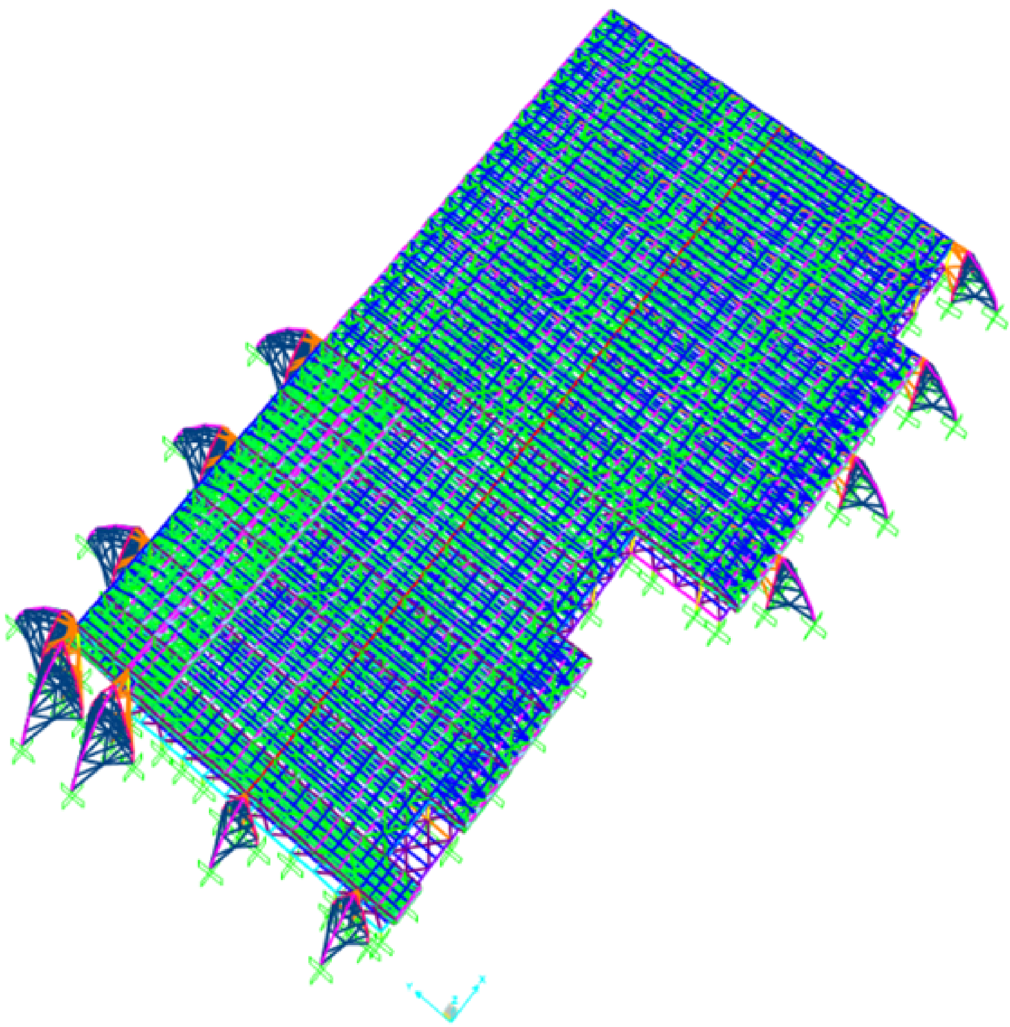

Figure 3.11: Layout Fifth configuration of Exoskeletons

As observed in Figure 3.6, our goal was to ensure that the structure remains away from the plateau with longer periods greater than Tc in the X-direction. However, when we applied our retrofitting solution, it automatically introduced a significant level of stiffness to the coupled system. With just four exoskeletons, the structure reached the beginning of the plateau.

A quick analysis to verify the efficiency of the exoskeletons revealed that, under seismic demand, the base structure maintained the same base shear force that leads to failure without retrofitting. This demonstrates that our initial hypothesis of improving the behavior of the less rigid structure is not valid. The exoskeletons were unable to reduce the base shear force that causes failure in the initial condition. This situation prompts us to consider an alternative strategy where we provide more stiffness to the system and potentially shift our structure to lower values than Tb.

3.5.2 Second Strategy

The second strategy for achieving the best final configuration involves checking the reduction in demand on the reference structure. The most straightforward way to do this is to ensure that the base shear of the reference structure is lower than the condition without retrofitting. At this stage, we also verify the vulnerability coefficient, considering the distribution of forces proportional to the floor forces (referred to as the SRSS distribution in this document). This allows us to quickly identify two key criteria for ensuring the efficiency of our design.

To make this comparison, we considered the base shear of the original structure obtained using the capacity curve in the X+ and Y- directions, along with distributions of forces proportional to the floor forces. Since the X-direction is the most critical, we used the final configuration from the previous analysis. However, as this configuration did not efficiently reduce the building's seismic response, we added exoskeletons to the other side of the building.

Next, we adjusted the dimensions of the exoskeleton cross-sections to control their stiffness. Increasing exoskeleton stiffness attracts higher seismic forces. Additionally, we aimed to ensure that plastic hinge formation in the exoskeletons occurs outside the seismic demand range, allowing them to remain within the elastic range. It's important to note that this type of three-dimensional exoskeleton exhibits limited ductility.

Table 3.8: Configuration N°6, Cross section properties of exoskeletons. X. Dir

Description				
Typ of element	Cross section	Area (mm2)	Fyd (Mpa)	P capacity (N)
Main arcs	HEA220	7684	350	2689400
skeletons Bracings	TUBO (219.1x5)	3363	350	1177050
Links	HEA220	7684	350	2689400

Table 3.9: Configuration N°6, Comparative between shear at the base and vulnerability index. X.Dir

Non retrofitted	Coupled Structure						
Vb (kN)	X Direction	Primary Vb (kN)	Exoskeleton Vb (kN)	Total (kN)	T (s)	Sa (g)	V. index
2009.37	Final Step	2055.511	21456.388	23511.899	0.3	0.73	1.413
	Elastic Demand	1454.7141	15184.988	16639.7021			

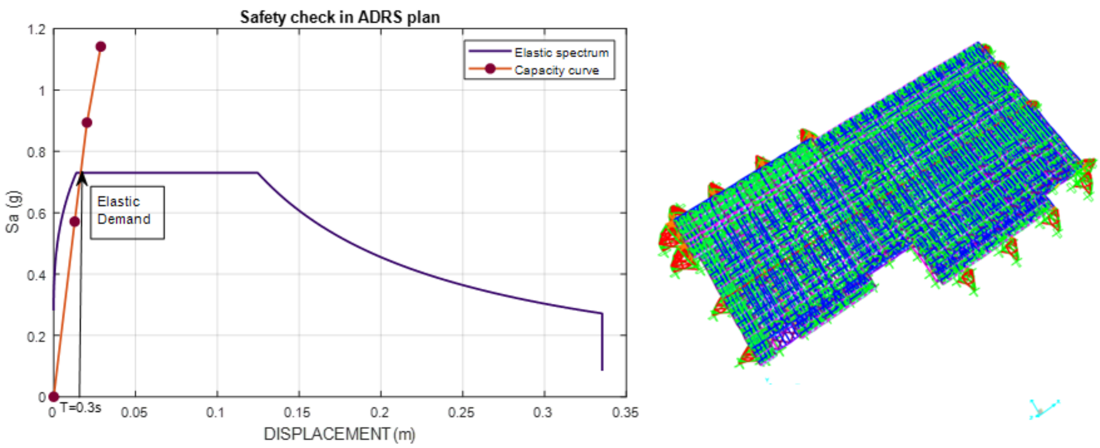

Figure 3.12: Configuration N°6: Safety check and Demand control. X. Dir

Table 3.10: Configuration N°7, Cross section properties of exoskeletons X.Dir

Description				
Typ of element	Cross section	Area (mm2)	Fyd (Mpa)	P capacity (N)
Main arcs	HEB 300	14900	350	5215000
skeletons Bracings	TUBO 244.5 X 5.4	4056	350	1419600
Links	HEB 300	14900	350	5215000

Table 3.11: Configuration N°7, Comparative between shear at the base and vulnerability index. X. Dir

Non retrofitted Vb (kN)	X Direction	Primary Vb (kN)	Exoskeleton Vb (kN)	Total (kN)	T(s) (s)	Sa (g) (g)	V. index
2009.37	Final Step	2735.83	36314.17	39050	0.23	0.66	2.79
	E. Demand	980.58	13015.83	13996.42			

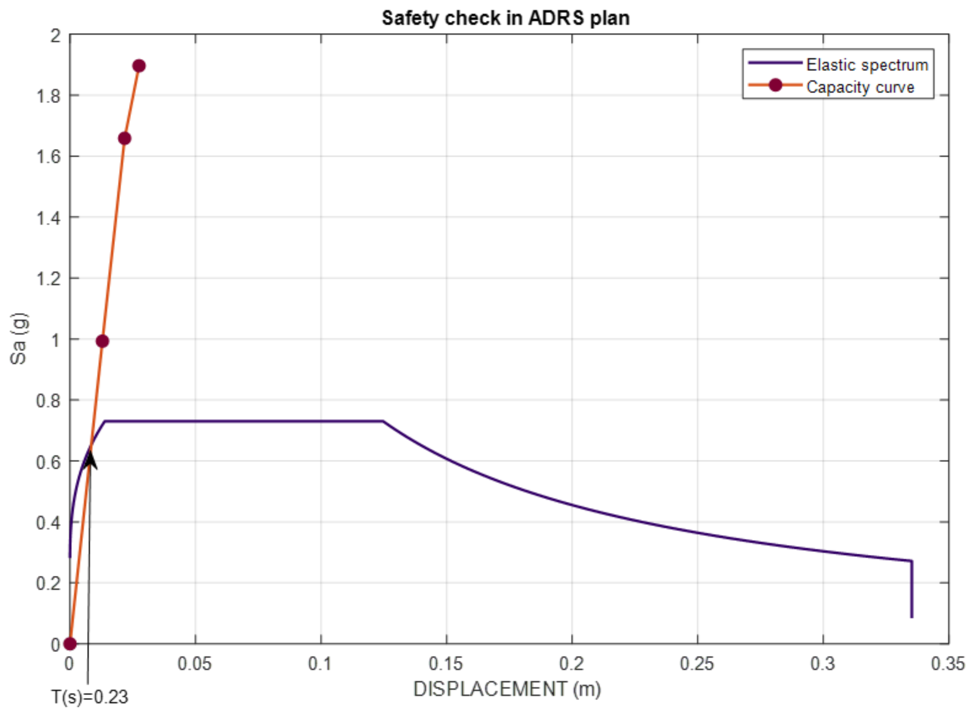

Figure 3.13: Configuration N°7: Safety check and Demand control. X. Dir

Table 3.12: Configuration N°8, Cross section properties of exoskeletons X.Dir

Description				
Typ of element	Cross section	Area (mm2)	Fyd (Mpa)	P capacity (N)
Main arcs	HEB 260	11800	350	4130000
skeletons Bracings	TUBO (219.1x5)	3363	350	1177050
Links	HEB 260	11800	350	4130000

Table 3.13: Configuration N°8, Comparative between shear at the base and vulnerability index. X. Dir

Non retrofitted Vb (kN)	X Direction	Primary Vb (kN)	Exoskeleton Vb (kN)	Total (kN)	T(s) (s)	Sa (g) (g)	V. index
2009.37	Final Step	2384.91	27831.09	30216	0.25	0.69	2.07
	E. Demand	1153.25	13457.97	14611.22			

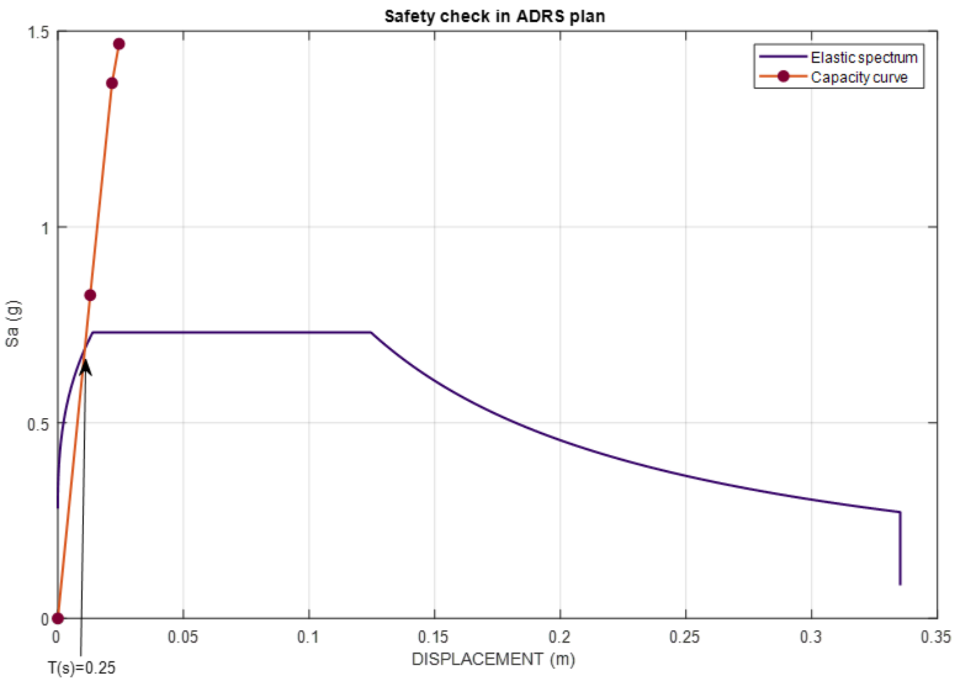

Figure 3.14: Configuration N°8: Safety check and Demand control. X. Dir

The decision to downsize the main elements from HEB300 to HEB260 was driven by the limited reduction in seismic demand. However, this change led to a significant increase in the structural weight, which, in turn, could potentially elevate the overall project cost. Exploring even smaller sections proved unfeasible, resulting in unfavorable outcomes. Nonetheless, this configuration aligns with the criteria for seismic demand reduction and the structural safety assessment. We proceed now to asses the Y direction.

Table 3.14: Configuration N°8, Cross section properties of exoskeletons Y.Dir

Description				
Typ of element	Cross section	Area (mm2)	Fyd (Mpa)	P capacity (N)
Main arcs	HEB 260	11800	350	4130000
skeletons Bracings	TUBO (219.1x5)	3363	350	9248825
Links	HEB 260	11800	350	4130000

Table 3.15: Configuration N°8, Comparative between shear at the base and vulnerability index. Y. Dir

Non retrofitted Vb (kN)	Y Direction	Primary Vb (kN)	Exoskeleton Vb (kN)	Total (kN)	T(s) (s)	Sa (g) (g)	V. index
4090	Final Step	11443.002	26843.998	38287	0.216	0.632	2.746
	E. Demand	4167.15	9775.67	13942.83			

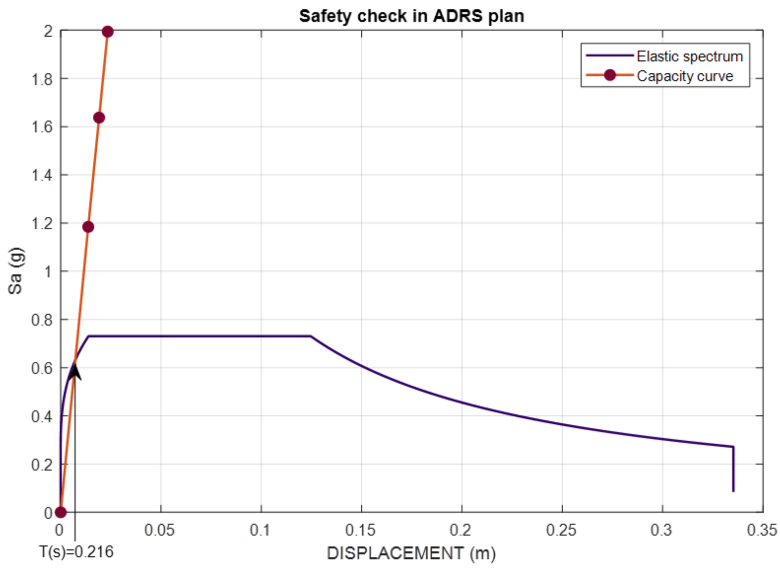

Figure 3.15: Configuration N°8: Safety check and Demand control. Y. Dir

Despite having a vulnerability index well above the minimum required by the code, it is evident that the exoskeletons cannot effectively mitigate the seismic demand in the Y-direction. This observation suggests that the original structure might enter the nonlinear range either before or simultaneously with the exoskeletons.

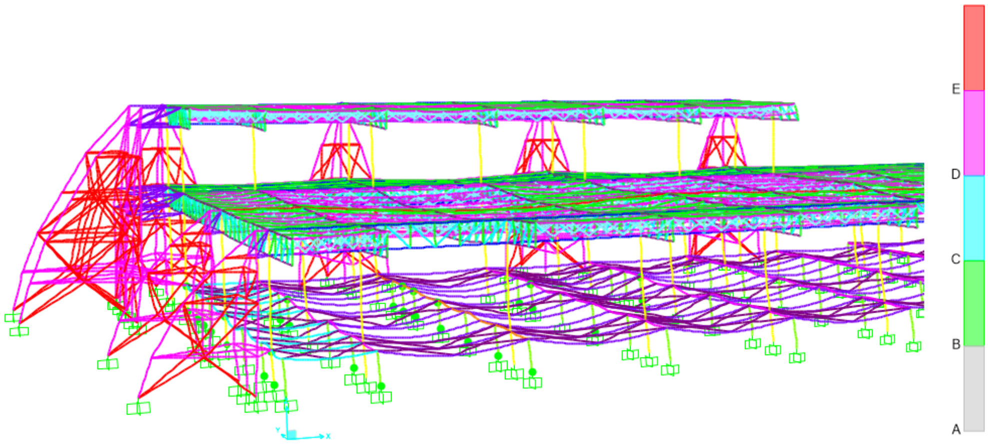

Figure 3.16: Plastic hinges formation at step 3 of Configuration N°8. Y. dir

We examined the plastic hinge formation patterns in our model and found that they begin forming prior to those in the exoskeletons. In the third step of the pushover analysis, the structure has already exceeded the seismic demand threshold from the elastic response spectrum. However, it indicates that the failure mode is due to the formation of plastic hinges in the original structure, presenting a brittle failure. This highlights the need for the exoskeletons to be connected at the same height where these hinges form.

Regarding the safety assessment of the overall structural system, we can confirm that it ensures the structural integrity. However, it does not guarantee the efficient performance of the appendage structure.

Due to constraints imposed by airport management, it is not possible to attach exoskeletons at a height exceeding +1.40 meters in the main entrance area. Nevertheless, a new configuration was proposed, allowing exoskeletons to be attached up to the height of 1.40 meters at the raising floor level.

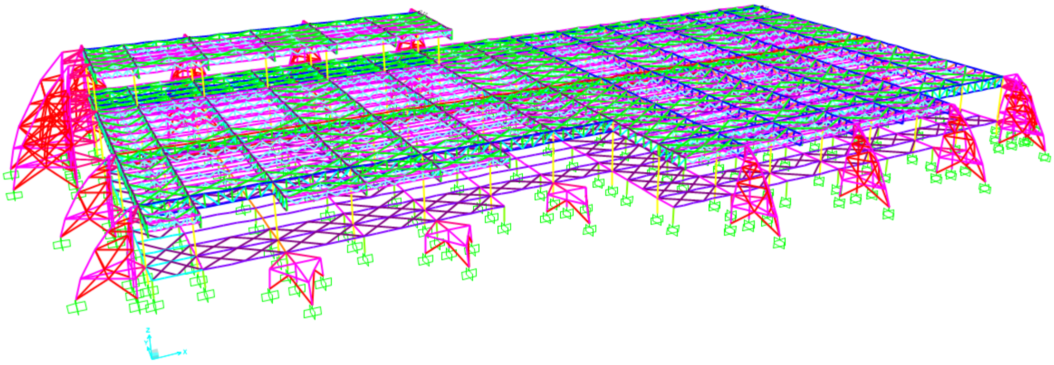

Figure 3.17: Northern view of the configuration N°9

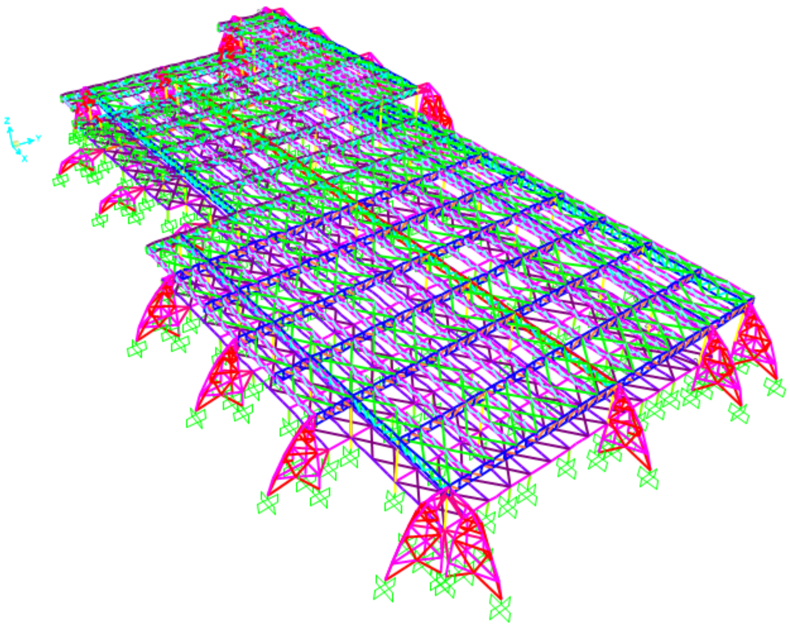

Figure 3.18: North-Western view of the configuration N°9

If we manage to reduce the seismic demand on the base structure, we can conclude that we have achieved the goal of finding the most efficient exoskeleton configuration that meets the minimum requirements of the code while also ensuring that the base structure always remains in the elastic range under any scenario

Table 3.16: Configuration N°9, Cross section properties of exoskeletons Y.Dir

Description				
Typ of element	Cross section	Area (mm2)	Fyd (Mpa)	P capacity (N)
Main arcs	HEB 260	11800	350	4130000
skeletons Bracings	TUBO (219.1x5)	3363	350	1177050
Links	HEB260	11800	350	4130000

Table 3.17: Configuration N°9, Comparative between shear at the base and vulnerability index. Y. Dir

Non retrofitted Vb (kN)	Y Direction	Primary Vb (kN)	Exoskeleton Vb (kN)	Total (kN)	T(s) (s)	Sa (g) (g)	V. index
4090	Final Step	12272.95	45389.05	57662	0.21	0.62	4.63
	E. Demand	2651.32	9805.37	12456.69			

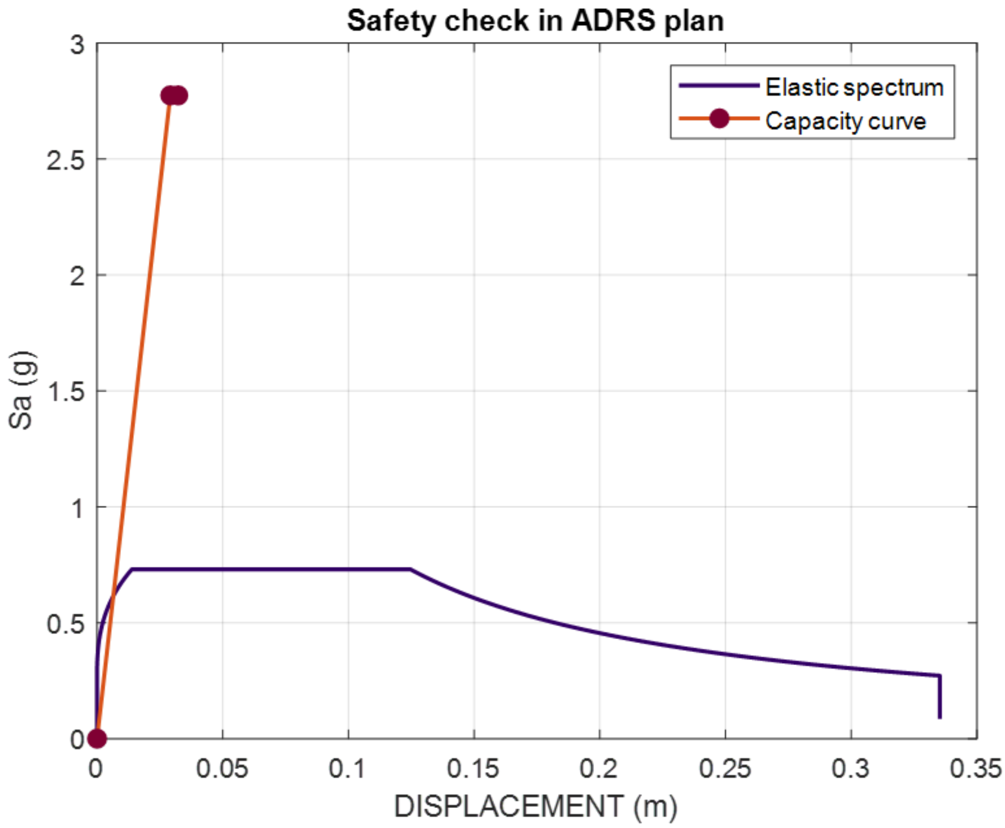

Figure 3.19: Configuration N°9: Safety check and Demand control. Y. Dir

Chapter 4

RESULTS AND DISCUSSIONS

In this chapter, we will repeat the analytical procedure used in the reference condition of the structure. The main objective is to verify the seismic vulnerability of the structure. We have previously assessed the effectiveness of the exoskeletons, with the aim of significantly reducing the seismic demand on the base structure.

Once we've confirmed that the exoskeletons can effectively reduce the seismic demand on the base structure, we can proceed with the final evaluation of the seismic vulnerability coefficient. As previously discussed, our goal was to ensure that the seismic demand does not adversely impact the overall behavior of the base structure under any circumstances and that it remains within the elastic range.

In the first strategy, we focused on reducing the vibration modes with the highest modal mass participation. The purpose was to force the structure to behave predominantly in the fundamental modes. Upon re-solving the eigenvalue problem, we observed a substantial reduction in the number of modes with modal mass participation totaling 90% in the X-axis. However, in the Y-axis, exoskeleton placement was determined by field restrictions, and the absence of exoskeletons on their North-South facades may have influenced the outcome.

It's essential to highlight that modal analysis significantly increases computational demands. Exoskeletons are characterized by a different fundamental frequency or period than the base structure. When they are connected, this results in a broad range of periods that must be analyzed to account for the modal mass participation in the structure. The base structure was initially analyzed for 40 vibration modes, capturing a minimum of 85% of the modal mass participation. In contrast, the coupled system model required a minimum of 250 vibration modes to achieve the same level of participation.

Table 4.1: Mass Participation ratios. Final scenario

Mass Participation ratios					
MODE	**Period**	**UY**	**MODE**	**Period**	**UX**
N°	Sec	Unitless	N°	Sec	Unitless
144.000	0.229	0.211	203	0.168	0.461
238.000	0.125	0.157	43	0.244	0.352
239.000	0.125	0.130	202	0.169	0.090
247.000	0.123	0.097		Sum	0.903
235.000	0.128	0.062			
223.000	0.138	0.043			
192.000	0.179	0.036			
221.000	0.142	0.035			
177.000	0.208	0.029			
250.000	0.120	0.025			
175.000	0.209	0.017			
161.000	0.225	0.014			
229.000	0.135	0.013			
178.000	0.205	0.012			
253.000	0.117	0.011			
230.000	0.134	0.010			
	Sum	0.901			

4.1 ASSESSMENT OF THE GROUP 1- LOAD PROFILE: EQUIVALENT TO THE STOREY FORCES

In subsection 2.6.2, we provided a detailed description of the procedure used to calculate the primary force distribution in our nonlinear static analysis. The calculation process for each mode and each frame of the structure is outlined in the appendix. This calculation is carried out using the principle of modal superposition, decoupling the floor forces for each analyzed mode.

It's crucial to note that each force distribution, representing the floor force, will have its unique transformation factor. The reliability of the adopted procedure is based on a theoretical framework that integrates overall deformation and floor mass, as mentioned earlier.

In our case, we will obtain one representative distribution in the X-direction and another in the Y-direction. As we observed in Chapter 2, the two selected distributions exhibit completely different behaviors, resulting in rather pessimistic outcomes due to their inadequate response to seismic demands.

The distributions we will obtain can be simplified for a visual assessment of the force distribution patterns. This will allow us to understand how the exoskeletons operate and how they can modify the force profiles in their respective groups 1 and 2.

This procedure, although seemingly straightforward, enables us to experiment with arch dimensions, cross-sectional element sizes, and the quantity of exoskeletons. It helps us predict whether the exoskeletons might concentrate seismic forces on a particular storey.

Table 4.2: Distribution Equivalent to the Storey Forces, Xdir

Distribution $\sqrt{\sum_{m=1}^{N_m}\left(\Gamma_m \phi_{mi} m_i S_a^{(m)}\right)^2}$		
FRAME 00	Final Force (N)	Norm Force
Ground Floor	8143.953248	8143.953248
FRAME NO		
First Floor	7479050.348	7479050.348
Ground Floor	2035062.413	2035062.413
FRAME 6		
Ground Floor	6263562.245	6263562.245
FRAME 7		
First Floor	4650793.218	4650793.218
Ground Floor	4639181.754	4639181.754
FRAME 9		
First Floor	1109522.045	1109522.045
Ground Floor	17298868.56	17298868.56
FRAME 11		
Ground Floor	27911549.3	27911549.3
FRAME 13		
First Floor	12408517.61	12408517.61
Ground Floor	5621777.192	5621777.192
FRAME 14		
First Floor	661719.2222	661719.2222
Ground Floor	4391544.032	4391544.032
FRAME 15		
Ground Floor	12648575.53	12648575.53
FRAME 16		
First Floor	887116.2025	887116.2025
Ground Floor	7901043.478	7901043.478
FRAME 17		
Ground Floor	16091390.12	16091390.12
FRAME MO		
Roof	2950634.899	2950634.899
First Floor	3975867.724	3975867.724
Ground Floor	1572944.463	1572944.463
FRAME 21		
Ground Floor	4857149.22	4857149.22
FRAME 23		
Roof	456919.0543	456919.0543
First Floor	4695923.54	4695923.54

Table 4.3: Distribution Equivalent to the Storey Forces, Ydir. Part (1)

Distribution	$\sqrt{\sum_{m=1}^{N_m} \left(\Gamma_m \phi_{mi} m_i S_a^{(m)}\right)^2}$	
FRAME B	Final Force (N)	Norm Force
Roof	233793.6992	0.064
First Floor	409875.2671	0.112
Ground Floor	532726.5367	0.146
FRAME C		
Roof	863756.3291	0.237
First Floor	2918413.643	0.799
Ground Floor	1388889.574	0.380
FRAME D		
Roof	792311.3243	0.217
First Floor	2180868.369	0.597
Ground Floor	1670101.789	0.457
FRAME E		
Roof	860466.1793	0.236
First Floor	1838347.068	0.503
First Floor	1588598.55	0.435
FRAME F		
Roof	427528.0719	0.117
First Floor	3191374.343	0.874
Ground Floor	1524816.783	0.418
FRAME G		
Roof	1172092.693	0.321
First Floor	1473942.867	0.404
Ground Floor	1428214.527	0.391
FRAME H		
Roof	442123.3072	0.121
First Floor	2678760.934	0.734
Ground Floor	1348669.317	0.369

Table 4.4: Distribution Equivalent to the Storey Forces, Ydir. Part (2))

Distribution	$\sqrt{\sum_{m=1}^{N_m}\left(\Gamma_m \phi_{mi} m_i S_a^{(m)}\right)^2}$	
FRAME I	Final Force (N)	Norm Force
First Floor	1712903.978	0.469
Ground Floor	1589105.11	0.435
FRAME J		
First Floor	3651453.336	1
Ground Floor	1842305.221	0.505
FRAME K		
First Floor	1521378.287	0.417
Ground Floor	1868258.827	0.512
FRAME L		
First Floor	3874402.38	1.061
Ground Floor	1920845.101	0.526
FRAME M		
First Floor	2869033.24	0.786
Ground Floor	1990516.484	0.545
FRAME N		
First Floor	3429573.647	0.939
Ground Floor	2047351.891	0.561
FRAME O		
First Floor	2668576.032	0.731
Ground Floor	2091990.504	0.573
FRAME P		
First Floor	974768.5096	0.267
Ground Floor	1109522.166	0.304

4.2 ASSESSMENT OF THE GROUP 2-LOAD PROFILE: UNIFORM ACCELERATION

For our analysis, the distribution of forces proportional to uniform storey accelerations maintains the same distribution as in the previous analysis. The exoskeletons do not contribute gravitational forces to our base system. Even when considering the self-weight of these elements, the variability in the distribution does not differ by more than 5%. Therefore, we will use the same distribution of forces with uniform accelerations. The equations and the procedure's explanation are detailed in the second chapter. Here, we will once again report the force profile that needs to be imposed on our new system.

Table 4.5: Distribution of uniform acceleration. X.Dir

D. UNIFORM	acc / X.dir	Acc (m/s2)	9.81	
FRAME 00	mass kN	mass kG	Force Profile (N)	Unscaled Distribution
Ground Floor	273.433	27872.88481	273433	0.086751305
FRAME NO				
First Floor	775.018	79002.85423	775018	0.245887742
Ground Floor	953.14	97160.04077	953140	0.302399999
FRAME 6				
Ground Floor	1716.067	174930.3772	1716067	0.544451664
FRAME 7				
First Floor	627.739	63989.70438	627739	0.199160955
Ground Floor	843.981	86032.72171	843981	0.267767436
FRAME 9				
First Floor	140.471	14319.16412	140471	0.044566832
Ground Floor	2413.118	245985.525	2413118	0.765603039
FRAME 11				
Ground Floor	3151.918	321296.4322	3151918	1
FRAME 13				
First Floor	1776.625	181103.4659	1776625	0.563664727
Ground Floor	2596.874	264717.0234	2596874	0.823902779
FRAME 14				
First Floor	183.49	18704.38328	183490	0.058215347
Ground Floor	1047.679	106797.0438	1047679	0.332394117
FRAME 15				
Ground Floor	2478.687	252669.419	2478687	0.786405928
FRAME 16				
First Floor	69.805	7115.698267	69805	0.022146833
Ground Floor	929.844	94785.3211	929844	0.295008944
FRAME 17				
Ground Floor	2298.94	234346.5851	2298940	0.729378112
FRAME MO				
Roof	543.184	55370.43833	543184	0.172334433
First Floor	1814.216	184935.3721	1814216	0.575591116
Ground Floor	1047.679	106797.0438	1047679	0.332394117
FRAME 21				
Ground Floor	513.538	52348.41998	513538	0.162928731
FRAME 23				
Roof	134.691	13729.96942	134691	0.042733028
First Floor	892.931	91022.52803	892931	0.283297662

Table 4.6: Distribution of uniform acceleration. Y.Dir (PART 1)

D. UNIFORM	acc / Y.dir	Acc (m/s2)	9.81	
FRAME B	mass kN	mass kG	Force Profile (N)	Unscaled Distribution
Roof	46.179	4707.33945	46179	0.0284
First floor	128.865	13136.08563	128865	0.0792
Ground Floor	372.221	37943.01733	372221	0.2289
FRAME C	-	-		
Roof	77.516	7901.732926	77516	0.0477
First floor	473.058	48222.01835	473058	0.2909
Ground Floor	1001.579	102097.7574	1001579	0.6158
FRAME D	-	-		
Roof	142.507	14526.70744	142507	0.0876
First Floor	473.037	48219.87768	473037	0.2908
Ground Floor	1268.546	129311.5189	1268546	0.7800
FRAME E	-	-		
Roof	95.627	9747.910296	95627	0.0588
First Floor	304.191	31008.25688	304191	0.1870
Ground Floor	1265.267	128977.2681	1265267	0.7779
FRAME F	-	-		
Roof	149.763	15266.36086	149763	0.0921
First Floor	816.122	83192.86442	816122	0.5018
Ground Floor	1265.324	128983.0785	1265324	0.7780
FRAME G	-	-		
Roof	96.754	9862.793068	96754	0.0595
First Floor	294.543	30024.77064	294543	0.1811
Ground Floor	1224.29	124800.2039	1224290	0.7527
FRAME H	-	-		
Roof	69.529	7087.56371	69529	0.0427
First Floor	511.405	52130.98879	511405	0.3144
Ground Floor	1181.936	120482.7727	1181936	0.7267
FRAME I	-	-		
First Floor	251.522	25639.3476	251522	0.1546
Ground Floor	1406.722	143396.738	1406722	0.8649

Table 4.7: Distribution of uniform acceleration. Y.Dir (PART 2)

D. UNIFORM	acc / Y.dir	Acc (m/s2)	9.81	
FRAME J	mass kN	mass kG	Force Profile (N)	Unscaled Distribution
First Floor	667.643	68057.39042	667643	0.4105
Ground Floor	1626.434	165793.476	1626434	1.0000
FRAME K	-	-		
First Floor	259.119	26413.76147	259119	0.1593
Ground Floor	1624.517	165598.0632	1624517	0.9988
FRAME L	-	-		
First Floor	588.086	59947.60449	588086	0.3616
Ground Floor	1626.433	165793.3741	1626433	1.0000
FRAME M	-	-		
First Floor	399.153	40688.3792	399153	0.2454
Ground Floor	1625.291	165676.9623	1625291	0.9993
FRAME N	-	-		
First Floor	533.763	54410.09174	533763	0.3282
Ground Floor	1599.726	163070.948	1599726	0.9836
FRAME O	-	-		
First Floor	320.274	32647.70642	320274	0.1969
Ground Floor	1555.668	158579.8165	1555668	0.9565
FRAME P	-	-		
First Floor	259.514	26454.0265	259514	0.1596
Ground Floor	783.038	79820.38736	783038	0.4814

4.3 IMPORTANCE OF THE FORCE DISTRIBUTION SCHEME IN THE STRUCTURE

The current force distribution reveals the following pattern. As one might expect, Group 2 remains unchanged regardless of the exoskeleton placement. However, Group 1 exhibits a significant difference, with force distributions on each storey taking entirely distinct forms. This demonstrates that in the X-direction, even the distributions of Group 1 and 2 exhibit a similar behavior, concentrating seismic force more intensely at the level of the raising floor. In Figure 4.1 we could perceive a similar trend of forces that could present also a similar response in the final demand.

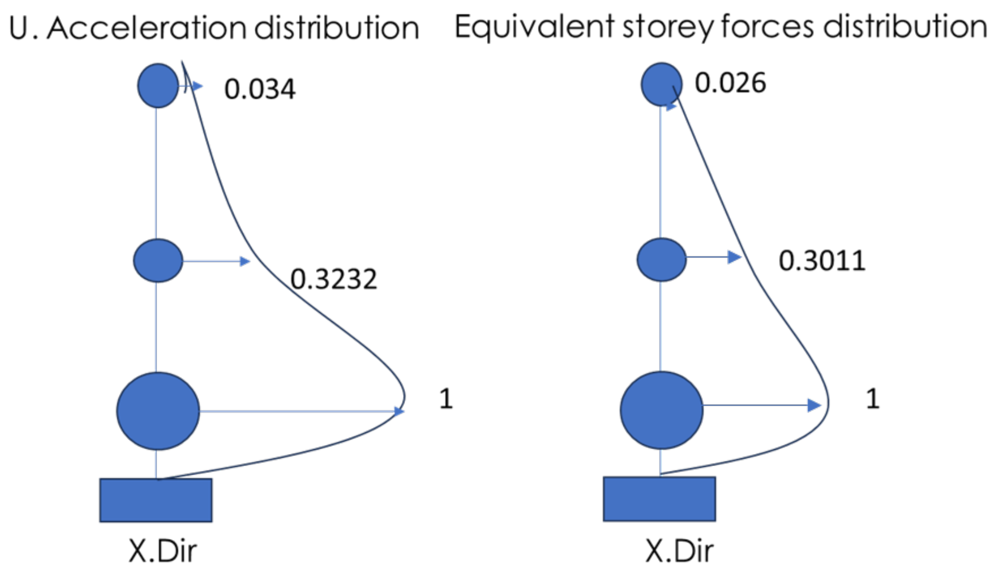

Figure 4.1: FINAL Scheme of the Forces distributions. X.Dir

The three-dimensional semi-spherical exoskeletons are attached to the structure, concentrating the forces at the +1.15m level in the X direction. In the Y direction, however, the concentration is at the +6.15m level. The behavior between these two distributions in the Y direction is significantly different. This suggests that one condition may be more detrimental than the other.

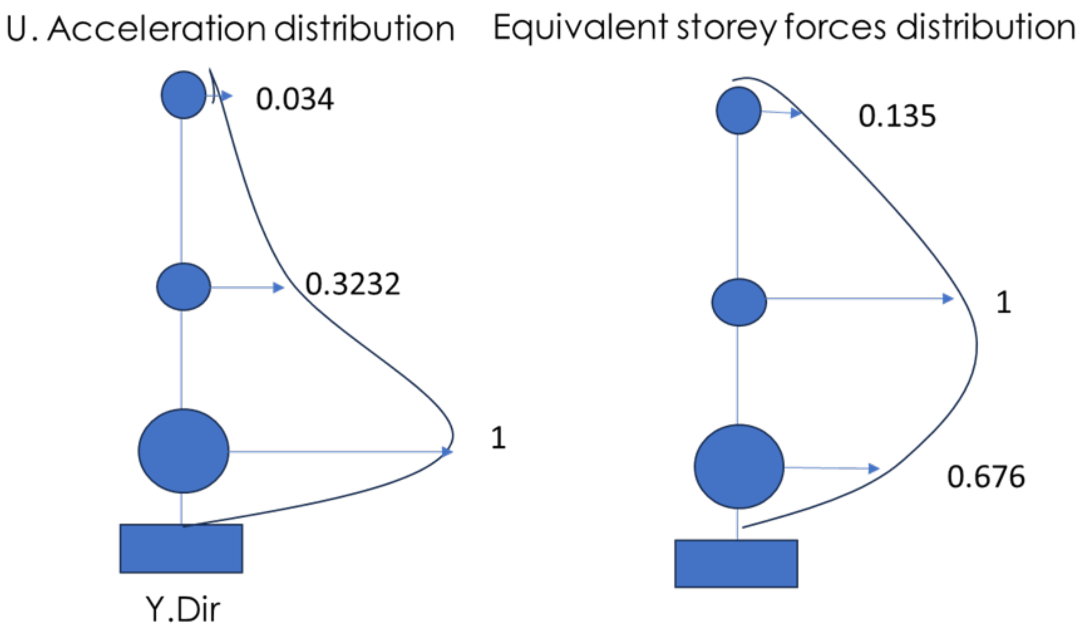

Figure 4.2: FINAL Scheme of the Forces distributions. Y.Dir

4.4 CAPACITY CURVES IN MDOF

The capacity curves obtained from the nonlinear analysis exhibit a more uniform behavior, as expected, in the X direction. In the previous subchapter, we noticed that both distributions had a similar shape. It's worth noting that only one distribution manages to project some of its deformations into a plastic range, suggesting the presence of a brittle failure at the end of the capacity curve. Contrasting the values obtained initially in the X direction, for example, we achieved an approximately 20 times the initial capacity. This suggests that by using a set of exoskeletons in just four axes, the global resistance of the system can be significantly increased.

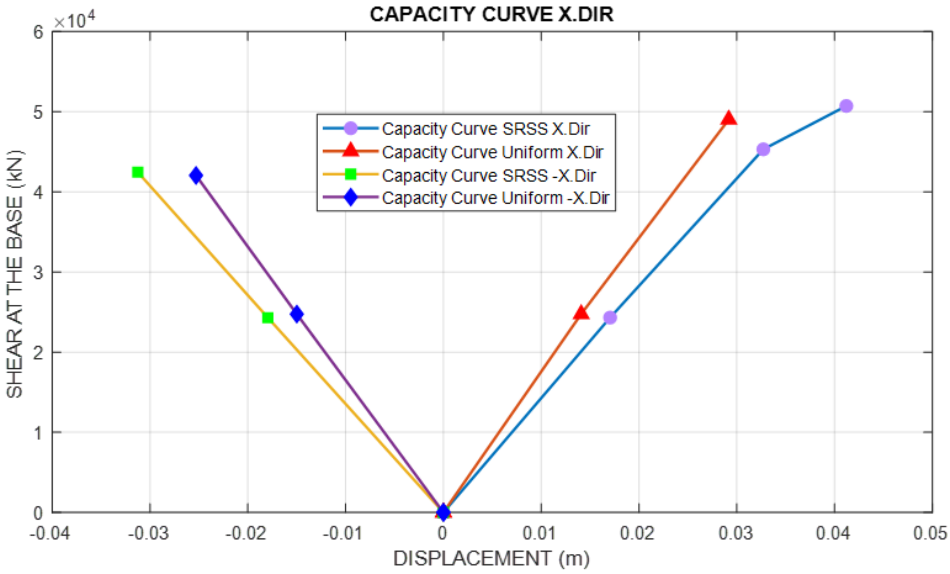

Figure 4.3: FINAL SCENARIO - Capacity curves in a MDOFS. X.Dir

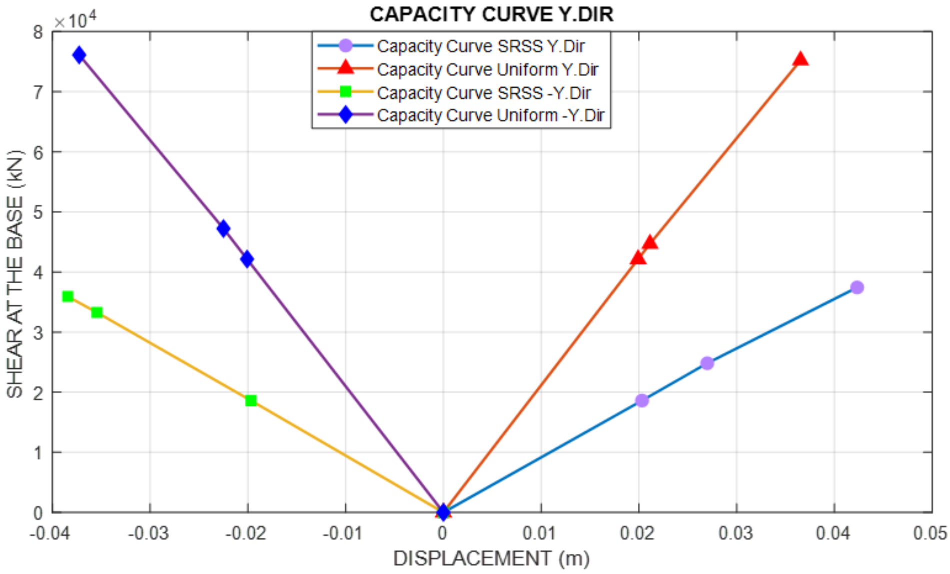

Figure 4.4: FINAL SCENARIO - Capacity curves in a MDOFS. Y.Dir

Regarding the Y direction, the response indicates an unfavorable outcome when using the group of forces proportional to the floor force. Not only that, but all distributions and directions where the load is applied exhibit a very linear behavior with brittle failure. It's worth mentioning that the overall system improves by a factor of 20, similar to the X-axis case. Now, we can proceed to assess vulnerability by transforming these curves into single-degree-of-freedom system representative curves.

4.5 CALCULATION OF THE FOUR TRANSFORMATION FACTOR

The theoretical framework upon which we based our hypothesis allows us to represent a curve from a multi-degree-of-freedom system and simplify it into a single-degree-of-freedom system. This is achieved through a relationship between the deformation pattern and the floor masses. The mathematical procedure is explained in Chapter 2. We will now report the values obtained.

Table 4.8: Transformation factor and equivalent mass derivation X direction. SRSS distribution

	FI	shape (m)	Norm shape	Mass kg	T. Factor	m* (kg)
Roof	fi 3	3.94E-06	0.75	69100.41	1.43	1689141.68
First Flor	fi 2	5.24E-06	1.00	640193.17		
Ground Floor	fi 1	2.64E-06	0.50	1980325.38		

Table 4.9: Transformation factor and equivalent mass derivation Y direction. SRSS distribution

	FI	Shape (m)	Norm shape	Mass kg	T. Factor	m* (kg)
Roof	fi 3	1.50E-02	0.86	69100.41	1.29	926874.41
First Flor	fi 2	1.73E-02	1.00	640193.17		
Ground Floor	fi 1	1.99E-03	0.11	1980325.38		

Table 4.10: Transformation factor and equivalent mass derivation X direction. Mass distribution

	FI	Shape (mm)	Norm shape	Mass kg	T. Factor	m* (kg)
Roof	fi 3	4.8005	1	69100.4077	1.50226173	1668391.76
First Flor	fi 2	4.264	0.88824081	640193.17		
Ground Floor	fi 1	2.49838462	0.52044258	1980325.38		

Table 4.11: Transformation factor and equivalent mass derivation Y direction. Mass distribution

	FI	Shape (mm)	Norm shape	Mass kg	T. Factor	m* (kg)
Roof	fi 3	5.229	0.8634078	69100.4077	1.5034052	1397753.43
First Flor	fi 2	7.12213333	1	640193.17		
Ground Floor	fi 1	2.54206667	0.11463743	1980325.38		

In the literature we have on nonlinear analysis, we can observe that the range of values for the transformation factor typically falls between 1.2 and 2. This range of values aligns with the results reported in our analysis, indicating consistency. While this factor is often obtained through modal analysis in buildings with diaphragm behavior and uniform masses, it's important to emphasize that its strict definition is not necessarily limited to a modal shape but can be applied to any type of deformations imposed on a system.

In our four cases, we applied linear loads proportional to each force distribution. Deformations at each node of the frames were obtained, and an arithmetic mean of the displacements per floor was calculated, resulting in a vector representing a discrete system. Subsequently, we computed the transformation factor and the equivalent mass of the system. This procedure is comprehensively illustrated in Chapter 2. These two parameters allow for the simplification to a single-degree-of-freedom system.

4.6 SAFETY ASSESSMENT

Our seismic vulnerability analysis is rooted in the relationship between capacity and demand, which evaluates ductility criteria directly associated with the fundamental period of the structure and its deformation capacity. Nonlinear analysis takes into account the plastic response that the overall system can exhibit, contrasted with the elastic response spectrum. In our case, we have decided not to change the failure mechanism that the structure exhibits, one characterized by low ductility. Instead, our objective is to control the displacement of the structure, force a global response in its predominant modes, and reduce the seismic demand through exoskeletons.

The procedure for calculating vulnerability follows these steps:

1. Obtain capacity curves for a multiple-degree-of-freedom system.
2. Calculate the transformation factor and equivalent mass.
3. Transform the multiple-degree-of-freedom system into a single-degree-of-freedom system by dividing the response and mass by the explained factors.
4. Report the ductility of the system through the ductility index.
5. Determine the performance point of the structure and verify if it exceeds the minimum limit established by the regulations.

The mathematical formulation of this process can be found in Chapter 2.9, under the section "Safety Assessment and Evaluation of Demand."

Table 4.12: Distribution SRSS (X+)

	SRSS (X+)		Vulnerability
T [s]	0.218	de,max [m]	0.007
m*	1689.142	du* [m]	0.023
Say [m/s^2]	18.759	dy* [m]	0.023
Say [g]	1.912	μc	1.017
Sae [g]	0.639	q *	1.004
q*	1.000	de,max * [m]	0.023
μd	1.000	ζ_E	3.026

Table 4.13: Distribution SRSS (X-)

	SRSS (X-)		Vulnerability
T [s]	0.222	de,max [m]	0.0079
m*	1689.142	du* [m]	0.0219
Say [m/s^2]	17.577	dy* [m]	0.0219
Say [g]	1.792	μc	1.0000
Sae [g]	0.642	q *	1.0000
q*	1.000	de,max * [m]	0.0219
μd	1.000	ζ_E	2.7827

Table 4.14: Distribution U. Mass (X+)

	U. Mass (X+)		Vulnerability
T [s]	0.195	de,max [m]	0.005652158
m*	1668.392	du* [m]	0.019422048
Say [m/s^2]	19.566	dy* [m]	0.018846132
Say [g]	1.994	μc	1.030558872
Sae [g]	0.598	q *	1.007190064
q*	1.000	de,max * [m]	0.018981637
μd	1.000	ζ_E	3.358299267

Table 4.15: Distribution U. Mass (X-)

	U. Mass (X-)		Vulnerability
T [s]	0.200	de,max [m]	0.006004544
m*	1668.392	du* [m]	0.016837945
Say [m/s^2]	16.778	dy* [m]	0.016837945
Say [g]	1.710	μc	1
Sae [g]	0.606	q *	1
q*	1.000	de,max * [m]	0.016837945
μd	1.000	ζ_E	2.804200344

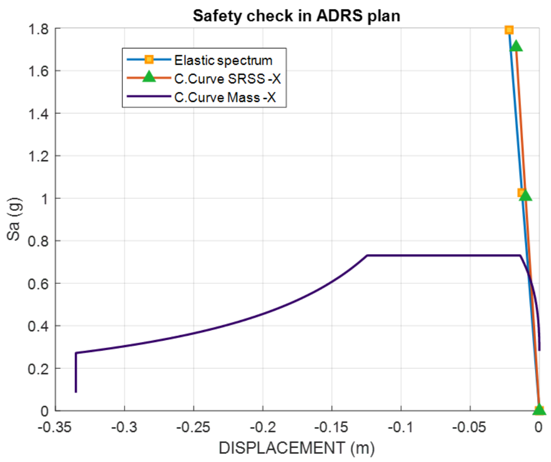

(a) -X.dir

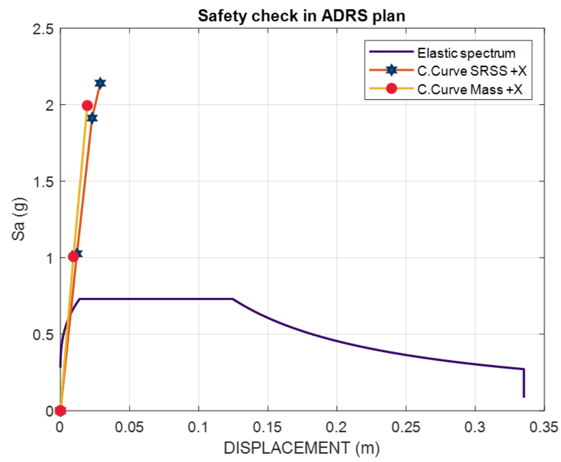

(b) X.dir

Table 4.16: Distribution SRSS (Y+)

	SRSS (Y+)		Vulnerability
T [s]	0.199	de,max [m]	0.006
m*	926.874	du* [m]	0.033
Say [m/s^2]	20.736	dy* [m]	0.021
Say [g]	2.114	μc	1.566
Sae [g]	0.606	q *	1.136
q*	1.000	de,max * [m]	0.024
d	1.000	ζ_E	3.966

Table 4.17: Distribution SRSS (Y-)

	SRSS (Y-)		Vulnerability
T [s]	0.196	de,max [m]	0.006
m*	926.874	du* [m]	0.030
Say [m/s^2]	27.788	dy* [m]	0.027
Say [g]	2.833	μc	1.090
Sae [g]	0.601	q *	1.021
q*	1.000	de,max * [m]	0.028
d	1.000	ζ_E	4.811

Table 4.18: Distribution U. Mass (Y+)

	U. Mass (Y+)		Vulnerability
T [s]	0.199	de,max [m]	0.006
m*	926.874	du* [m]	0.033
Say [m/s^2]	20.736	dy* [m]	0.021
Say [g]	2.114	μc	1.566
Sae [g]	0.606	q *	1.136
q*	1.000	de,max * [m]	0.024
d	1.000	ζ_E	3.966

Table 4.19: Distribution U. Mass (Y-)

	U. Mass (Y-)		Vulnerability
T [s]	0.197	de,max [m]	0.006
m*	926.874	du* [m]	0.030
Say [m/s²]	26.788	dy* [m]	0.027
Say [g]	2.833	μc	1.090
S_{ae} [g]	0.601	q *	1.021
q*	1.000	de,max * [m]	0.028
μ_d	1.000	ζ_E	4.811

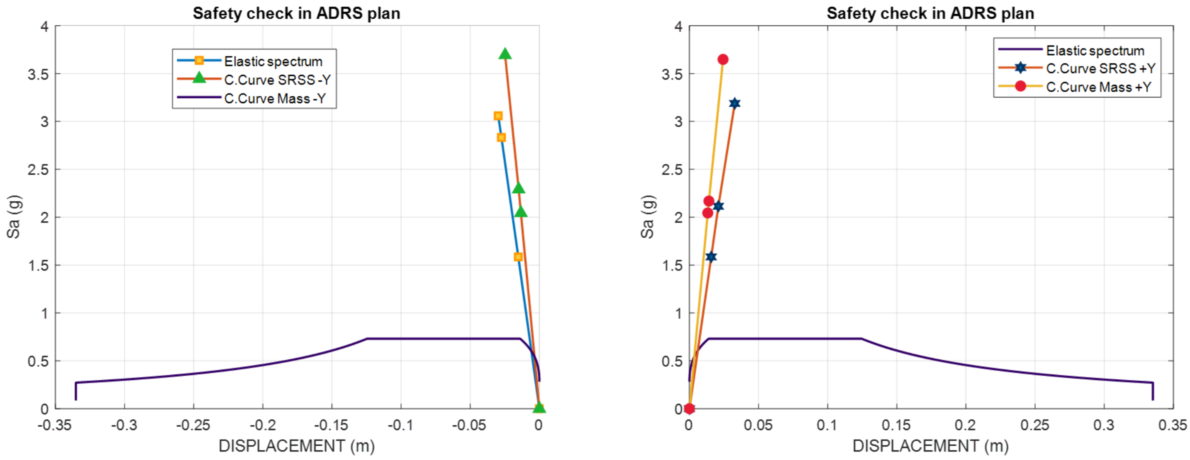

(a) -Y.dir (b) Y.dir

Figure 4.6: Safety ChecK Y dir

Chapter 5

CONCLUSIONS AND FUTURE DEVELOPMENTS

In this thesis, the vulnerability assessment of Foggia's airport and the rehabilitation solution with innovative 3D arch exoskeleton systems have been proposed.
According to the Italian Standard Regulation, the final goal consists of the evaluation of the factor for the assessment of the seismic safety of the structure.

At first, a comprehensive study of the historical reports and technical drawings has been conducted aiming to assess the real level of knowledge of the structure. No-invasive and invasive survey as well as the characterization of the mechanical properties of the material has been described.

The adopted modeling strategies represent a crucial aspect of this thesis. A refined FE model was required aiming to provide a realistic behaviour of the structural seismic response. The difficulties that occur during the modeling phase are mainly attributable to:

- The structure is entirely made of steel with a low intrinsic dissipation capacity and a total lack of dissipative or isolation devices resulting in a pure elastic behavior. This fact has been demonstrated by the analysis conducted on the case study;

- The presence of a huge number of different truss beam topologies and as well as connections placed to different positions inside the building;

- The high flexibility of the entire structures which allows high displacement that has been shown to exceed 10 cm. This inner flexibility is emphasized by the fact that no vertical or horizontal bracing has been identified during the survey;
- The total inconsistency of the rigid floor assumption for each deck at each level of the structure;
- Such deformability of the structure leads to a huge number of fundamental modes that must be considered in both the performed Linear and Static Non-Linear analysis
- The necessity to implement a suitable load profile able to represent in a realistic way the multi-modal dependence of the structure according to the current Italian Standard Regulation NTC2018;
- Implement smart modeling strategies for avoiding false warnings or numerical instabilities during the analysis and structural verification phase such as unrealistic flexural-buckling failure at the level of single truss beams.

After the definition of the numerical model by adopting the well-known FEM solver SAP2000 and a preliminary calibration of itself, the structure has been verified under gravitational load. Results obtained by the ULS analysis demonstrate the safety level of the structure though critical aspect related to the serviceability at the level of the rising floor has been observed.

Then, linear and Static non-linear analysis has been performed in order to evaluate the seismic response of the structure. With specific regard to the latter, a crucial aspect was related to the evaluation of the Transformation factor Γ to move from a multi-degree system to a single one. Due to the lack of knowledge of a well-defined procedure, several approaches have been performed and a final comparison with the proposed evaluation methodology has been provided. It is worth noting that the statistical combination via ADSR of the Transformation factor of each mode leads to unrealistic results with a final value of Γ higher than 5. Alternative approaches as the mathematical and weighted average of the transformation factor seem to provide more realistic results. For this specific kind of structure in which the number of fundamental modes was approximately equal to 10 in both directions with the highest mass participation factor equal to 20%, the suggestions provided by academics authors [19] [3]are impractical.

The proposed approach introduced in this thesis is based on the assumption that the multi-degree pushover curves obtained by a multi-modal load profile give the most representative seismic behavior of the structure. For this reason, the eigenvectors ϕ adopted for the evaluation of the Transformation factor were assumed to be equal to the displacement profile obtained by the multi-modal load distribution. The value of Γ obtained by following this approach is according to some of the mentioned approaches and it seems to be the most reasonable for this type of structure.

The feasibility of the results has been demonstrated by the accordance between the ζ factor obtained from the two analyses. As expected, the structure turns out not to meet the verification under seismic action with a vulnerability index equal to 2.782 and 3.966 along the x and y directions, respectively.

Aiming to provide a feasible solution for the seismic consolidation of the structure, exoskeletons have been preferred due to their no-invasive nature and the possibility of maintaining the full operability of all the activities hosted by the airport. Specifically, a 3D trussed Arch exoskeleton has been designed because of its overall stability with respect to bi-directional seismic actions.

For the seismic assessment of the airport, the same previous linear and non-static analyses were performed by varying the number and position of the exoskeletons as well as their sizing. In order to improve the efficiency of the external retrofitting systems, horizontal bracings have been provided at the level of each deck of the structure. Among all the possible configurations, the final one has been obtained by aiming for the best rigid behavior of the deck.

The retrofitted solutions show that the presence of the external exoskeleton allows the unloading of the structure by almost half guaranteeing the structural safety under seismic load. Specifically, the final vulnerability index of the retrofitting system has been calculated equal to 2.782 in X direction and 3.966 in Y direction

As future developments, the presence of dissipative devices between the exoskeletons and the existing structures could be an aspect of crucial interest for academicians and practitioners. Moreover, a comprehensive study focused on the validity of the recommendations provided by the Italian standard regulation should be provided and the stiffness proposed approach should be overcome.

Chapter 6

Appendix

Table 6.1: Equivalent storey force, Mode 1

MODE 1		Γ n	2.108	acc (m/s2)	2.768
FRAME 00	SHAPE	NORM SHAPE	mass kN	mass kg	Force profile (N)
Ground Floor	0.000016	0.000254	273.433	27872.885	41.236
FRAME NO	SHAPE	NORM SHAPE			
First Floor	0.009114	0.144416	775.018	79002.854	66576.951
Ground Floor	0.001509	0.023911	953.140	97160.041	13556.545
FRAME 6	SHAPE	NORM SHAPE			
Ground Floor	0.000441	0.006988	1716.067	174930.377	7133.061
FRAME 7	SHAPE	NORM SHAPE			
First Floor	0.013276	0.210365	627.739	63989.704	78550.589
Ground Floor	0.001321	0.020932	843.981	86032.722	10508.448
FRAME 9	SHAPE	NORM SHAPE			
First Floor	0.014712	0.233119	140.471	14319.164	19478.768
Ground Floor	0.000710	0.011250	2413.118	245985.525	16148.790
FRAME 11	SHAPE	NORM SHAPE			
Ground Floor	0.000146	0.002313	3151.918	321296.432	4337.414
FRAME 13	SHAPE	NORM SHAPE			
First Floor	0.024523	0.388579	1776.625	181103.466	410650.594
Ground Floor	0.003665	0.058074	2596.874	264717.023	89707.333
FRAME 14	SHAPE	NORM SHAPE			
First Floor	0.027795	0.440425	183.490	18704.383	48070.891
Ground Floor	0.002601	0.041214	1047.679	106797.044	25684.533
FRAME 15	SHAPE	NORM SHAPE			
Ground Floor	0.000646	0.010236	2478.687	252669.419	15092.365
FRAME 16	SHAPE	NORM SHAPE			
First Floor	0.038980	0.617657	69.805	7115.698	25646.698
Ground Floor	0.000068	0.001077	929.844	94785.321	595.967
FRAME 17	SHAPE	NORM SHAPE			
Ground Floor	0.000834	0.013215	2298.940	234346.585	18071.607
FRAME MO	SHAPE	NORM SHAPE			
Roof	0.070118	1.111053	543.184	55370.438	358987.707
First Floor	0.039626	0.627893	1814.216	184935.372	677598.314
Ground Floor	0.006466	0.102457	1047.679	106797.044	63850.901
FRAME 21	SHAPE	NORM SHAPE			
Ground Floor	0.000080	0.001268	513.538	52348.420	387.227
FRAME 23	SHAPE	NORM SHAPE			
Roof	0.056101	0.888947	134.691	13729.969	71221.689
First Floor	0.040705	0.644990	892.931	91022.528	342585.319

Table 6.2: Equivalent storey force, Mode 21

MODE 21		Γ n	1.388	Acc (m/s2)	7.165
FRAME 00	SHAPE	NORM SHAPE	mass kN	mass kG	Force profile (N)
Ground Floor	0.000001	0.000234	273.433	27872.885	64.746
FRAME NO	SHAPE	NORM SHAPE			
First Floor	0.000259	0.049664	775.018	79002.854	39023.231
Ground Floor	0.000119	0.022819	953.14	97160.041	22050.342
FRAME 6	SHAPE	NORM SHAPE			
Ground Floor	-0.001821	-0.349185	1716.067	174930.377	-607513.391
FRAME 7	SHAPE	NORM SHAPE			
First Floor	-0.000651	-0.124832	627.739	63989.704	-79445.951
Ground Floor	-0.001821	-0.349185	843.981	86032.722	-298781.900
FRAME 9	SHAPE	NORM SHAPE			
First Floor	-0.001186	-0.227421	140.471	14319.164	-32387.918
Ground Floor	0.018031	3.457526	2413.118	245985.525	8458825.037
FRAME 11	SHAPE	NORM SHAPE			
Ground Floor	0.038321	7.348226	3151.918	321296.432	23481369.010
FRAME 13	SHAPE	NORM SHAPE			
First Floor	-0.001155	-0.221477	1776.625	181103.466	-398923.318
Ground Floor	0.002600	0.498562	2596.874	264717.023	1312610.566
FRAME 14	SHAPE	NORM SHAPE			
First Floor	-0.002086	-0.400000	183.49	18704.383	-74411.211
Ground Floor	-0.010488	-2.011122	1047.679	106797.044	-2136154.139
FRAME 15	SHAPE	NORM SHAPE			
Ground Floor	-0.004589	-0.879962	2478.687	252669.419	-2211319.096
FRAME 16	SHAPE	NORM SHAPE			
First Floor	-0.003317	-0.636050	69.805	7115.698	-45013.592
Ground Floor	0.000345	0.066155	929.844	94785.321	62364.990
FRAME 17	SHAPE	NORM SHAPE			
Ground Floor	0.000229	0.043912	2298.94	234346.585	102346.923
FRAME MO	SHAPE	NORM SHAPE			
Roof	0.004102	0.786577	543.184	55370.438	433165.934
First Floor	0.000061	0.011697	1814.216	184935.372	21514.462
Ground Floor	0.000017	0.003260	1047.679	106797.044	3462.492
FRAME 21	SHAPE	NORM SHAPE			
Ground Floor	0.000000	0.000078	513.538	52348.420	40.793
FRAME 23	SHAPE	NORM SHAPE			
Roof	0.006328	1.213423	134.691	13729.969	165697.790
First Floor	-0.000391	-0.074976	892.931	91022.528	-67874.451

Table 6.3: Equivalent storey force, Mode 26

MODE 26		Partic	1.056	Acc (m/s2)	7.165
FRAME 00	SHAPE	NORM SHAPE	mass kN	mass kG	Force profile (N)
Ground Floor	-0.000046	0.00311116	273.433	27872.885	656.158
FRAME NO	SHAPE	NORM SHAPE			
First Floor	-0.03211	2.1717223	775.018	79002.854	1298230.744
Ground Floor	-0.001709	0.11558622	953.140	97160.041	84976.444
FRAME 6	SHAPE	NORM SHAPE			
Ground Floor	0.037586	-2.54208515	1716.067	174930.377	-3364806.887
FRAME 7	SHAPE	NORM SHAPE			
First Floor	0.007822	-0.52903182	627.739	63989.704	-256151.390
Ground Floor	0.001981	-0.13398262	843.981	86032.722	-87220.172
FRAME 9	SHAPE	NORM SHAPE			
First Floor	0.013584	-0.91873795	140.471	14319.164	-99543.783
Ground Floor	-0.001443	0.09759562	2413.118	245985.525	181653.883
FRAME 11	SHAPE	NORM SHAPE			
Ground Floor	0.005303	-0.3586622	3151.918	321296.432	-871959.538
FRAME 13	SHAPE	NORM SHAPE			
First Floor	-0.002733	0.18484326	1776.625	181103.466	253300.003
Ground Floor	0.007773	-0.52571776	2596.874	264717.023	-1053026.598
FRAME 14	SHAPE	NORM SHAPE			
First Floor	-0.015506	1.04873017	183.490	18704.383	148426.681
Ground Floor	0.042693	-2.88749112	1047.679	106797.044	-2333375.895
FRAME 15	SHAPE	NORM SHAPE			
Ground Floor	0.022948	-1.55206114	2478.687	252669.419	-2967333.264
FRAME 16	SHAPE	NORM SHAPE			
First Floor	-0.033265	2.24983937	69.805	7115.698	121136.174
Ground Floor	0.000575	-0.03888945	929.844	94785.321	-27891.876
FRAME 17	SHAPE	NORM SHAPE			
Ground Floor	-0.000275	0.0185993	2298.940	234346.585	32980.719
FRAME MO	SHAPE	NORM SHAPE			
Roof	-0.018278	1.23621115	543.184	55370.438	517935.211
First Floor	0.008809	-0.59578641	1814.216	184935.372	-833710.743
Ground Floor	0.00169	-0.11430117	1047.679	106797.044	-92366.553
FRAME 21	SHAPE	NORM SHAPE			
Ground Floor	0.000031	-0.00209665	513.538	52348.420	-830.489
FRAME 23	SHAPE	NORM SHAPE			
Roof	-0.011293	0.76378885	134.691	13729.969	79350.141
First Floor	0.014013	-0.94775287	892.931	91022.528	-652752.912

Table 6.4: Equivalent storey force, Mode 28

MODE 28		Participation	0.8469834	Acc (m/s2)	7.165
FRAME 00	SHAPE	NORM SHAPE	mass kN	mass kG	Force profile (N)
Ground Floor	-0.000051	0.0098	273.433	27872.885	1650.142
FRAME NO	SHAPE	NORM SHAPE			
First Floor	-0.016548	3.1655	775.018	79002.854	1517600.361
Ground Floor	-0.003344	0.6397	953.140	97160.041	377157.792
FRAME 6	SHAPE	NORM SHAPE			
Ground Floor	0.003272	-0.6259	1716.067	174930.377	-664427.585
FRAME 7	SHAPE	NORM SHAPE			
First Floor	0.014541	-2.7815	627.739	63989.704	-1080123.725
Ground Floor	0.003098	-0.5926	843.981	86032.722	-309395.650
FRAME 9	SHAPE	NORM SHAPE			
First Floor	0.015852	-3.0323	140.471	14319.164	-263494.077
Ground Floor	0.000676	-0.1293	2413.118	245985.525	-193030.251
FRAME 11	SHAPE	NORM SHAPE			
Ground Floor	0.001300	-0.2487	3151.918	321296.432	-484862.261
FRAME 13	SHAPE	NORM SHAPE			
First Floor	-0.016842	3.2217	1776.625	181103.466	3540703.430
Ground Floor	-0.002300	0.4400	2596.874	264717.023	706771.183
FRAME 14	SHAPE	NORM SHAPE			
First Floor	-0.008091	1.5477	183.490	18704.383	175676.925
Ground Floor	0.001794	-0.3432	1047.679	106797.044	-222408.201
FRAME 15	SHAPE	NORM SHAPE			
Ground Floor	0.002051	-0.3923	2478.687	252669.419	-601571.799
FRAME 16	SHAPE	NORM SHAPE			
First Floor	0.028720	-5.4938	69.805	7115.698	-237230.807
Ground Floor	-0.012351	2.3626	929.844	94785.321	1358977.713
FRAME 17	SHAPE	NORM SHAPE			
Ground Floor	-0.052171	9.9797	2298.940	234346.585	14192435.124
FRAME MO	SHAPE	NORM SHAPE			
Roof	0.004233	-0.8097	543.184	55370.438	-272079.209
First Floor	0.000729	-0.1394	1814.216	184935.372	-156500.828
Ground Floor	-0.009794	1.8735	1047.679	106797.044	1214195.051
FRAME 21	SHAPE	NORM SHAPE			
Ground Floor	-0.000140	0.0268	513.538	52348.420	8507.476
FRAME 23	SHAPE	NORM SHAPE			
Roof	-0.001698	0.3248	134.691	13729.969	27063.028
First Floor	-0.004039	0.7726	892.931	91022.528	426768.025

Table 6.5: Equivalent storey force, Mode 36

MODE 36		Participation	1.058	Acc (m/s2)	7.165
FRAME 00	SHAPE	NORM SHAPE	mass kN	mass kG	Force profile (N)
Ground Floor	0.000031	-0.009	273.433	27872.885	-1995.226
FRAME NO	SHAPE	NORM SHAPE			
First Floor	0.001373	-0.418	775.018	79002.854	-250473.535
Ground Floor	0.001439	-0.438	953.140	97160.041	-322847.188
FRAME 6	SHAPE	NORM SHAPE			
Ground Floor	-0.007830	2.386	1716.067	174930.377	3162827.605
FRAME 7	SHAPE	NORM SHAPE			
First Floor	-0.002534	0.772	627.739	63989.704	374425.347
Ground Floor	-0.022343	6.808	843.981	86032.722	4438678.341
FRAME 9	SHAPE	NORM SHAPE			
First Floor	0.000815	-0.248	140.471	14319.164	-26947.830
Ground Floor	-0.026496	8.074	2413.118	245985.525	15050065.60
FRAME 11	SHAPE	NORM SHAPE			
Ground Floor	0.020163	-6.144	3151.918	321296.432	-14959241.7
FRAME 13	SHAPE	NORM SHAPE			
First Floor	-0.004800	1.463	1776.625	181103.466	2007319.600
Ground Floor	-0.006611	2.014	2596.874	264717.023	4041080.986
FRAME 14	SHAPE	NORM SHAPE			
First Floor	-0.005159	1.572	183.490	18704.383	222821.681
Ground Floor	0.000756	-0.230	1047.679	106797.044	-186435.904
FRAME 15	SHAPE	NORM SHAPE			
Ground Floor	0.000744	-0.227	2478.687	252669.419	-434084.365
FRAME 16	SHAPE	NORM SHAPE			
First Floor	0.004701	-1.432	69.805	7115.698	-77242.496
Ground Floor	-0.002461	0.750	929.844	94785.321	538643.254
FRAME 17	SHAPE	NORM SHAPE			
Ground Floor	-0.000619	0.189	2298.940	234346.585	334963.746
FRAME MO	SHAPE	NORM SHAPE			
Roof	-0.003822	1.165	543.184	55370.438	488671.679
First Floor	-0.000267	0.081	1814.216	184935.372	114019.668
Ground Floor	0.000361	-0.110	1047.679	106797.044	-89025.610
FRAME 21	SHAPE	NORM SHAPE			
Ground Floor	0.000203	-0.062	513.538	52348.420	-24538.507
FRAME 23	SHAPE	NORM SHAPE			
Roof	0.005286	-1.611	134.691	13729.969	-167588.902
First Floor	-0.002253	0.687	892.931	91022.528	473542.117

Table 6.6: Equivalent storey force, Mode 32

MODE 32		Participation	1.027	Acc (m/s2)	7.165
FRAME 00	SHAPE	NORM SHAPE	mass kN	mass kG	Force profile (N)
Ground Floor	0.000007	0.001245	273.433	27872.885	255.269
FRAME NO	SHAPE	NORM SHAPE			
First Floor	0.001278	0.212786	775.018	79002.854	123653.127
Ground Floor	0.000357	0.059440	953.140	97160.041	42480.280
FRAME 6	SHAPE	NORM SHAPE			
Ground Floor	-0.000482	-0.080253	1716.067	174930.377	-103262.763
FRAME 7	SHAPE	NORM SHAPE			
First Floor	-0.001796	-0.299032	627.739	63989.704	-140749.838
Ground Floor	-0.001209	-0.201297	843.981	86032.722	-127385.921
FRAME 9	SHAPE	NORM SHAPE			
First Floor	-0.000952	-0.158507	140.471	14319.164	-16694.987
Ground Floor	-0.001546	-0.257408	2413.118	245985.525	-465747.476
FRAME 11	SHAPE	NORM SHAPE			
Ground Floor	0.001681	0.279885	3151.918	321296.432	661462.282
FRAME 13	SHAPE	NORM SHAPE			
First Floor	0.001190	0.198134	1776.625	181103.466	263939.987
Ground Floor	-0.008480	-1.411913	2596.874	264717.023	-2749218.083
FRAME 14	SHAPE	NORM SHAPE			
First Floor	0.002687	0.447383	183.490	18704.383	61552.051
Ground Floor	-0.018193	-3.029119	1047.679	106797.044	-2379551.013
FRAME 15	SHAPE	NORM SHAPE			
Ground Floor	0.037443	6.234228	2478.687	252669.419	11586567.291
FRAME 16	SHAPE	NORM SHAPE			
First Floor	-0.001378	-0.229436	69.805	7115.698	-12008.761
Ground Floor	0.066458	11.065200	929.844	94785.321	7714713.844
FRAME 17	SHAPE	NORM SHAPE			
Ground Floor	0.009274	1.544113	2298.940	234346.585	2661688.264
FRAME MO	SHAPE	NORM SHAPE			
Roof	-0.009512	-1.583740	543.184	55370.438	-645032.017
First Floor	-0.000420	-0.069930	1814.216	184935.372	-95126.331
Ground Floor	-0.006966	-1.159833	1047.679	106797.044	-911117.043
FRAME 21	SHAPE	NORM SHAPE			
Ground Floor	-0.000266	-0.044289	513.538	52348.420	-17053.624
FRAME 23	SHAPE	NORM SHAPE			
Roof	0.011051	1.839982	134.691	13729.969	185824.348
First Floor	0.003060	0.509487	892.931	91022.528	341115.763

Table 6.7: Equivalent storey force, Mode 29

MODE 29		Participation	2.817	Acc (m/s2)	7.165
FRAME 00	SHAPE	NORM SHAPE	mass kN	mass kG	Force profile (N)
Ground Floor	-0.000131	-0.010418	273.433	27872.885	-5862.151
FRAME NO	SHAPE	NORM SHAPE			
First Floor	-0.040387	-3.211945	775.018	79002.854	-5122572.763
Ground Floor	-0.008427	-0.670192	953.140	97160.041	-1314511.658
FRAME 6	SHAPE	NORM SHAPE			
Ground Floor	0.007977	0.634404	1716.067	174930.377	2240312.409
FRAME 7	SHAPE	NORM SHAPE			
First Floor	0.039514	3.142516	627.739	63989.704	4059428.151
Ground Floor	0.008660	0.688723	843.981	86032.722	1196149.090
FRAME 9	SHAPE	NORM SHAPE			
First Floor	0.038772	3.083506	140.471	14319.164	891332.271
Ground Floor	0.002220	0.176555	2413.118	245985.525	876730.845
FRAME 11	SHAPE	NORM SHAPE			
Ground Floor	0.002966	0.235884	3151.918	321296.432	1529962.582
FRAME 13	SHAPE	NORM SHAPE			
First Floor	-0.039699	-3.157229	1776.625	181103.466	-11542771.240
Ground Floor	-0.004614	-0.366948	2596.874	264717.023	-1960935.102
FRAME 14	SHAPE	NORM SHAPE			
First Floor	-0.013935	-1.108239	183.490	18704.383	-418460.169
Ground Floor	0.008806	0.700334	1047.679	106797.044	1509877.358
FRAME 15	SHAPE	NORM SHAPE			
Ground Floor	0.007749	0.616272	2478.687	252669.419	3143417.758
FRAME 16	SHAPE	NORM SHAPE			
First Floor	0.071578	5.692540	69.805	7115.698	817712.889
Ground Floor	0.005758	0.457929	929.844	94785.321	876226.747
FRAME 17	SHAPE	NORM SHAPE			
Ground Floor	0.018825	1.497137	2298.940	234346.585	7082675.980
FRAME MO	SHAPE	NORM SHAPE			
Roof	0.024917	1.981629	543.184	55370.438	2215019.090
First Floor	-0.010428	-0.829330	1814.216	184935.372	-3096169.782
Ground Floor	0.001729	0.137506	1047.679	106797.044	296454.457
FRAME 21	SHAPE	NORM SHAPE			
Ground Floor	0.000005	0.000385	513.538	52348.420	406.690
FRAME 23	SHAPE	NORM SHAPE			
Roof	0.000231	0.018371	134.691	13729.969	5091.964
First Floor	-0.030008	-2.386512	892.931	91022.528	-4385203.017

Table 6.8: Equivalent storey force, Mode 24

MODE 24		Participation	3.603	Acc (m/s2)	7.165
FRAME 00	SHAPE	NORM SHAPE	mass kN	mass kG	Force profile (N)
Ground Floor	0.00020	0.007	273.433	27872.885	4969.91575
FRAME NO	SHAPE	NORM SHAPE			
First Floor	0.07239	2.475	775.018	79002.854	5048345.79
Ground Floor	0.01710	0.585	953.140	97160.041	1466816.28
FRAME 6	SHAPE	NORM SHAPE			
Ground Floor	0.02250	0.769	1716.067	174930.377	3473497.31
FRAME 7	SHAPE	NORM SHAPE			
First Floor	-0.03368	-1.152	627.739	63989.704	-1902495.83
Ground Floor	-0.00556	-0.190	843.981	86032.722	-422007.137
FRAME 9	SHAPE	NORM SHAPE			
First Floor	-0.04666	-1.595	140.471	14319.164	-589738.557
Ground Floor	-0.00168	-0.057	2413.118	245985.525	-363914.452
FRAME 11	SHAPE	NORM SHAPE			
Ground Floor	0.00125	0.043	3151.918	321296.432	355363.412
FRAME 13	SHAPE	NORM SHAPE			
First Floor	0.01060	0.362	1776.625	181103.466	1693727.19
Ground Floor	0.00300	0.102	2596.874	264717.023	699833.028
FRAME 14	SHAPE	NORM SHAPE			
First Floor	0.02273	0.777	183.490	18704.383	375299.229
Ground Floor	0.01185	0.405	1047.679	106797.044	1117008.99
FRAME 15	SHAPE	NORM SHAPE			
Ground Floor	0.00569	0.195	2478.687	252669.419	1268832.67
FRAME 16	SHAPE	NORM SHAPE			
First Floor	0.03119	1.066	69.805	7115.698	195906.405
Ground Floor	-0.00018	-0.006	929.844	94785.321	-14641.8135
FRAME 17	SHAPE	NORM SHAPE			
Ground Floor	-0.00177	-0.061	2298.940	234346.585	-366347.243
FRAME MO	SHAPE	NORM SHAPE			
Roof	0.03181	1.087	543.184	55370.438	1554591.92
First Floor	-0.01364	-0.466	1814.216	184935.372	-2226313.96
Ground Floor	-0.00261	-0.089	1047.679	106797.044	-246045.528
FRAME 21	SHAPE	NORM SHAPE			
Ground Floor	-0.00004	-0.002	513.538	52348.420	-2033.16204
FRAME 23	SHAPE	NORM SHAPE			
Roof	0.02669	0.913	134.691	13729.969	323469.905
First Floor	-0.01636	-0.559	892.931	91022.528	-1314220.64

Table 6.9: Equivalent storey force, Mode 38

MODE 38		Participation	0.9998	Acc (m/s2)	7.165
FRAME 00	SHAPE	NORM SHAPE	mass kN	mass kG	Force profile (N)
Ground Floor	0.00000020	-0.000019	273.433	27872.885	-3.780
FRAME NO	SHAPE	NORM SHAPE			
First Floor	0.00000507	-0.000477	775.018	79002.854	-270.029
Ground Floor	0.00000930	-0.000876	953.140	97160.041	-609.903
FRAME 6	SHAPE	NORM SHAPE			
Ground Floor	-0.00005400	0.005086	1716.067	174930.377	6373.266
FRAME 7	SHAPE	NORM SHAPE			
First Floor	-0.00001200	0.001130	627.739	63989.704	518.077
Ground Floor	-0.00015500	0.014599	843.981	86032.722	8997.015
FRAME 9	SHAPE	NORM SHAPE			
First Floor	0.00001600	-0.001507	140.471	14319.164	-154.576
Ground Floor	-0.00018300	0.017236	2413.118	245985.525	30371.323
FRAME 11	SHAPE	NORM SHAPE			
Ground Floor	0.00013500	-0.012715	3151.918	321296.432	-29264.610
FRAME 13	SHAPE	NORM SHAPE			
First Floor	-0.00004700	0.004427	1776.625	181103.466	5742.853
Ground Floor	-0.00001100	0.001036	2596.874	264717.023	1964.616
FRAME 14	SHAPE	NORM SHAPE			
First Floor	-0.00005400	0.005086	183.490	18704.383	681.460
Ground Floor	0.00007100	-0.006687	1047.679	106797.044	-5115.884
FRAME 15	SHAPE	NORM SHAPE			
Ground Floor	-0.00012200	0.011490	2478.687	252669.419	20797.713
FRAME 16	SHAPE	NORM SHAPE			
First Floor	0.00004300	-0.004050	69.805	7115.698	-206.438
Ground Floor	-0.00012700	0.011961	929.844	94785.321	8121.717
FRAME 17	SHAPE	NORM SHAPE			
Ground Floor	0.00012900	-0.012150	2298.940	234346.585	-20396.301
FRAME MO	SHAPE	NORM SHAPE			
Roof	0.00012600	-0.011867	543.184	55370.438	-4707.080
First Floor	0.00001500	-0.001413	1814.216	184935.372	-1871.606
Ground Floor	-0.00020000	0.018837	1047.679	106797.044	14410.940
FRAME 21	SHAPE	NORM SHAPE			
Ground Floor	-0.13752000	12.952202	513.538	52348.420	4857049.314
FRAME 23	SHAPE	NORM SHAPE			
Roof	-0.00021300	0.020061	134.691	13729.969	1973.114
First Floor	0.00011900	-0.011208	892.931	91022.528	-7308.007

Distribution in Y direction:

Table 6.10: Equivalent storey force, Mode 5 (PART 1)

MODE 5		Participation	2.072	acc (m/s2)	5.088
FRAME B	SHAPE	NORM SHAPE	mass kN	mass kG	Force profile (N)
Roof	-0.055	0.958	46.179	4707.33945	47572.38454
First floor	-0.044	0.777	128.865	13136.08563	107603.6211
Ground Floor	-0.003	0.054	372.221	37943.01733	21582.07395
FRAME C	SHAPE	NORM SHAPE	-	-	
Roof	-0.064	1.117	77.516	7901.732926	93029.94196
First floor	-0.048	0.831	473.058	48222.01835	422801.3421
Ground Floor	-0.003	0.052	1001.579	102097.7574	55515.79667
FRAME D	SHAPE	NORM SHAPE	-	-	
Roof	-0.066	1.148	142.507	14526.70744	175812.4518
First Floor	-0.052	0.906	473.037	48219.87768	460877.4146
Ground Floor	-0.002	0.038	1268.546	129311.5189	52139.51595
FRAME E	SHAPE	NORM SHAPE	-	-	
Roof	-0.065	1.134	95.627	9747.910296	116519.8962
First Floor	-0.050	0.866	304.191	31008.25688	283263.4311
Ground Floor	-0.002	0.037	1265.267	128977.2681	50840.63516
FRAME F	SHAPE	NORM SHAPE	-	-	
Roof	-0.059	1.029	149.763	15266.36086	165597.4801
First Floor	-0.045	0.788	816.122	83192.86442	691415.6243
Ground Floor	-0.002845	0.049696803	1265.324	128983.0785	67592.58089
FRAME G	SHAPE	NORM SHAPE	-	-	
Roof	-0.051737	0.90374816	96.754	9862.793068	93990.76494
First Floor	-0.039539	0.690672024	294.543	30024.77064	218670.0983
Ground Floor	-0.002696	0.047094053	1224.29	124800.2039	61975.3807
FRAME H	SHAPE	NORM SHAPE	-	-	
Roof	-0.040723	0.711354278	69.529	7087.56371	53164.38087
First Floor	-0.031291	0.546594964	511.405	52130.98879	300468.8298
Ground Floor	-0.001806	0.031547426	1181.936	120482.7727	40079.90837
FRAME I	SHAPE	NORM SHAPE	-	-	
First Floor	-0.022966	0.40117286	251.522	25639.3476	108461.6861
Ground Floor	-0.00096	0.016769396	1406.722	143396.738	25356.8047
FRAME J	SHAPE	NORM SHAPE	-	-	
First Floor	-0.017496	0.305622239	667.643	68057.39042	219330.0225
Ground Floor	-0.0009	0.015721309	1626.434	165793.476	27484.88772

Table 6.11: Equivalent storey force, Mode 5 (PART 2)

MODE 5		Participation	2.072	acc (m/s2)	5.088
FRAME K	SHAPE	NORM SHAPE	mass kN	mass kG	Force profile (N)
First Floor	-0.012913	0.225565842	259.119	26413.76147	62826.29123
Ground Floor	-0.000472	0.008244953	1624.517	165598.0632	14397.30723
FRAME L	SHAPE	NORM SHAPE	-	-	
First Floor	-0.008583	0.14992888	588.086	59947.60449	94775.25604
Ground Floor	-0.000441	0.007703441	1626.433	165793.3741	13467.5867
FRAME M	SHAPE	NORM SHAPE	-	-	
First Floor	-0.004535	0.079217927	399.153	40688.3792	33988.47682
Ground Floor	-0.000235	0.004105008	1625.291	165676.9623	7171.566104
FRAME N	SHAPE	NORM SHAPE	-	-	
First Floor	-0.000787	0.013747411	533.763	54410.09174	7887.478911
Ground Floor	-0.00004	0.000698725	1599.726	163070.948	1201.491237
FRAME O	SHAPE	NORM SHAPE	-	-	
First Floor	0.00194	-0.033888154	320.274	32647.70642	-11666.44202
Ground Floor	0.000096	-0.00167694	1555.668	158579.8165	-2804.162418
FRAME P	SHAPE	NORM SHAPE	-	-	
First Floor	0.004333	-0.075689367	259.514	26454.0265	-21113.70717
Ground Floor	0.000201	-0.003511092	783.038	79820.38736	-2955.247843

Table 6.12: Equivalent storey force, Mode 6 (PART 1)

MODE 6		Partic	1.068	Acc (m/s2)	6.284
FRAME B	SHAPE	NORM SHAPE	mass kN	mass kG	Force profile (N)
Roof	-0.0511	-2.8180	46.179	4707.339	-89049.118
First floor	-0.0412	-2.2718	128.865	13136.086	-200335.986
Ground Floor	-0.0029	-0.1592	372.221	37943.017	-40544.262
FRAME C	SHAPE	NORM SHAPE	-	-	
Roof	-0.0536	-2.9537	77.516	7901.733	-156674.835
First floor	-0.0386	-2.1275	473.058	48222.018	-688699.877
Ground Floor	-0.0025	-0.1399	1001.579	102097.757	-95904.255
FRAME D	SHAPE	NORM SHAPE	-	-	
Roof	-0.0366	-2.0197	142.507	14526.707	-196953.188
First Floor	-0.0278	-1.5340	473.037	48219.878	-496546.047
Ground Floor	-0.0014	-0.0755	1268.546	129311.519	-65497.468
FRAME E	SHAPE	NORM SHAPE	-	-	
Roof	-0.0148	-0.8187	95.627	9747.910	-53571.575
First Floor	-0.0106	-0.5830	304.191	31008.257	-121365.327
Ground Floor	-0.0005	-0.0280	1265.267	128977.268	-24259.290
FRAME F	SHAPE	NORM SHAPE	-	-	
Roof	0.0091	0.5020	149.763	15266.361	51448.600
First Floor	0.0079	0.4350	816.122	83192.864	242940.053
Ground Floor	0.0006	0.0328	1265.324	128983.078	28367.456
FRAME G	SHAPE	NORM SHAPE	-	-	
Roof	0.0312	1.7208	96.754	9862.793	113930.971
First Floor	0.0257	1.4155	294.543	30024.771	285302.285
Ground Floor	0.0020	0.1094	1224.29	124800.204	91630.322
FRAME H	SHAPE	NORM SHAPE	-	-	
Roof	0.0472	2.6022	69.529	7087.564	123810.112
First Floor	0.0375	2.0681	511.405	52130.989	723739.218
Ground Floor	0.0025	0.1362	1181.936	120482.773	110140.552
FRAME I	SHAPE	NORM SHAPE	-	-	
First Floor	0.0434	2.3926	251.522	25639.348	411801.297
Ground Floor	0.0021	0.1141	1406.722	143396.738	109797.136
FRAME J	SHAPE	NORM SHAPE	-	-	
First Floor	0.0440	2.4269	667.643	68057.390	1108763.813
Ground Floor	0.0025	0.1397	1626.434	165793.476	155490.490

Table 6.13: Equivalent storey force, Mode 6 (PART 2)

MODE 6		Partic	1.068	Acc (m/s2)	6.284
FRAME K	SHAPE	NORM SHAPE	mass kN	mass kG	Force profile (N)
First Floor	0.0437	2.4116	259.119	26413.761	427603.655
Ground Floor	0.0019	0.1021	1624.517	165598.063	113552.693
FRAME L	SHAPE	NORM SHAPE	-	-	
First Floor	0.0425	2.3448	588.086	59947.60449	943614.9006
Ground Floor	0.0025	0.1361	1626.433	165793.3741	151438.927
FRAME M	SHAPE	NORM SHAPE	-	-	
First Floor	0.0409	2.2543	399.153	40688.3792	615725.1006
Ground Floor	0.0024	0.1328	1625.291	165676.9623	147713.3712
FRAME N	SHAPE	NORM SHAPE	-	-	
First Floor	0.0389	2.1429	533.763	54410.09174	782697.6726
Ground Floor	0.0023	0.1272	1599.726	163070.948	139231.3721
FRAME O	SHAPE	NORM SHAPE	-	-	
First Floor	0.0353	1.9442	320.274	32647.70642	426101.4401
Ground Floor	0.0021	0.1137	1555.668	158579.8165	121070.3439
FRAME P	SHAPE	NORM SHAPE	-	-	
First Floor	0.0305	1.6805	259.514	26454.0265	298435.9855
Ground Floor	0.0015	0.0850	783.038	79820.38736	45542.58462

Table 6.14: Equivalent storey force, Mode 8 (PART 1)

MODE 8		Partic	0.387	Acc (m/s2)	6.969
FRAME B	SHAPE	NORM SHAPE	mass kN	mass kG	Force profile (N)
Roof	-0.0028	0.4366	46.179	4707.33945	5539.760281
First floor	-0.0019	0.2933	128.865	13136.0856	10384.33077
Ground Floor	-0.0001	0.0191	372.221	37943.0173	1955.472915
FRAME C	SHAPE	NORM SHAPE	-	-	
Roof	-0.0038	0.6069	77.516	7901.73293	12927.10345
First floor	-0.0019	0.3072	473.058	48222.0183	39927.87664
Ground Floor	0.0006	-0.0989	1001.579	102097.757	-27222.3182
FRAME D	SHAPE	NORM SHAPE	-	-	
Roof	-0.0052	0.8286	142.507	14526.7074	32446.24504
First Floor	-0.0025	0.3995	473.037	48219.8777	51920.3659
Ground Floor	0.0020	-0.3113	1268.546	129311.519	-108502.066
FRAME E	SHAPE	NORM SHAPE	-	-	
Roof	-0.0069	1.0840	95.627	9747.9103	28481.98217
First Floor	-0.0033	0.5180	304.191	31008.2569	43293.31815
Ground Floor	0.0028	-0.4406	1265.267	128977.268	-153158.292
FRAME F	SHAPE	NORM SHAPE	-	-	
Roof	-0.0079	1.2406	149.763	15266.3609	51049.92067
First Floor	-0.0041	0.6411	816.122	83192.8644	143755.8927
Ground Floor	0.0027	-0.4213	1265.324	128983.078	-146462.841
FRAME G	SHAPE	NORM SHAPE	-	-	
Roof	-0.0089	1.4108	96.754	9862.79307	37504.95713
First Floor	-0.0050	0.7872	294.543	30024.7706	63711.52379
Ground Floor	0.0021	-0.3250	1224.29	124800.204	-109341.281
FRAME H	SHAPE	NORM SHAPE	-	-	
Roof	-0.0088	1.3924	69.529	7087.56371	26601.4944
First Floor	-0.0061	0.9576	511.405	52130.9888	134556.0275
Ground Floor	0.0009	-0.1427	1181.936	120482.773	-46339.0658
FRAME I	SHAPE	NORM SHAPE	-	-	
First Floor	-0.0064	1.0148	251.522	25639.3476	70131.29236
Ground Floor	-0.0003	0.0419	1406.722	143396.738	16185.26135
FRAME J	SHAPE	NORM SHAPE	-	-	
First Floor	-0.0054	0.8465	667.643	68057.3904	155285.7162
Ground Floor	-0.0007	0.1060	1626.434	165793.476	47383.21533

Table 6.15: Equivalent storey force, Mode 8 (PART 2)

MODE 8		Partic	0.387	Acc (m/s2)	6.969
FRAME K	SHAPE	NORM SHAPE	mass kN	mass kG	Force profile (N)
First Floor	-0.0039	0.6216	259.119	26413.7615	44258.75343
Ground Floor	-0.0005	0.0822	1624.517	165598.063	36676.94611
FRAME L	SHAPE	NORM SHAPE	-	-	
First Floor	-0.0023	0.3601	588.086	59947.6045	58190.31779
Ground Floor	-0.0003	0.0496	1626.433	165793.374	22173.3539
FRAME M	SHAPE	NORM SHAPE	-	-	
First Floor	-0.0005	0.0776	399.153	40688.3792	8509.155358
Ground Floor	0.0001	-0.0134	1625.291	165676.962	-5998.12648
FRAME N	SHAPE	NORM SHAPE	-	-	
First Floor	0.0013	-0.2087	533.763	54410.0917	-30613.7722
Ground Floor	0.0007	-0.1124	1599.726	163070.948	-49383.375
FRAME O	SHAPE	NORM SHAPE	-	-	
First Floor	0.0030	-0.4679	320.274	32647.7064	-41174.2459
Ground Floor	0.0009	-0.1438	1555.668	158579.817	-61464.4322
FRAME P	SHAPE	NORM SHAPE	-	-	
First Floor	0.0041	-0.6498	259.514	26454.0265	-46331.8307
Ground Floor	0.0004	-0.0555	783.038	79820.3874	-11933.1615

Table 6.16: Equivalent storey force, Mode 12 (PART 1)

MODE 12		Participation	0.559	Acc (m/s2)	7.069
FRAME B	SHAPE	NORM SHAPE	mass kN	mass kG	Force profile (N)
Roof	0.0176	-5.2846	46.179	4707.339	-98371.207
First floor	0.0135	-4.0530	128.865	13136.086	-210535.152
Ground Floor	0.0009	-0.2818	372.221	37943.017	-42283.779
FRAME C	SHAPE	NORM SHAPE	-	-	
Roof	0.0188	-5.6273	77.516	7901.733	-175833.127
First floor	0.0123	-3.6942	473.058	48222.018	-704434.582
Ground Floor	-0.0003	0.0857	1001.579	102097.757	34617.549
FRAME D	SHAPE	NORM SHAPE	-	-	
Roof	0.0115	-3.4462	142.507	14526.707	-197965.835
First Floor	0.0080	-2.3915	473.037	48219.878	-456015.680
Ground Floor	-0.0013	0.3784	1268.546	129311.519	193468.671
FRAME E	SHAPE	NORM SHAPE	-	-	
Roof	0.0023	-0.6937	95.627	9747.910	-26741.697
First Floor	0.0016	-0.4779	304.191	31008.257	-58597.589
Ground Floor	0.0004	-0.1262	1265.267	128977.268	-64373.830
FRAME F	SHAPE	NORM SHAPE	-	-	
Roof	-0.0072	2.1664	149.763	15266.361	130781.875
First Floor	-0.0051	1.5308	816.122	83192.864	503594.488
Ground Floor	0.0010	-0.3046	1265.324	128983.078	-155360.470
FRAME G	SHAPE	NORM SHAPE	-	-	
Roof	-0.0155	4.6598	96.754	9862.793	181739.299
First Floor	-0.0113	3.3971	294.543	30024.771	403331.385
Ground Floor	-0.0005	0.1529	1224.290	124800.204	75457.003
FRAME H	SHAPE	NORM SHAPE	-	-	
Roof	-0.0203	6.0812	69.529	7087.564	170437.305
First Floor	-0.0138	4.1316	511.405	52130.989	851708.095
Ground Floor	0.0002	-0.0495	1181.936	120482.773	-23568.013
FRAME I	SHAPE	NORM SHAPE	-	-	
First Floor	-0.0131	3.9415	251.522	25639.348	399620.458
Ground Floor	0.0008	-0.2356	1406.722	143396.738	-133621.363
FRAME J	SHAPE	NORM SHAPE	-	-	
First Floor	-0.0113	3.3728	667.643	68057.390	907699.079
Ground Floor	0.0007	-0.2093	1626.434	165793.476	-137194.575

Table 6.17: Equivalent storey force, Mode 12 (PART 2)

MODE 12		Participation	0.559	Acc (m/s2)	7.069
FRAME K	SHAPE	NORM SHAPE	mass kN	mass kg	Force (N)
First Floor	-0.0093	2.7948	259.119	26413.761	291912.996
Ground Floor	0.0015	-0.4557	1624.517	165598.063	-298409.6895
FRAME L	SHAPE	NORM SHAPE	-	-	
First Floor	-0.0073	2.2011	588.086	59947.6045	521795.4565
Ground Floor	0.0017	-0.4995	1626.433	165793.374	-327458.484
FRAME M	SHAPE	NORM SHAPE	-	-	
First Floor	-0.0055	1.6606	399.153	40688.3792	267187.3147
Ground Floor	0.0011	-0.3406	1625.291	165676.962	-223128.2371
FRAME N	SHAPE	NORM SHAPE	-	-	
First Floor	-0.0040	1.1860	533.763	54410.0917	255181.8731
Ground Floor	0.0002	-0.0672	1599.726	163070.948	-43305.06493
FRAME O	SHAPE	NORM SHAPE	-	-	
First Floor	-0.0029	0.8607	320.274	32647.7064	111121.9743
Ground Floor	-0.0003	0.0809	1555.668	158579.817	50760.48406
FRAME P	SHAPE	NORM SHAPE	-	-	
First Floor	-0.0018	0.5396	259.514	26454.0265	56451.87473
Ground Floor	-0.0002	0.0474	783.038	79820.3874	14951.50801

Table 6.18: Equivalent storey force, Mode 7 (PART 1)

MODE 7		Participation	1.207	Acc (m/s2)	6.802
FRAME B	SHAPE	NORM SHAPE	mass kN	mass kG	Force profile (N)
Roof	-0.0342	3.3913	46.179	4707.339	131065.830
First floor	-0.0268	2.6611	128.865	13136.086	286998.322
Ground Floor	-0.0019	0.1879	372.221	37943.017	58541.851
FRAME C	SHAPE	NORM SHAPE	-	-	
Roof	-0.0371	3.6828	77.516	7901.733	238918.526
First floor	-0.0257	2.5524	473.058	48222.018	1010505.072
Ground Floor	-0.0020	0.2017	1001.579	102097.757	169086.212
FRAME D	SHAPE	NORM SHAPE	-	-	
Roof	-0.0237	2.3540	142.507	14526.707	280755.339
First Floor	-0.0174	1.7295	473.037	48219.878	684704.245
Ground Floor	-0.0013	0.1337	1268.546	129311.519	141997.833
FRAME E	SHAPE	NORM SHAPE	-	-	
Roof	-0.0063	0.6283	95.627	9747.910	50281.363
First Floor	-0.0042	0.4128	304.191	31008.257	105081.266
Ground Floor	-0.0002	0.0231	1265.267	128977.268	24480.693
FRAME F	SHAPE	NORM SHAPE	-	-	
Roof	0.0118	-1.1745	149.763	15266.361	-147208.126
First Floor	0.0097	-0.9670	816.122	83192.864	-660491.295
Ground Floor	0.0013	-0.1258	1265.324	128983.078	-133231.404
FRAME G	SHAPE	NORM SHAPE	-	-	
Roof	0.0272	-2.6948	96.754	9862.793	-218214.849
First Floor	0.0222	-2.2030	294.543	30024.771	-543057.693
Ground Floor	0.0028	-0.2751	1224.290	124800.204	-281916.034
FRAME H	SHAPE	NORM SHAPE	-	-	
Roof	0.0359	-3.5574	69.529	7087.564	-207003.215
First Floor	0.0249	-2.4659	511.405	52130.989	-1055429.904
Ground Floor	0.0028	-0.2730	1181.936	120482.773	-270003.974
FRAME I	SHAPE	NORM SHAPE	-	-	
First Floor	0.0192	-1.9029	251.522	25639.348	-400557.527
Ground Floor	0.0014	-0.1431	1406.722	143396.738	-168445.396
FRAME J	SHAPE	NORM SHAPE	-	-	
First Floor	0.0085	-0.8387	667.643	68057.390	-468641.533
Ground Floor	0.0007	-0.0700	1626.434	165793.476	-95216.271

Table 6.19: Equivalent storey force, Mode 7 (PART 2)

MODE 7		Participation	1.207	Acc (m/s2)	6.802
FRAME K	SHAPE	NORM SHAPE	mass kN	mass kg	Force (N)
First Floor	-0.0027	0.2695	259.119	26413.761	58440.595
Ground Floor	-0.0002	0.0186	1624.517	165598.063	25226.179
FRAME L	SHAPE	NORM SHAPE	-	-	
First Floor	-0.0139	1.3760	588.086	59947.6045	677236.3795
Ground Floor	-0.0012	0.1190	1626.433	165793.374	161935.0897
FRAME M	SHAPE	NORM SHAPE	-	-	
First Floor	-0.0247	2.4531	399.153	40688.3792	819490.1508
Ground Floor	-0.0022	0.2162	1625.291	165676.962	294085.74
FRAME N	SHAPE	NORM SHAPE	-	-	
First Floor	-0.0348	3.4553	533.763	54410.0917	1543521.65
Ground Floor	-0.0033	0.3285	1599.726	163070.948	439835.6119
FRAME O	SHAPE	NORM SHAPE	-	-	
First Floor	-0.0412	4.0926	320.274	32647.7064	1096982.391
Ground Floor	-0.0038	0.3741	1555.668	158579.817	487016.7231
FRAME P	SHAPE	NORM SHAPE	-	-	
First Floor	-0.0441	4.3753	259.514	26454.0265	950288.4306
Ground Floor	-0.0026	0.2568	783.038	79820.3874	168280.0824

Table 6.20: Equivalent storey force, Mode 10 (PART 1)

MODE 10		Participation	1.073	Acc (m/s2)	7.010
FRAME B	SHAPE	NORM SHAPE	mass kN	mass kG	Force profile (N)
Roof	-0.004	-1.753	46.179	4707.339	-62042.173
First floor	-0.003	-1.533	128.865	13136.086	-151490.538
Ground Floor	0.000	-0.395	372.221	37943.017	-112747.211
FRAME C	SHAPE	NORM SHAPE	-	-	
Roof	-0.003	-1.447	77.516	7901.733	-85959.127
First floor	-0.003	-1.309	473.058	48222.018	-474732.659
Ground Floor	-0.002	-2.648	1001.579	102097.757	-2033413.161
FRAME D	SHAPE	NORM SHAPE	-	-	
Roof	0.000	-0.158	142.507	14526.707	-17299.348
First Floor	-0.001	-0.357	473.037	48219.878	-129466.796
Ground Floor	-0.002	-3.855	1268.546	129311.519	-3748795.738
FRAME E	SHAPE	NORM SHAPE	-	-	
Roof	0.003	1.326	95.627	9747.910	97211.832
First Floor	0.002	0.783	304.191	31008.257	182594.355
Ground Floor	0.000	-0.243	1265.267	128977.268	-235970.667
FRAME F	SHAPE	NORM SHAPE	-	-	
Roof	0.005	2.527	149.763	15266.361	290102.070
First Floor	0.004	1.812	816.122	83192.864	1133851.773
Ground Floor	0.002	3.425	1265.324	128983.078	3322743.366
FRAME G	SHAPE	NORM SHAPE	-	-	
Roof	0.007	3.271	96.754	9862.793	242615.191
First Floor	0.005	2.460	294.543	30024.771	555525.636
Ground Floor	0.001	1.899	1224.290	124800.204	1782188.295
FRAME H	SHAPE	NORM SHAPE	-	-	
Roof	0.007	3.234	69.529	7087.564	172353.652
First Floor	0.004	1.735	511.405	52130.989	680224.655
Ground Floor	-0.002	-2.994	1181.936	120482.773	-2713206.584
FRAME I	SHAPE	NORM SHAPE	-	-	
First Floor	0.002	0.763	251.522	25639.348	147139.106
Ground Floor	-0.002	-2.949	1406.722	143396.738	-3179915.618
FRAME J	SHAPE	NORM SHAPE	-	-	
First Floor	0.001	0.401	667.643	68057.390	205352.643
Ground Floor	-0.001	-1.443	1626.434	165793.476	-1799609.511

Table 6.21: Equivalent storey force, Mode 10 (PART 2)

MODE 10		Participation	1.073	Acc (m/s2)	7.010
FRAME K	SHAPE	NORM SHAPE	mass kN	mass kg	Force (N)
First Floor	0.000	0.211	259.119	26413.761	41875.976
Ground Floor	0.000	-0.731	1624.517	165598.063	-910944.346
FRAME L	SHAPE	NORM SHAPE	-	-	
First Floor	0.000	0.069	588.086	59947.6045	31315.02967
Ground Floor	0.000	-0.315	1626.433	165793.374	-392900.9299
FRAME M	SHAPE	NORM SHAPE	-	-	
First Floor	0.000	-0.038	399.153	40688.3792	-11742.0098
Ground Floor	0.000	-0.026	1625.291	165676.962	-32549.22731
FRAME N	SHAPE	NORM SHAPE	-	-	
First Floor	0.000	-0.129	533.763	54410.0917	-52869.60327
Ground Floor	0.000	0.286	1599.726	163070.948	350407.3621
FRAME O	SHAPE	NORM SHAPE	-	-	
First Floor	0.000	-0.177	320.274	32647.7064	-43410.9227
Ground Floor	0.000	0.322	1555.668	158579.817	383594.8031
FRAME P	SHAPE	NORM SHAPE	-	-	
First Floor	0.000	-0.229	259.514	26454.0265	-45515.325
Ground Floor	0.000	0.012	783.038	79820.3874	7400.769512

Table 6.22: Equivalent storey force, Mode 13 (PART 1)

MODE 13		Participation	0.730	Acc (m/s2)	7.086
FRAME B	SHAPE	NORM SHAPE	mass kN	mass kG	Force profile (N)
Roof	0.0013	-0.5944	46.179	4707.339	-14466.519
First floor	0.0012	-0.5279	128.865	13136.086	-35856.805
Ground Floor	0.0001	-0.0420	372.221	37943.017	-8246.651
FRAME C	SHAPE	NORM SHAPE	-	-	
Roof	0.0008	-0.3490	77.516	7901.733	-14256.156
First floor	0.0008	-0.3810	473.058	48222.018	-95002.654
Ground Floor	0.0008	-0.3747	1001.579	102097.757	-197803.290
FRAME D	SHAPE	NORM SHAPE	-	-	
Roof	-0.0003	0.1433	142.507	14526.707	10761.907
First Floor	-0.0001	0.0447	473.037	48219.878	11156.400
Ground Floor	0.0002	-0.1089	1268.546	129311.519	-72831.127
FRAME E	SHAPE	NORM SHAPE	-	-	
Roof	-0.0014	0.6513	95.627	9747.910	32827.536
First Floor	-0.0008	0.3720	304.191	31008.257	59640.320
Ground Floor	-0.0010	0.4385	1265.267	128977.268	292380.016
FRAME F	SHAPE	NORM SHAPE	-	-	
Roof	-0.0023	1.0478	149.763	15266.361	82701.185
First Floor	-0.0014	0.6238	816.122	83192.864	268304.491
Ground Floor	0.0004	-0.1758	1265.324	128983.078	-117258.711
FRAME G	SHAPE	NORM SHAPE	-	-	
Roof	-0.0030	1.3619	96.754	9862.793	69448.334
First Floor	-0.0018	0.8281	294.543	30024.771	128548.776
Ground Floor	0.0008	-0.3652	1224.290	124800.204	-235661.932
FRAME H	SHAPE	NORM SHAPE	-	-	
Roof	-0.0032	1.4338	69.529	7087.564	52540.346
First Floor	-0.0020	0.8932	511.405	52130.989	240738.572
Ground Floor	-0.0008	0.3625	1181.936	120482.773	225819.842
FRAME I	SHAPE	NORM SHAPE	-	-	
First Floor	-0.0018	0.7946	251.522	25639.348	105338.861
Ground Floor	0.0002	-0.1094	1406.722	143396.738	-81099.358
FRAME J	SHAPE	NORM SHAPE	-	-	
First Floor	-0.0022	0.9786	667.643	68057.390	344346.736
Ground Floor	0.0021	-0.9619	1626.434	165793.476	-824521.223

Table 6.23: Equivalent storey force, Mode 13 (PART 2)

MODE 13		Participation	0.730	Acc (m/s2)	7.086
FRAME K	SHAPE	NORM SHAPE	mass kN	mass kg	Force (N)
First Floor	-0.0029	1.3257	259.119	26413.761	181052.736
Ground Floor	0.0017	-0.7517	1624.517	165598.063	-643591.471
FRAME L	SHAPE	NORM SHAPE	-	-	
First Floor	-0.0038	1.7149	588.086	59947.6045	531535.0868
Ground Floor	-0.0006	0.2626	1626.433	165793.374	225115.8533
FRAME M	SHAPE	NORM SHAPE	-	-	
First Floor	-0.0045	2.0485	399.153	40688.3792	430946.2138
Ground Floor	-0.0016	0.7413	1625.291	165676.962	634992.724
FRAME N	SHAPE	NORM SHAPE	-	-	
First Floor	-0.0049	2.2356	533.763	54410.0917	628921.3646
Ground Floor	-0.0001	0.0488	1599.726	163070.948	41158.84029
FRAME O	SHAPE	NORM SHAPE	-	-	
First Floor	-0.0047	2.1113	320.274	32647.7064	356389.8458
Ground Floor	0.0008	-0.3788	1555.668	158579.817	-310566.5714
FRAME P	SHAPE	NORM SHAPE	-	-	
First Floor	-0.0043	1.9378	259.514	26454.0265	265037.939
Ground Floor	-0.0001	0.0276	783.038	79820.3874	11379.06148

Table 6.24: Equivalent storey force, Mode 20 (PART 1)

MODE 20		Participation	0.771	Acc (m/s2)	7.165
FRAME B	SHAPE	NORM SHAPE	mass kN	mass kG	Force profile (N)
Roof	0.0024	-0.9777	46.179	4707.33945	-25435.2352
First floor	0.0007	-0.2921	128.865	13136.0856	-21203.2936
Ground Floor	0.0000	-0.0199	372.221	37943.0173	-4169.85871
FRAME C	SHAPE	NORM SHAPE	-	-	
Roof	-0.0035	1.4703	77.516	7901.73293	64206.1434
First floor	-0.0001	0.0563	473.058	48222.0183	15015.2487
Ground Floor	0.0000	0.0000	1001.579	102097.757	-7.00335676
FRAME D	SHAPE	NORM SHAPE	-	-	
Roof	-0.0025	1.0357	142.507	14526.7074	83148.695
First Floor	-0.0008	0.3128	473.037	48219.8777	83353.0114
Ground Floor	0.0000	0.0079	1268.546	129311.519	5625.21404
FRAME E	SHAPE	NORM SHAPE	-	-	
Roof	-0.0012	0.4826	95.627	9747.9103	26000.7388
First Floor	-0.0003	0.1264	304.191	31008.2569	21653.3667
Ground Floor	0.0000	0.0024	1265.267	128977.268	1695.89996
FRAME F	SHAPE	NORM SHAPE	-	-	
Roof	-0.0001	0.0406	149.763	15266.3609	3425.38852
First Floor	0.0004	-0.1599	816.122	83192.8644	-73522.7294
Ground Floor	0.0000	-0.0033	1265.324	128983.078	-2337.09853
FRAME G	SHAPE	NORM SHAPE	-	-	
Roof	0.0005	-0.2221	96.754	9862.79307	-12103.555
First Floor	0.0010	-0.4039	294.543	30024.7706	-67024.341
Ground Floor	0.0000	-0.0166	1224.29	124800.204	-11429.4024
FRAME H	SHAPE	NORM SHAPE	-	-	
Roof	0.0008	-0.3294	69.529	7087.56371	-12900.6723
First Floor	-0.0001	0.0269	511.405	52130.9888	7758.13902
Ground Floor	0.0000	0.0016	1181.936	120482.773	1091.81481
FRAME I	SHAPE	NORM SHAPE	-	-	
First Floor	-0.0021	0.8725	251.522	25639.3476	123627.07
Ground Floor	0.0000	0.0124	1406.722	143396.738	9849.3771
FRAME J	SHAPE	NORM SHAPE	-	-	
First Floor	-0.0032	1.3170	667.643	68057.3904	495352.158
Ground Floor	-0.0001	0.0257	1626.434	165793.476	23534.6295

Table 6.25: Equivalent storey force, Mode 20 (PART 2)

MODE 20		Participation	0.771	Acc (m/s2)	7.165
FRAME K	SHAPE	NORM SHAPE	mass kN	mass kg	Force (N)
First Floor	-0.0040	1.6538	259.119	26413.7615	241417.653
Ground Floor	0.0000	0.0104	1624.517	165598.063	9478.58481
FRAME L	SHAPE	NORM SHAPE	-	-	
First Floor	-0.0046	1.9215	588.086	59947.6045	636576.814
Ground Floor	-0.0001	0.0468	1626.433	165793.374	42893.7338
FRAME M	SHAPE	NORM SHAPE	-	-	
First Floor	-0.0052	2.1406	399.153	40688.3792	481345.693
Ground Floor	0.0000	-0.0070	1625.291	165676.962	-6448.5086
FRAME N	SHAPE	NORM SHAPE	-	-	
First Floor	-0.0056	2.3362	533.763	54410.0917	702473.251
Ground Floor	-0.0004	0.1665	1599.726	163070.948	150089.699
FRAME O	SHAPE	NORM SHAPE	-	-	
First Floor	-0.0060	2.4708	320.274	32647.7064	445798.446
Ground Floor	0.0015	-0.6355	1555.668	158579.817	-556956.798
FRAME P	SHAPE	NORM SHAPE	-	-	
First Floor	-0.0063	2.6212	259.514	26454.0265	383210.903
Ground Floor	0.0018	-0.7275	783.038	79820.3874	-320912.461

Table 6.26: Equivalent storey force, Mode 31 (PART 1)

MODE 31		Participation	0.9780	Acc (m/s2)	7.165
FRAME B	SHAPE	NORM SHAPE	mass kN	mass kG	Force profile (N)
Roof	0.0017	0.1251	46.179	4707.339	4125.974
First floor	0.0038	0.2826	128.865	13136.086	26015.603
Ground Floor	0.0071	0.5301	372.221	37943.017	140966.063
FRAME C	SHAPE	NORM SHAPE	-	-	
Roof	-0.0001	-0.0048	77.516	7901.733	-263.842
First floor	-0.0008	-0.0616	473.058	48222.018	-20831.351
Ground Floor	0.0062	0.4589	1001.579	102097.757	328390.816
FRAME D	SHAPE	NORM SHAPE	-	-	
Roof	0.0037	0.2748	142.507	14526.707	27973.896
First Floor	-0.0092	-0.6819	473.037	48219.878	-230442.882
Ground Floor	-0.0006	-0.0428	1268.546	129311.519	-38792.411
FRAME E	SHAPE	NORM SHAPE	-	-	
Roof	0.0133	0.9932	95.627	9747.910	67853.801
First Floor	-0.0095	-0.7042	304.191	31008.257	-153041.851
Ground Floor	-0.0004	-0.0280	1265.267	128977.268	-25301.294
FRAME F	SHAPE	NORM SHAPE	-	-	
Roof	0.0214	1.5904	149.763	15266.361	170160.915
First Floor	-0.0077	-0.5724	816.122	83192.864	-333731.852
Ground Floor	-0.0005	-0.0339	1265.324	128983.078	-30685.931
FRAME G	SHAPE	NORM SHAPE	-	-	
Roof	0.0293	2.1832	96.754	9862.793	150906.963
First Floor	-0.0047	-0.3535	294.543	30024.771	-74391.547
Ground Floor	-0.0003	-0.0236	1224.290	124800.204	-20640.313
FRAME H	SHAPE	NORM SHAPE	-	-	
Roof	0.0247	1.8382	69.529	7087.564	91308.782
First Floor	-0.0013	-0.0971	511.405	52130.989	-35466.250
Ground Floor	-0.0001	-0.0054	1181.936	120482.773	-4588.699
FRAME I	SHAPE	NORM SHAPE	-	-	
First Floor	-0.0001	-0.0070	251.522	25639.348	-1257.409
Ground Floor	0.0000	-0.0002	1406.722	143396.738	-184.865
FRAME J	SHAPE	NORM SHAPE	-	-	
First Floor	0.0001	0.0050	667.643	68057.390	2378.986
Ground Floor	0.0000	0.0002	1626.434	165793.476	267.886

Table 6.27: Equivalent storey force, Mode 31 (PART 2)

MODE 31		Participation	0.9780	Acc (m/s2)	7.165
FRAME K	SHAPE	NORM SHAPE	mass kN	mass kg	Force (N)
First Floor	0.0001	0.0066	259.119	26413.761	1212.704
Ground Floor	0.0000	0.0002	1624.517	165598.063	222.731
FRAME L	SHAPE	NORM SHAPE	-	-	
First Floor	0.0001	0.0047	588.086	59947.6045	1970.39865
Ground Floor	0.0000	0.0002	1626.433	165793.374	256.29524
FRAME M	SHAPE	NORM SHAPE	-	-	
First Floor	0.0000	0.0009	399.153	40688.3792	254.737778
Ground Floor	0.0000	0.0000	1625.291	165676.962	44.6710692
FRAME N	SHAPE	NORM SHAPE	-	-	
First Floor	-0.0001	-0.0042	533.763	54410.0917	-1589.67815
Ground Floor	0.0000	-0.0002	1599.726	163070.948	-203.25183
FRAME O	SHAPE	NORM SHAPE	-	-	
First Floor	-0.0002	-0.0122	320.274	32647.7064	-2793.4329
Ground Floor	0.0000	-0.0005	1555.668	158579.817	-590.149243
FRAME P	SHAPE	NORM SHAPE	-	-	
First Floor	-0.0002	-0.0173	259.514	26454.0265	-3215.80292
Ground Floor	0.0000	-0.0007	783.038	79820.3874	-416.442984

Table 6.28: Equivalent storey force, Mode 4 (PART 1)

MODE 4		Participation	2.066	Acc (m/s2)	5.019
FRAME B	SHAPE	NORM SHAPE	mass kN	mass kG	Force profile (N)
Roof	-0.0027	0.2005	46.179	4707.339	9788.114
First floor	-0.0067	0.5030	128.865	13136.086	68526.332
Ground Floor	-0.0005	0.0356	372.221	37943.017	13992.441
FRAME C	SHAPE	NORM SHAPE	-	-	
Roof	-0.0103	0.7765	77.516	7901.733	63638.972
First floor	-0.0089	0.6718	473.058	48222.018	335961.128
Ground Floor	-0.0006	0.0415	1001.579	102097.757	43939.566
FRAME D	SHAPE	NORM SHAPE	-	-	
Roof	-0.0135	1.0148	142.507	14526.707	152886.548
First Floor	-0.0103	0.7775	473.037	48219.878	388804.358
Ground Floor	-0.0004	0.0327	1268.546	129311.519	43855.792
FRAME E	SHAPE	NORM SHAPE	-	-	
Roof	-0.0154	1.1590	95.627	9747.910	117176.373
First Floor	-0.0114	0.8561	304.191	31008.257	275312.099
Ground Floor	-0.0005	0.0368	1265.267	128977.268	49172.526
FRAME F	SHAPE	NORM SHAPE	-	-	
Roof	-0.0163	1.2249	149.763	15266.361	193938.362
First Floor	-0.0122	0.9134	816.122	83192.864	788131.318
Ground Floor	-0.0008	0.0574	1265.324	128983.078	76728.686
FRAME G	SHAPE	NORM SHAPE	-	-	
Roof	-0.0173	1.3019	96.754	9862.793	133175.158
First Floor	-0.0124	0.9355	294.543	30024.771	291299.801
Ground Floor	-0.0008	0.0633	1224.290	124800.204	81927.155
FRAME H	SHAPE	NORM SHAPE	-	-	
Roof	-0.0176	1.3223	69.529	7087.564	97199.337
First Floor	-0.0096	0.7204	511.405	52130.989	389491.458
Ground Floor	-0.0005	0.0411	1181.936	120482.773	51382.208
FRAME I	SHAPE	NORM SHAPE	-	-	
First Floor	-0.0052	0.3899	251.522	25639.348	103686.856
Ground Floor	-0.0002	0.0162	1406.722	143396.738	24036.887
FRAME J	SHAPE	NORM SHAPE	-	-	
First Floor	-0.0036	0.2725	667.643	68057.390	192346.279
Ground Floor	-0.0002	0.0141	1626.434	165793.476	24171.830

Table 6.29: Equivalent storey force, Mode 4 (PART 2)

MODE 4		Participation	2.066	Acc (m/s2)	5.019
FRAME B	SHAPE	NORM SHAPE	mass kN	mass kG	Force
FRAME K	SHAPE	NORM SHAPE	-	-	
First Floor	-0.0027	0.2028	259.119	26413.761	55561.336
Ground Floor	-0.0001	0.0074	1624.517	165598.063	12781.768
FRAME L	SHAPE	NORM SHAPE	-	-	
First Floor	-0.0019	0.1419	588.086	59947.6045	88241.7901
Ground Floor	-0.0001	0.0073	1626.433	165793.374	12538.3212
FRAME M	SHAPE	NORM SHAPE	-	-	
First Floor	-0.0012	0.0878	399.153	40688.3792	37052.1761
Ground Floor	-0.0001	0.0045	1625.291	165676.962	7750.21695
FRAME N	SHAPE	NORM SHAPE	-	-	
First Floor	-0.0005	0.0372	533.763	54410.0917	20998.3487
Ground Floor	0.0000	0.0019	1599.726	163070.948	3178.46249
FRAME O	SHAPE	NORM SHAPE	-	-	
First Floor	-0.0001	0.0089	320.274	32647.7064	3029.00594
Ground Floor	0.0000	0.0004	1555.668	158579.817	692.243466
FRAME P	SHAPE	NORM SHAPE	-	-	
First Floor	0.0000	-0.0037	259.514	26454.0265	-1010.62108
Ground Floor	0.0000	-0.0002	783.038	79820.3874	-158.816268

Table 6.30: Equivalent storey force, Mode 11 (PART 1)

MODE 11		Participation	2.039	Acc (m/s2)	7.052
FRAME B	SHAPE	NORM SHAPE	mass kN	mass kG	Force profile (N)
Roof	0.0046	-4.9241	46.179	4707.339	-333268.408
First floor	0.0038	-4.0200	128.865	13136.086	-759252.080
Ground Floor	0.0003	-0.2975	372.221	37943.017	-162277.679
FRAME C	SHAPE	NORM SHAPE	-	-	
Roof	0.0046	-4.8752	77.516	7901.733	-553871.854
First floor	0.0034	-3.6227	473.058	48222.018	-2511705.143
Ground Floor	0.0012	-1.2440	1001.579	102097.757	-1826173.304
FRAME D	SHAPE	NORM SHAPE	-	-	
Roof	0.0020	-2.1418	142.507	14526.707	-447328.543
First Floor	0.0015	-1.6180	473.037	48219.878	-1121746.956
Ground Floor	0.0007	-0.7522	1268.546	129311.519	-1398425.590
FRAME E	SHAPE	NORM SHAPE	-	-	
Roof	-0.0010	1.0634	95.627	9747.910	149043.999
First Floor	-0.0006	0.6374	304.191	31008.257	284182.608
Ground Floor	-0.0013	1.3609	1265.267	128977.268	2523662.041
FRAME F	SHAPE	NORM SHAPE	-	-	
Roof	-0.0038	4.0200	149.763	15266.361	882379.772
First Floor	-0.0025	2.7037	816.122	83192.864	3234020.410
Ground Floor	-0.0006	0.6300	1265.324	128983.078	1168305.237
FRAME G	SHAPE	NORM SHAPE	-	-	
Roof	-0.0060	6.4072	96.754	9862.793	908569.475
First Floor	-0.0041	4.3759	294.543	30024.771	1889036.643
Ground Floor	0.0016	-1.6711	1224.290	124800.204	-2998561.146
FRAME H	SHAPE	NORM SHAPE	-	-	
Roof	-0.0070	7.4504	69.529	7087.564	759223.613
First Floor	-0.0045	4.8062	511.405	52130.989	3602362.812
Ground Floor	0.0001	-0.1307	1181.936	120482.773	-226359.620
FRAME I	SHAPE	NORM SHAPE	-	-	
First Floor	-0.0037	3.9340	251.522	25639.348	1450205.588
Ground Floor	-0.0014	1.4873	1406.722	143396.738	3066452.203
FRAME J	SHAPE	NORM SHAPE	-	-	
First Floor	-0.0020	2.0748	667.643	68057.390	2030235.548
Ground Floor	-0.0006	0.5960	1626.434	165793.476	1420689.564

Table 6.31: Equivalent storey force, Mode 11 (PART 2)

MODE 11		Participation	2.039	Acc (m/s2)	7.052
FRAME B	SHAPE	NORM SHAPE	mass kN	mass kG	Force
FRAME K	SHAPE	NORM SHAPE	-	-	
First Floor	-0.0001	0.1328	259.119	26413.761	50432.344
Ground Floor	0.0009	-0.9349	1624.517	165598.063	-2225905.985
FRAME L	SHAPE	NORM SHAPE	-	-	
First Floor	0.0016	-1.6509	588.086	59947.6045	-1422956.88
Ground Floor	0.0018	-1.9176	1626.433	165793.374	-4571021.545
FRAME M	SHAPE	NORM SHAPE	-	-	
First Floor	0.0029	-3.0713	399.153	40688.3792	-1796748.843
Ground Floor	0.0014	-1.4788	1625.291	165676.962	-3522656.125
FRAME N	SHAPE	NORM SHAPE	-	-	
First Floor	0.0039	-4.0912	533.763	54410.0917	-3200529.752
Ground Floor	-0.0003	0.3601	1599.726	163070.948	844394.0922
FRAME O	SHAPE	NORM SHAPE	-	-	
First Floor	0.0040	-4.2240	320.274	32647.7064	-1982749.934
Ground Floor	-0.0010	1.0454	1555.668	158579.817	2383482.137
FRAME P	SHAPE	NORM SHAPE	-	-	
First Floor	0.0040	-4.2516	259.514	26454.0265	-1617103.289
Ground Floor	0.0000	-0.0340	783.038	79820.3874	-39015.09792

Chapter 7

Bibliography

[1] F. E. M. Agency. *Techniques for the seismic rehabilitation of existing buildings*. Www Militarybookshop Company U, 2006.

[2] M. Amini and M. Poursha. A single-run multi-mode pushover analysis for seismic evaluation of tall buildings. In *16th World Conference on Earthquake Engineering, 16WCEE*, 2017.

[3] A. K. Chopra. Dynamics of structures, 2010.

[4] Computers and I. Structures. Csi analysis reference manual for sap2000, 2017.

[5] F. Di Trapani. Evaluation of the demand and safety assessment (n2 method) – fajfar, 2022. Lectures of 2022.

[6] I. Erdem, U. Akyuz, U. Ersoy, and G. Ozcebe. An experimental study on two different strengthening techniques for rc frames. *Engineering Structures*, 28(13):1843–1851, 2006.

[7] S. Erlicher, O. Lherminier, and M. Huguet. The e-dva method: A new approach for multi-modal pushover analysis under multi-component earthquakes. *Soil Dynamics and Earthquake Engineering*, 132:106069, 2020.

[8] A. Formisano, A. Massimilla, G. Di Lorenzo, and R. Landolfo. Seismic retrofit of gravity load designed rc buildings using external steel concentric bracing systems. *Engineering Failure Analysis*, 111:104485, 2020.

[9] D. A. Foutch, K. Hjelmstad, E. D. V. Calderón, E. F. Gutiérrez, and R. E. Downs. The mexico earthquake of september 19, 1985—case studies of seismic strengthening for two buildings in mexico city. *Earthquake Spectra*, 5(1):153–174, 1989.

[10] T. Görgülü, Y. S. Tama, S. Yilmaz, H. Kaplan, and Z. Ay. Strengthening of reinforced concrete structures with external steel shear walls. *Journal of Constructional Steel Research*, 70:226–235, 2012.

[11] M. Y. Kaltakci, M. H. Arslan, U. S. Yilmaz, and H. D. Arslan. A new approach on the strengthening of primary school buildings in turkey: An application of external shear wall. *Building and Environment*, 43(6):983–990, 2008.

[12] M. Y. Kaltakci, M. H. Arslan, U. S. Yilmaz, and H. D. Arslan. A new approach on the strengthening of primary school buildings in turkey: An application of external shear wall. *Building and Environment*, 43(6):983–990, 2008.

[13] H. Kaplan, S. Yilmaz, N. Cetinkaya, and E. Atimtay. Seismic strengthening of rc structures with exterior shear walls. *Sadhana*, 36:17–34, 2011.

[14] L. Martelli, L. Restuccia, and G. Ferro. The exoskeleton: a solution for seismic retrofitting of existing buildings. *Procedia Structural Integrity*, 25:294–304, 2020.

[15] L. Martelli, L. Restuccia, and G. Ferro. The exoskeleton technology as a solution to seismic adjustment of existing buildings. *Procedia Structural Integrity*, 26:175–186, 2020.

[16] J. P. Moehle. State of research on seismic retrofit of concrete building structures in the us. In *US-Japan symposium and workshop on seismic retrofit of concrete structures*, volume 16, 2000.

[17] N. Mordà and A. Mancini. Norme tecniche per le costruzioni (ntc 2018) d. min. infrastrutture e trasporti 17 gennaio 2018, 2018.

[18] F. NEHRP. Techniques for the seismic rehabilitation of existing buildings, fema 547. *Building Seismic Safety Council for the Federal Emergency Management Agency*, 2006.

[19] R. Pinho, F. Bianchi, R. Nascimbene, et al. *Valutazione sismica e tecniche di intervento per edifici esistenti in ca.* Maggioli spa, 2019.

[20] H. Sezen, A. Whittaker, K. Elwood, and K. Mosalam. Performance of reinforced concrete buildings during the august 17, 1999 kocaeli, turkey earthquake, and seismic design and construction practise in turkey. *Engineering Structures*, 25(1):103–114, 2003.

[21] A. Wada, Z. Qu, H. Ito, S. Motoyui, H. Sakata, and K. Kasai. Seismic retrofit using rocking walls and steel dampers. In *Improving the seismic performance of existing buildings and other structures*, pages 1010–1021. 2010.